

**TARGETING GROWTH AND ATROPHY PATHWAYS TO AMELIORATE
MUSCLE ATROPHY AND WEAKNESS DURING DISUSE**

by

Jay J. Salazar

A dissertation submitted in partial fulfillment
of the requirements for the degree of
Doctor of Philosophy
(Molecular and Integrative Physiology)
in the University of Michigan
2009

Doctoral Committee:

Associate Professor Susan Brooks Herzog, Chair
Professor John A. Faulkner
Professor Steven A. Goldstein
Assistant Professor Daniel E. Michele

© Jay J. Salazar

2009

Dedicated to my parents, Daisy Lopez de Salazar & Jesus R. Salazar
for their sacrifice in allowing me to leave Venezuela as a child
to pursue my American Dream.

To my grandmothers Maria de Lopez and Marina de Salazar
for providing the conduits that allowed me to reach the American shores.
To my 2nd Mom Xiomara de Hung, for inspiring me to love the sciences.

Dedicado a mis padres, Daisy Lopez de Salazar & Jesus R. Salazar
por sus sacrificios en dejarme salir de Venezuela desde joven
en búsqueda del Sueño Americano.

A mis abuelas Maria de Lopez and Marina de Salazar
por crear los medios que me ayudaron a llegar a las costas Americanas.
A mi segunda madre, Xiomara de Hung, por inspirarme a amar las ciencias.

Acknowledgements

Although medical research is unheard of in my native Venezuela, I dreamed as a child of three things; to get a taste of the American dream, the opportunity to be part of the scientific discovery process, and to contribute something towards NASA's space program. I am so privileged to say that Dr. Susan Brooks assisted me in fulfilling the latter two with the work in this dissertation. While I know that I am not the typical research student, Dr. Brooks patiently provided me with a high level of mentorship that I never envisioned, gave me the academic freedom to explore the worlds of muscle and spaceflight, and guided me to grow as the scientist that I am today.

I would also like to offer many thanks to Dr. Daniel Michele for being like a second mentor to me. His guidance and teachings were instrumental in the work presented in this dissertation. The Michele lab was my second home and I am so grateful for all the time that he invested in me. To Dr. John Faulkner, many thanks for his advice during my second rotation, opening his lab to me, and helping me through my preliminary examinations and committee meetings. I also extend my gratitude to Dr. Steven Goldstein for his advice and efforts as a member of my dissertation committee.

I would like to thank everyone in the Muscle Mechanics Lab but especially Cheryl Hassett and Carol Davis who assisted me with everything, and Ajit Gogawale, Amber Lee, and Jonathan Gumucio for help analyzing histological and electron microscope images. I also want to thank Dr. Mark Isken for his support. Finally, to the people that are the pillars in my life: my friends, Ana, Alex, Sue, & Steve, for opening my eyes to a

new world; my sisters, Daisy & Zuly, for all the support, love, and grief; and my family in Caracas & Ojeda who are everything to me.

TABLE OF CONTENTS

Dedication	ii
Acknowledgements	iii
List of Figures.....	vi
Abstract.....	ix
Chapters	
1. INTRODUCTION	1
2. INHIBITION OF CALPAIN PREVENTS MUSCLE WEAKNESS AND DISRUPTION OF SARCOMERE STRUCTURE DURING HINDLIMB SUSPENSION	24
3. TREATMENT WITH DEACETYLASE INHIBITORS DURING HINDLIMB SUSPENSION DOES NOT PREVENT MUSCLE WEAKNESS BUT RESULTS IN LARGER INDIVIDUAL FIBERS	63
4. SUMMARY AND CONCLUSIONS	92

List of Figures

Figure 2.1.	Characterization of cp mice	45
Figure 2.2	Soleus muscle mass for wt and cp mice following hindlimb suspension	46
Figure 2.3A	Representative cross sections for soleus muscles of control non-suspended wt and cp mice	47
Figure 2.3B	Individual type 1 fiber cross sectional areas (CSAs) for soleus muscles of wt and cp mice following hindlimb suspension	48
Figure 2.3C	Individual type 2 fiber cross sectional areas (CSAs) for soleus muscles of wt and cp mice following hindlimb suspension	48
Figure 2.4	Soleus muscle maximum isometric forces for wt and cp mice following hind limb suspension	49
Figure 2.5	Soleus muscle maximum isometric specific forces for wt and cp mice following hindlimb suspension	50
Figure 2.6	Sarcomere structure for soleus muscles of non-suspended wt and cp mice and mice exposed to 14 days of hindlimb suspension	51
Figure 2.7	Thick filament lengths for soleus muscles of non-suspended wt and cp mice and mice exposed to 14 days of hindlimb suspension	52

Figure 2.8	<i>Changes in passive resistance to stretch for soleus muscles on wt and cp mice following 14 days of hindlimb suspension</i>	53
Figure 2.9	<i>Force deficits following lengthening contractions of soleus muscles of wt and cp mice following hindlimb suspension</i>	54
Figure 2.10	<i>Masses, maximum isometric forces, and maximum specific forces for EDL muscle of wt and cp mice following HS</i>	55
Figure 3.1	<i>Effects of 21 days of TSA treatment on soleus muscles of non-suspended mice</i>	80
Figure 3.2	<i>Soleus muscle mass following 14 and 21 days of hindlimb suspension for TSA and vehicle treated mice</i>	81
Figure 3.3	<i>Soleus muscle maximum isometric force following 14 and 21 days of hindlimb suspension for TSA and vehicle treated mice</i>	82
Figure 3.4	<i>Soleus muscle maximum isometric specific force following 14 and 21 days of hindlimb suspension for TSA and vehicle treated mice</i>	83
Figure 3.5	<i>Force deficits following lengthening contractions of soleus muscles following 14 and 21 days of hindlimb suspension for TSA and vehicle treated mice</i>	84
Figure 3.6	<i>Individual fiber cross-sectional areas (CSAs) for soleus muscles following 21 days of hindlimb suspension for TSA and vehicle treated mice</i>	85

Figure 3.7 **Total number of fibers that appear in a muscle cross section for soleus muscles following 21 days of hindlimb suspension for TSA and vehicle treated mice..... 86**

Abstract

With unloading, muscle atrophy and weakness occur due to changes in both protein synthesis and degradation. The long term goal is to increase understanding of mechanisms underlying the losses in mass and force generation associated with muscle disuse. Our approach was to target both protein degradation, through inhibition of the protease calpain, and growth pathways, through inhibition of deacetylase activity, during hindlimb suspension (HS) to assess the effectiveness for ameliorating structural and functional declines in muscle with unloading. Calpain was inhibited by muscle-specific over-expression of calpastatin in transgenic (*cp*) mice, and in separate experiments, deacetylase activity was inhibited by treatment with trichostatin A (TSA), previously shown to promote myoblast fusion in culture and induce hypertrophy in dystrophic muscle *in vivo*. Compared with non-suspended control mice, after 14 days of HS, soleus muscles of wild type (*wt*) mice showed declines of 25-40% in mass, maximum isometric force (P_o), and specific P_o normalized for total muscle fiber cross-sectional area (CSA), while muscles of *cp* mice exhibited similar declines in mass but no change in specific P_o . Consistent with preservation of specific P_o during HS, muscles of *cp* mice also maintained sarcomere structure, in contrast to *wt* muscles that demonstrated misalignment of Z-lines and decreased uniformity of thick filament lengths. We conclude that inhibition of calpain proteolytic activity during unloading preserves sarcomere structure and isometric force generating capacity but does not protect from muscle

atrophy. In contrast, treatment with TSA did little to ameliorate the loss of muscle mass during HS and provided no protection from the decrease in specific P_o induced by unloading. Although treatment with TSA was ineffective for protecting muscles from atrophy or weakness, individual fiber CSAs were 30-40% larger in TSA treated than in vehicle treated mice after 21 days of HS. These findings indicate that inhibition of deacetylase activity is capable of inducing fiber growth, even in atrophying muscle. In conclusion, calpain inhibition may be an effective target for preventing muscle weakness during disuse, by minimizing proteolytic damage to the force generating apparatus, especially in combination with therapies targeting growth pathways for preventing muscle fiber atrophy.

CHAPTER 1

INTRODUCTION

The fully differentiated skeletal muscle cell is uniquely suited to generate force and, through its attachment through tendons or tendon-like structures to the skeleton, to produce movement. A structural hierarchy divides the whole muscle tissue into individual parallel running fibers, in which eighty percent of the volume is occupied by parallel running approximately cylindrical myofibrils. The myofibrils are in turn composed of a highly ordered array of interdigitating protein filaments. Cyclical interactions between the myosin molecules of the thick filaments and the actin molecules of the thin filaments result in the sliding of thick and thin filaments past one another and the generation of movement. Under circumstances when filament sliding is resisted, the cyclical interactions result in force generation. During development, individual skeletal muscle fibers differentiate into various types with widely varying contractile properties, providing the ability for the muscular system to match its structure and function to the habitual level of activity. Moreover, alterations in activity patterns, such as changes in loading, can induce adaptations in the expression and organization of muscle specific proteins to once again match the new pattern of activity (Lieber 2002). Fiber types vary with respect the myosin isoforms expressed, type 1 slow or type 2 fast, and the capacity for oxidative metabolism depending on the required function.

Skeletal Muscle Unloading by Hindlimb Suspension Induces Muscle Atrophy and Weakness

Deficits in skeletal muscle structure and function are prominent features of several diseases including HIV/AIDS (Gonzalez-Cadavid *et al.* 1998), cancer (Spencer & Mellgren 2002; Russell *et al.* 2009), muscular dystrophy (Spencer & Mellgren 2002), sepsis (Williams *et al.* 1999), and diabetes (Price & Mitch 1998). In addition, unloading of skeletal muscle during space flight (Gardetto *et al.* 1989; Tischler *et al.* 1993; Tischler & Slentz 1995; Widrick *et al.* 1997; Widrick *et al.* 1999; Bodine *et al.* 2001) or during a period of bed rest (Gardetto *et al.* 1989; Tischler *et al.* 1993; Tischler & Slentz 1995; Widrick *et al.* 1997; Widrick *et al.* 1999; Bodine *et al.* 2001) or immobilization due to casting of a limb (Gardetto *et al.* 1989; Tischler *et al.* 1993; Tischler & Slentz 1995; Widrick *et al.* 1997; Widrick *et al.* 1999; Bodine *et al.* 2001) induces substantial muscle atrophy, weakness, and changes in protein expression. A commonly used experimental method for unloading the skeletal muscles of the hind limbs of rodents is hindlimb suspension (HS), also sometimes referred to as hindlimb unweighting (HU). Multiple modified versions of the original methodology described by Morey *et al.* (1979) have since resulted in over 1300 publications. Most HS methods are similar, and involve placing some form of small harness on the rodent's tail that is used to suspend the hind legs just slightly off of the floor of the cage. The tail is then connected by a pulley to a rod so that the animals can move freely around the cage with easy access to food and water.

In conjunction with NASA, investigators have performed parallel studies demonstrating the similarity of the responses of skeletal muscles from rodents exposed to HS to those of muscles of rodents during the actual weightlessness of space (Tischler

et al. 1993; Ikemoto *et al.* 2001). One response consistently reported following both HS and true weightlessness was a similar pattern of muscle atrophy. During HS, skeletal muscle mass declines rapidly by as much as 40% within 2 weeks for rats (Fitts *et al.* 1986). During HS of rats as well as during space flight, the soleus muscles, normally weight bearing postural muscles, show a large degree of muscle atrophy while the extensor digitorum longus (EDL) muscles, non-weight bearing muscles, are much less affected. In addition to the muscle atrophy induced by HS, associated losses in force are also observed. Following 14 days of HS, both soleus and adductor longus muscles display atrophy, and permeabilized fibers from both muscles generate lower forces than fibers from muscles of non-suspended animals. Moreover, fibers from soleus muscles exhibit weakness, i.e. a decrease in maximum isometric force in excess of what could be explained by atrophy, resulting in a decreased specific force (kN/m^2) (Riley *et al.* 2005). Despite the consistency of the findings that slow muscles are primarily affected with HS or space flight in rats, studies utilizing muscle biopsy material from astronauts have shown that type 1 and type 2 fibers are similarly affected (Fitts *et al.* 2000).

The mechanism underlying the loss of muscle mass and force during unloading induced by HS has been attributed to an imbalance in protein turnover where protein degradation is increased and protein synthesis is diminished (Haddad *et al.* 2003a; Haddad *et al.* 2003b). The rate of myofibrillar protein synthesis declines rapidly over the first several days following the initiation of HS (Thomason *et al.* 1989). The rapid decrease in myofibril protein synthesis rate does not appear to be due to decreased transcription, based on the observation that myosin heavy chain mRNA concentration was not decreased after 7 days of HS, a time point when myofibrillar protein synthesis had decreased by 59%. Subsequent to the rapid decline in protein synthesis, the rate of

protein degradation slowly increases, peaking around Day 15 for soleus muscles of young rats and returning to pre-suspension values after about 3 weeks (Thomason *et al.* 1989). Further investigations of single fibers from rat soleus muscles showed a 25% reduction in the density of thin filaments following 14 days of HS that accompanied the decreased specific force values (Riley *et al.* 2005) and parallel findings from muscle samples of astronauts in orbit for 17 days on the space shuttle indicated that, compared with preflight samples, there was a 26% decrease in number of thin filaments and a 23% increase in susceptibility to contraction induced injury (Riley *et al.* 2000). Finally, six weeks of bed rest induced a 40% reduction in specific force with a parallel decline in myofibrillar protein content per muscle fiber volume (Larsson *et al.* 1996). Each of these findings is consistent with a tip in the balance toward increased protein degradation with insufficient protein synthesis to compensate.

Detailed analyses of specific proteins targeted for degradation during disuse atrophy have focused recently on the giant sarcomere protein titin. Titin filaments bind on one end to the Z-disc and on the other to multiple points along the thick filaments and serves as template for sarcomere assembly. Titin is well recognized as the main determinant within muscle fibers of passive tension (Horowitz *et al.* 1986; Funatsu *et al.* 1990; Prado *et al.* 2005) and as such acts to maintain the thick filaments of the A-band in the central portion of the sarcomere. Recently, Udaka and colleagues concluded that muscle disuse, achieved through immobilization of a limb by casting, induced changes within sarcomeres that were due to the preferential loss of titin in comparison to the unchanged levels of other myofibrillar proteins (Udaka *et al.* 2008). Among the findings of the Udaka study were the observations of decreased mean thick filament length, decreased uniformity of thick filament length, decreased maximum isometric specific

force, and decreased passive force in response to six weeks of limb immobilization. Other investigators have reported decreased passive tension of whole soleus muscles (Caiozzo *et al.* 2007) and permeabilized single soleus fibers (Toursel *et al.* 2002) following HS that was accompanied by decreased titin levels in the muscles (Toursel *et al.* 2002).

Thus, while disuse clearly results in reductions in muscle protein levels as well as decreases in force generating capability, the molecular mechanisms for these changes are still incompletely understood. Although skeletal muscle has an enormous capacity to remodel and adapt in response to alterations in usage, an increased understanding of the regulatory events that contribute to the loss of muscle mass and force would improve our ability to design interventions aimed at maintaining functional capacity under circumstances when muscles are exposed to decreased loads (Stein & Wade 2005). Thus, the long term goal of this thesis work is to increase understanding of the mechanisms underlying the losses in mass and force associated with unloading. Our approach was to target both muscle protein degradation and growth pathways during HS to assess the effectiveness for ameliorating structural and functional declines.

Protein Degradation Pathways in Skeletal Muscle

Skeletal muscle contains four primary proteolytic systems that contribute to the turnover of muscle proteins: 1. the lysosomal system, 2. the caspase system, 3. the ubiquitin-proteasome system, and 4. the calpain system (Goll *et al.* 2008). Several studies have investigated the relative contributions to disuse skeletal muscle atrophy of these various proteolytic systems (Taillandier *et al.* 1996; Spencer *et al.* 1997; Bodine *et al.* 2001). One study performed on rats flown on the Space Shuttle STS-90 analyzed

three of the major proteolytic pathways, namely the calpain, lysosomal, and ubiquitin-proteasome pathways, and reported increased cleavage of myosin heavy chain that was specifically correlated with increased expression of components of the ubiquitin-proteasome system (Ikemoto *et al.* 2001). Furthermore, daily injections of a calpain inhibitor did not prevent the muscle atrophy in the rats leading the authors to conclude that the atrophy was mediated specifically by the ubiquitin proteasome system (Ikemoto *et al.* 2001), although no data confirming entry of the inhibitor into the muscles let alone the inhibition of calpain activity was provided (Tidball & Spencer 2002).

Additional support for the importance of the ubiquitin-proteasome system in muscle atrophy was provided by the highly significant work of Bodine and her colleagues in the early part of this decade (Bodine *et al.* 2001). That study demonstrated that the expression of two muscle-specific ubiquitin ligases, namely the Muscle Atrophy F-box (MAFbx, also known as atrogin-1) and the Muscle RING Finger-1 (MuRF1), increased in response to multiple different interventions that induced muscle atrophy. Moreover, over-expression of MAFbx in myotubes was reported to reduce myotube size, whereas mice deficient in either MAFbx or MuRF1 displayed an attenuation of muscle atrophy following denervation compared with wild type littermates (Bodine *et al.* 2001). Despite this compelling evidence supporting a role of MAFbx and MuRF1 in myofibrillar protein degradation during muscle atrophy, the exact role, mode of regulation, and target substrates of MAFbx and MuRF1 remain unknown (Glickman & Ciechanover 2002). Of particular importance, is the observation that the ubiquitin-proteasome system does not appear able to target and degrade intact myofibrils (Koochmaraie 1992; Solomon & Goldberg 1996; Williams *et al.* 1999; Jagoe & Goldberg 2001). Thus, myofibrillar proteins may need to first be cleaved and/or released from the myofibrils by

other degradative pathways to provide substrate for ubiquitination. The accumulation of the resultant protein fragments has been hypothesized to then generate a positive feedback signal resulting in increased proteasome activity (Li *et al.* 2004b).

The calpain system has been postulated to be the proteolytic system that is critical for cytoskeletal remodeling during the early phase of the muscle response to alterations in loading (Kandarian & Stevenson 2002; Goll *et al.* 2003; Fareed *et al.* 2006). Although numerous myofibrillar proteins are substrates for calpain, conflicting observations have been made about the action of calpains during skeletal muscle atrophy. Some investigators have reported no increases in the mRNA or activity of calpains during HS or spaceflight (Spencer *et al.* 1997; Ikemoto *et al.* 2001; Stevenson *et al.* 2003), while others have reported significant increases during unloading by HS or spinal cord transection (Taillandier *et al.* 1996; Haddad *et al.* 2003a). Other studies showed that inhibition of calpains *in vitro* prevented accelerated proteolysis in muscles harvested after 3 days of HS (Tischler *et al.* 1990), whereas another study indicated that *in vitro* inhibition of calpains after 9 days of HS prevented only a small percentage of muscle proteolysis (Taillandier *et al.* 1996). While the contradictory nature of these investigations is difficult to completely resolve, it is fair to say that the extent to which such *in vitro* assessments mimic the proteolytic process in an atrophying muscle *in vivo* is unclear. Despite the disparities among *in vitro* studies, support for the importance of calpain as a mediator of protein degradation in skeletal muscle during atrophy is provided by the observation that treatment of rats with calpain inhibitors prevented sepsis-induced muscle proteolysis with no change in the expression of the MAFbx and MURF-1 ubiquitin ligases (Fareed *et al.* 2006). Even more compelling is the report that inhibition of calpain through transgenic over-expression of the endogenous calpain

inhibitor, calpastatin, attenuated muscle fiber atrophy associated with HS (Tidball & Spencer 2002).

The use of general protease inhibitors, like the Bowman-Birk inhibitor, a non-specific serine protease inhibitor known to inhibit a large number of proteases, has been reported to effectively attenuate the loss of muscle mass during HS (Morris *et al.* 2005). However, due to the broad spectrum of known and unknown targets of these drugs, such studies do little to help clarify important mechanisms. Finally, rigorous isometric exercise interventions have been pursued as a means to ameliorate muscle atrophy during disuse (Haddad *et al.* 2006). Although the exercise was able to fully blunt the increased expression of markers believed to be mediating muscle atrophy, including atrogen-1, MURF-1, and myostatin, the exercise failed to counteract disuse atrophy (Haddad *et al.* 2006). Based on large bodies of work, summarized only briefly here, the conclusion is that the functional connections between the calpain, lysosomal, caspase, and ubiquitin-proteasome systems remain unknown (Taillandier *et al.* 1996; Taillandier *et al.* 2004).

Inhibition of the Calpain System Reduces Muscle Fiber Atrophy

The calpain system is primarily comprised of three polypeptides: two Ca²⁺-dependent proteases, calpain 1 and 2, along with an endogenous inhibitor of the two calpains; calpastatin. In addition to the ubiquitous calpains 1 and 2, a third calpain, calpain 3, is expressed in skeletal muscle (Goll *et al.* 2003; Bartoli & Richard 2005). Calpain 1 and calpain 2 are heterodimers containing identical 28 kDa subunits and an 80 kDa subunit that shares 55-66% homology between these two calpains (Goll *et al.* 2003). The terms μ -calpain (for calpain 1) and m-calpain (for calpain 2) were initially

used to refer to the micromolar and millimolar Ca^{2+} concentrations required for their activation. Calpains 1 and 2 are activated at Ca^{2+} concentrations of 3 μM to 50 μM and 400 μM to 800 μM , respectively, and undergo autolysis at Ca^{2+} concentrations of 50 μM to 150 μM and 550 μM to 800 μM , respectively (Goll *et al.* 2003). Moreover, the activation of the calpains requires sustained elevations in Ca^{2+} concentrations on the order of many seconds to minutes, preventing calpain activation in response to contraction-associated increases in $[\text{Ca}^{2+}]$, which transiently reach 10s of μM (Murphy *et al.* 2006). Although there is some controversy about the significance of the autolysis of the calpains, several studies report that auto-cleaved calpains 1 and 2 proteins are unstable and lose their proteolytic activity (Pal *et al.* 2001; Nakagawa *et al.* 2001; Li *et al.* 2004a).

Calpains 1 and 2 are primarily associated with the Z-lines of the myofibrils in skeletal muscle fibers and with the cytoskeleton and the plasma membrane in non-muscle cells, and over 100 proteins have been shown to be cleaved by calpains *in vitro* (Goll *et al.* 2003). Calpain activity has been reported to rapidly increase, within 12 hours, in soleus muscles in response to HS (Enns & Belcastro 2006). The ratio of calpain activity to calpastatin activity was also significantly elevated over the same period of time (Enns *et al.* 2007). Moreover, a significant inverse relationship ($r^2 = 0.7$) was demonstrated between the ratio of calpain 1/calpastatin activity and the level of desmin, a muscle-specific intermediate filament protein and known calpain substrate, although the decrease in the levels of desmin did not reach statistical significance during the HS (Enns *et al.* 2007). The conclusion is that calpain activation, in particular calpain 1, is an early event following muscle unloading and the resultant increase in the proteolytic potential of the calpain-calpastatin system contributes to the depletion of

myofibrillar proteins. Despite this conclusion regarding the role of calpain 1 in muscle protein degradation during HS, the absence of calpain 1 in homozygous knock out mice has no apparent skeletal muscle phenotype (Azam *et al.* 2001). In contrast, disruption of the calpain 2 gene is embryonically lethal (Zimmerman *et al.* 2000), and although calpain 3 deficient mice exhibit smaller fibers than wild type littermates, calpain 3 activity is not increased during muscle atrophy (Bartoli & Richard 2005).

Another approach to altering the calpain/calpastatin activity ratio is to increase calpastatin activity. Transgenic mice over-expressing calpastatin 30- to 50-fold showed evidence for inhibition of calpain activity and the partial prevention of the muscle fiber atrophy induced by HS (Tidball & Spencer 2002). However, no studies have investigated the effects of inhibition of the calpain system on skeletal muscle force generation, integrity of the force generating apparatus, or the ability of the muscle to withstand contraction-induced injury.

Treatment with Deacetylase Inhibitors Increases Muscle Cell Size *In Vitro* and Induces Fiber Hypertrophy in Dystrophic Muscles *In Vitro*

In addition to approaches targeting protein degradation systems to ameliorate declines in skeletal muscles mass and function during disuse, modulation of positive or negative regulators of muscle growth also represents a strategy to alleviate such declines as well as to provide insights into the mechanisms underlying disuse atrophy. Recent investigations have used modulators of protein acetylation as a way to mediate hypertrophy in skeletal muscle (Minetti *et al.* 2006). The level of histone acetylation is an important means by which transcription is regulated.

Histones associate with DNA to form the complex chromatin structure into which

the DNA is organized and packaged within the nucleus of eukaryotic cells. The modification of core histones by acetylation and deacetylation is of fundamental importance to conformational changes of the chromatin. The core histone proteins are acetylated, by histone acetyltransferases, on lysine residues in the N-terminal tail and on the surface of the nucleosome core. Upon acetylation, chromatin conformation is transformed into a more relaxed structure. A relaxed chromatin structure allows the transcriptional machinery access to promoters increasing transcriptional activity (Clayton *et al.* 2006). In contrast, the relaxation of the chromatin structure is reversed by the action of histone deacetylases, resulting in the condensation of chromatin conformation and gene silencing. Histone deacetylases are also involved in the reversible acetylation of non-histone proteins. Protein acetylation positively influences cell proliferation and differentiation in skeletal muscle.

Although the important targets underlying the positive effects of increased levels of protein acetylation in muscle are unknown, studies of C2C12 skeletal muscle cell lines showed that treatment with deacetylase inhibitors, including trichostatin A (TSA), valproic acid, and phenylbutyrate, resulted in the formation of larger myotubes compared with myotubes formed in cultures in the absence of the drug (Iezzi *et al.* 2002; Iezzi *et al.* 2004). Similar results were reported for human primary myoblast cultures providing motivation for the use of these drugs *in vivo* mice (Iezzi *et al.* 2002; Iezzi *et al.* 2004). In addition, treatment of both *mdx* and alpha-sarcoglycan deficient mice, models of Duchenne and limb girdle type 2D muscular dystrophies, respectively, with TSA was reported to increase muscle fiber size, enhance exercise performance, improve muscle force generation, and decrease susceptibility to contraction-induced injury to levels comparable to those of wild type mice (Minetti *et al.* 2006). Moreover, treatment with

TSA increased expression of markers of satellite cell activation and improved regeneration of injured muscles in wild type mice (Iezzi *et al.* 2002; Iezzi *et al.* 2004).

The effects of deacetylase inhibitors appear to be mediated through the actions of a member of the transforming growth factor-beta (TGF- β) family of cytokines, follistatin. Support for this hypothesis is provided by the observation that TSA treatment of C2C12 myoblasts increased follistatin expression while preventing follistatin transcription rendered myoblasts insensitive to TSA treatment. Furthermore, treatment of C2C12 cells with follistatin inhibitors greatly reduced TSA-mediated myoblast fusion (Iezzi *et al.* 2002; Iezzi *et al.* 2004). In addition, the beneficial effects of TSA treatment in *mdx* mice (Minetti *et al.* 2006) and the enhanced regeneration observed following TSA treatment in wild type mice (Iezzi *et al.* 2002; Iezzi *et al.* 2004) were, in both cases, accompanied by increased follistatin expression. Although the mechanism by which follistatin acts is not known, a recent study presented compelling evidence that the skeletal muscle hypertrophy induced by follistatin over-expression was dependent at least in part through the activation of satellite cells (Gilson *et al.* 2009).

One pathway by which follistatin may influence satellite cell activation is through its interaction with another TGF- β family member, myostatin (Lee & McPherron 2001). Myostatin is a negative regulator of skeletal muscle mass that appears to act, at least in part, by inhibiting the proliferation, differentiation, and self-renewal of myoblasts (Thomas *et al.* 2000; Taylor *et al.* 2001; McCroskery *et al.* 2003), and a reduction in myostatin levels, achieved either through inactivation of the myostatin genes or through postnatal inhibition of myostatin, results in dramatic increases in skeletal muscle mass (Grobet *et al.*, 2003; McPherron *et al.*, 1997; McPherron and Lee, 1997; Whittemore *et al.*, 2003). Despite a known role of follistatin in inhibiting myostatin *in vivo* (Lee & McPherron 2001),

over-expression of follistatin in myostatin-deficient mice results in additional muscle hypertrophy on top of the increases induced by the lack of myostatin (Gilson *et al.* 2009) indicating the ability of follistatin to act in a myostatin-independent manner. The ability of myostatin inhibition, follistatin over-expression, or treatment with deacetylase inhibitors to prevent the loss of muscle mass during hindlimb suspension has not been explored, but atrophy was not prevented in myostatin deficient mice exposed to HS (McMahon *et al.* 2003). In fact, following 7 days of HS, muscle mass decreased to a greater extent in the myostatin deficient mice compared with their wild type littermates (McMahon *et al.* 2003).

Study Aims and Hypotheses

The purpose of this thesis is to investigate the impact of manipulating pathways that modulate either muscle protein degradation, through the inhibition of the calcium-activated protease calpain, or muscle growth pathways, through the inhibition of deacetylase activity, to ameliorate the declines in skeletal muscle mass and force generating capacity that occur in response to disuse. Using the widely recognized HS model of muscle disuse in mice, the overall hypothesis that inhibition of either calpain activity or protein deacetylase activity would ameliorate the development of disuse-induced muscle atrophy and weakness was tested. To address this hypothesis two experimental chapters are presented.

For Chapter 2, a colony of transgenic mice was generated that over-expressed calpastatin by ~20-fold in a muscle specific manner. Calpastatin over-expressing transgenic mice (*cp* mice) and wild type littermates (*wt* mice) were subjected to 3, 9, or 14 days of HS. After a given period of HS, soleus and EDL muscles were removed and

evaluated for mass; isometric contractile properties, passive resistance to stretch, and susceptibility to lengthening-contraction induced injury measured *in vitro*; individual fiber cross-sectional areas determined from histological samples; and disruption of the underlying sarcomere structure through analysis of electron micrographs.

In Chapter 3, a study is described in which C57BL/6 control mice were treated with either the deacetylase inhibitor trichostatin A (TSA) or vehicle during a period of 14 or 21 days of HS. Based on findings in Chapter 2 that 14 days of HS had no effect on mass or force generation of the EDL muscles of mice, we concentrated our studies in Chapter 3 on the soleus muscle. Again, following HS, muscles were removed and evaluated for mass, isometric contractile properties, susceptibility to lengthening-contraction induced injury, and individual fiber cross-sectional areas.

The results of Chapter 2 indicate that calpain activity is critical mediator of the disruption of the sarcomere structure leading to decreased isometric force generating capability induced in soleus muscles during unloading associated with HS. In contrast, inhibition of calpain activity does not prevent the loss of soleus muscle mass associated with unloading. Our findings in Chapter 3 showed that treatment with TSA provides no protection from the substantial decrease in specific force induced by unloading, but individual fiber CSAs were 30-40% larger in TSA treated mice compared with those in vehicle treated animals after 21 days of HS. Thus, calpain inhibition may be an important and effective target for preventing muscle weakness during disuse, by minimizing proteolytic damage to the force generating apparatus, especially in combination with additional therapies aimed at preventing muscle atrophy by stimulating muscle fiber growth.

References

1. Azam, M., S. S. Andrabi, K. E. Sahr, L. Kamath, A. Kuliopulos and A. H. Chishti. 2001. Disruption of the mouse mu-calpain gene reveals an essential role in platelet function. *Mol. Cell Biol.*, 21: 2213-2220.
2. Bartoli, M. and I. Richard. 2005. Calpains in muscle wasting. *Int. J. Biochem. Cell Biol.*, 37: 2115-2133.
3. Bodine, S. C., E. Latres, S. Baumhueter, V. K. Lai, L. Nunez, B. A. Clarke, W. T. Poueymirou, F. J. Panaro, E. Na, K. Dharmarajan, Z. Q. Pan, D. M. Valenzuela, T. M. DeChiara, T. N. Stitt, G. D. Yancopoulos and D. J. Glass. 2001. Identification of ubiquitin ligases required for skeletal muscle atrophy. *Science*, 294: 1704-1708.
4. Caiozzo, V. J., H. Richmond, S. Kaska and D. Valeroso. 2007. The mechanical behavior of activated skeletal muscle during stretch: effects of muscle unloading and MyHC isoform shifts. *J. Appl. Physiol.*, 103: 1150-1160.
5. Clayton, A. L., C. A. Hazzalin and L. C. Mahadevan. 2006. Enhanced histone acetylation and transcription: a dynamic perspective. *Mol. Cell*, 23: 289-296.
6. Enns, D. L. and A. N. Belcastro. 2006. Early activation and redistribution of calpain activity in skeletal muscle during hindlimb unweighting and reweighting. *Can. J. Physiol Pharmacol.*, 84: 601-609.
7. Enns, D. L., T. Raastad, I. Ugelstad and A. N. Belcastro. 2007. Calpain/calpastatin activities and substrate depletion patterns during hindlimb unweighting and reweighting in skeletal muscle. *Eur. J. Appl. Physiol.*, 100: 445-455.

8. Fareed, M. U., A. R. Evenson, W. Wei, M. Menconi, V. Poylin, V. Petkova, B. Pignol and P. O. Hasselgren. 2006. Treatment of rats with calpain inhibitors prevents sepsis-induced muscle proteolysis independent of atrogin-1/MAFbx and MuRF1 expression. *Am. J. Physiol Regul. Integr. Comp Physiol*, 290: R1589-R1597.
9. Fitts, R. H., J. M. Metzger, D. A. Riley and B. R. Unsworth. 1986. Models of disuse: a comparison of hindlimb suspension and immobilization. *J. Appl. Physiol*, 60: 1946-1953.
10. Fitts, R. H., D. R. Riley and J. J. Widrick. 2000. Physiology of a microgravity environment invited review: microgravity and skeletal muscle. *J. Appl. Physiol*, 89: 823-839.
11. Funatsu, T., H. Higuchi and S. Ishiwata. 1990. Elastic filaments in skeletal muscle revealed by selective removal of thin filaments with plasma gelsolin. *J. Cell Biol.*, 110: 53-62.
12. Gardetto, P. R., J. M. Schluter and R. H. Fitts. 1989. Contractile function of single muscle fibers after hindlimb suspension. *J. Appl. Physiol*, 66: 2739-2749.
13. Gilson, H., O. Schakman, S. Kalista, P. Lause, K. Tsuchida and J. P. Thissen. 2009. Follistatin induces muscle hypertrophy through satellite cell proliferation and inhibition of both myostatin and activin. *Am. J. Physiol Endocrinol. Metab*, 297: E157-E164.
14. Glickman, M. H. and A. Ciechanover. 2002. The ubiquitin-proteasome proteolytic pathway: destruction for the sake of construction. *Physiol Rev.*, 82: 373-428.
15. Goll, D. E., G. Neti, S. W. Mares and V. F. Thompson. 2008. Myofibrillar protein turnover: the proteasome and the calpains. *J. Anim Sci.*, 86: E19-E35.

16. Goll, D. E., V. F. Thompson, H. Li, W. Wei and J. Cong. 2003. The calpain system. *Physiol Rev.*, 83: 731-801.
17. Gonzalez-Cadavid, N. F., W. E. Taylor, K. Yarasheski, I. Sinha-Hikim, K. Ma, S. Ezzat, R. Shen, R. Lalani, S. Asa, M. Mamita, G. Nair, S. Arver and S. Bhasin. 1998. Organization of the human myostatin gene and expression in healthy men and HIV-infected men with muscle wasting. *Proc. Natl. Acad. Sci. U. S. A*, 95: 14938-14943.
18. Haddad, F., G. R. Adams, P. W. Bodell and K. M. Baldwin. 2006. Isometric resistance exercise fails to counteract skeletal muscle atrophy processes during the initial stages of unloading. *J. Appl. Physiol*, 100: 433-441.
19. Haddad, F., R. R. Roy, H. Zhong, V. R. Edgerton and K. M. Baldwin. 2003a. Atrophy responses to muscle inactivity. I. Cellular markers of protein deficits. *J. Appl. Physiol*, 95: 781-790.
20. Haddad, F., R. R. Roy, H. Zhong, V. R. Edgerton and K. M. Baldwin. 2003b. Atrophy responses to muscle inactivity. II. Molecular markers of protein deficits. *J. Appl. Physiol*, 95: 791-802.
21. Horowitz, R., E. S. Kempner, M. E. Bisher and R. J. Podolsky. 1986. A physiological role for titin and nebulin in skeletal muscle. *Nature*, 323: 160-164.
22. Iezzi, S., G. Cossu, C. Nervi, V. Sartorelli and P. L. Puri. 2002. Stage-specific modulation of skeletal myogenesis by inhibitors of nuclear deacetylases. *Proc. Natl. Acad. Sci. U. S. A*, 99: 7757-7762.

23. Iezzi, S., P. M. Di, C. Serra, G. Caretti, C. Simone, E. Maklan, G. Minetti, P. Zhao, E. P. Hoffman, P. L. Puri and V. Sartorelli. 2004. Deacetylase inhibitors increase muscle cell size by promoting myoblast recruitment and fusion through induction of follistatin. *Dev. Cell*, 6: 673-684.
24. Ikemoto, M., T. Nikawa, S. Takeda, C. Watanabe, T. Kitano, K. M. Baldwin, R. Izumi, I. Nonaka, T. Towatari, S. Teshima, K. Rokutan and K. Kishi. 2001. Space shuttle flight (STS-90) enhances degradation of rat myosin heavy chain in association with activation of ubiquitin-proteasome pathway. *FASEB J.*, 15: 1279-1281.
25. Jagoe, R. T. and A. L. Goldberg. 2001. What do we really know about the ubiquitin-proteasome pathway in muscle atrophy? *Curr. Opin. Clin. Nutr. Metab Care*, 4: 183-190.
26. Kandarian, S. C. and E. J. Stevenson. 2002. Molecular events in skeletal muscle during disuse atrophy. *Exerc. Sport Sci. Rev.*, 30: 111-116.
27. Koochmaraie, M. 1992. Ovine skeletal muscle multicatalytic proteinase complex (proteasome): purification, characterization, and comparison of its effects on myofibrils with mu-calpains. *J. Anim Sci.*, 70: 3697-3708.
28. Larsson, L., X. Li, H. E. Berg and W. R. Frontera. 1996. Effects of removal of weight-bearing function on contractility and myosin isoform composition in single human skeletal muscle cells. *Pflugers Arch.*, 432: 320-328.
29. Lee, S. J. and A. C. McPherron. 2001. Regulation of myostatin activity and muscle growth. *Proc. Natl. Acad. Sci. U. S. A.*, 98: 9306-9311.
30. Li, H., V. F. Thompson and D. E. Goll. 2004a. Effects of autolysis on properties of mu- and m-calpain. *Biochim. Biophys. Acta*, 1691: 91-103.

31. Li, Y., S. Gazdciu, Z. Q. Pan and S. Y. Fuchs. 2004b. Stability of homologue of Slimb F-box protein is regulated by availability of its substrate. *J. Biol. Chem.*, 279: 11074-11080.
32. Lieber, R. L. 2002. *Skeletal Muscle Structure, Function, and Plasticity*, Second Edition edn. Lippincott Williams & Wilkins, Baltimore.
33. McCroskery, S., M. Thomas, L. Maxwell, M. Sharma and R. Kambadur. 2003. Myostatin negatively regulates satellite cell activation and self-renewal. *J. Cell Biol.*, 162: 1135-1147.
34. McMahon, C. D., L. Popovic, J. M. Oldham, F. Jeanplong, H. K. Smith, R. Kambadur, M. Sharma, L. Maxwell and J. J. Bass. 2003. Myostatin-deficient mice lose more skeletal muscle mass than wild-type controls during hindlimb suspension. *Am. J. Physiol Endocrinol. Metab*, 285: E82-E87.
35. Minetti, G. C., C. Colussi, R. Adami, C. Serra, C. Mozzetta, V. Parente, S. Fortuni, S. Straino, M. Sampaolesi, P. M. Di, B. Illi, P. Gallinari, C. Steinkuhler, M. C. Capogrossi, V. Sartorelli, R. Bottinelli, C. Gaetano and P. L. Puri. 2006. Functional and morphological recovery of dystrophic muscles in mice treated with deacetylase inhibitors. *Nat. Med.*, 12: 1147-1150.
36. Morris, C. A., L. D. Morris, A. R. Kennedy and H. L. Sweeney. 2005. Attenuation of skeletal muscle atrophy via protease inhibition. *J. Appl. Physiol*, 99: 1719-1727.
37. Murphy, R. M., E. Verburg and G. D. Lamb. 2006. Ca²⁺ activation of diffusible and bound pools of mu-calpain in rat skeletal muscle. *J. Physiol*, 576: 595-612.

38. Nakagawa, K., H. Masumoto, H. Sorimachi and K. Suzuki. 2001. Dissociation of m-calpain subunits occurs after autolysis of the N-terminus of the catalytic subunit, and is not required for activation. *J. Biochem. (Tokyo)*, 130: 605-611.
39. Pal, G. P., J. S. Elce and Z. Jia. 2001. Dissociation and aggregation of calpain in the presence of calcium. *J. Biol. Chem.*, 276: 47233-47238.
40. Prado, L. G., I. Makarenko, C. Andresen, M. Kruger, C. A. Opitz and W. A. Linke. 2005. Isoform diversity of giant proteins in relation to passive and active contractile properties of rabbit skeletal muscles. *J. Gen. Physiol*, 126: 461-480.
41. Price, S. R. and W. E. Mitch. 1998. Mechanisms stimulating protein degradation to cause muscle atrophy. *Curr. Opin. Clin. Nutr. Metab Care*, 1: 79-83.
42. Riley, D. A., J. L. Bain, J. G. Romatowski and R. H. Fitts. 2005. Skeletal muscle fiber atrophy: altered thin filament density changes slow fiber force and shortening velocity. *Am. J. Physiol Cell Physiol*, 288: C360-C365.
43. Riley, D. A., J. L. Bain, J. L. Thompson, R. H. Fitts, J. J. Widrick, S. W. Trappe, T. A. Trappe and D. L. Costill. 2000. Decreased thin filament density and length in human atrophic soleus muscle fibers after spaceflight. *J. Appl. Physiol*, 88: 567-572.
44. Russell, S. T., P. M. Siren, M. J. Siren and M. J. Tisdale. 2009. Attenuation of skeletal muscle atrophy in cancer cachexia by D-myo-inositol 1,2,6-triphosphate. *Cancer Chemother. Pharmacol.*, 64: 517-527.
45. Solomon, V. and A. L. Goldberg. 1996. Importance of the ATP-ubiquitin-proteasome pathway in the degradation of soluble and myofibrillar proteins in rabbit muscle extracts. *J. Biol. Chem.*, 271: 26690-26697.

46. Spencer, M. J., B. Lu and J. G. Tidball. 1997. Calpain II expression is increased by changes in mechanical loading of muscle in vivo. *J. Cell Biochem.*, 64: 55-66.
47. Spencer, M. J. and R. L. Mellgren. 2002. Overexpression of a calpastatin transgene in mdx muscle reduces dystrophic pathology. *Hum. Mol. Genet.*, 11: 2645-2655.
48. Stein, T. P. and C. E. Wade. 2005. Metabolic consequences of muscle disuse atrophy. *J. Nutr.*, 135: 1824S-1828S.
49. Stevenson, E. J., P. G. Giresi, A. Koncarevic and S. C. Kandarian. 2003. Global analysis of gene expression patterns during disuse atrophy in rat skeletal muscle. *J. Physiol*, 551: 33-48.
50. Taillandier, D., E. Aurousseau, D. Meynial-Denis, D. Bechet, M. Ferrara, P. Cottin, A. Ducastaing, X. Bigard, C. Y. Guezennec, H. P. Schmid and . 1996. Coordinate activation of lysosomal, Ca²⁺-activated and ATP-ubiquitin-dependent proteinases in the unweighted rat soleus muscle. *Biochem. J.*, 316 (Pt 1): 65-72.
51. Taillandier, D., L. Combaret, M. N. Pouch, S. E. Samuels, D. Bechet and D. Attaix. 2004. The role of ubiquitin-proteasome-dependent proteolysis in the remodelling of skeletal muscle. *Proc. Nutr. Soc.*, 63: 357-361.
52. Taylor, W. E., S. Bhasin, J. Artaza, F. Byhower, M. Azam, D. H. Willard, Jr., F. C. Kull, Jr. and N. Gonzalez-Cadauid. 2001. Myostatin inhibits cell proliferation and protein synthesis in C2C12 muscle cells. *Am. J. Physiol Endocrinol. Metab*, 280: E221-E228.

53. Thomas, M., B. Langley, C. Berry, M. Sharma, S. Kirk, J. Bass and R. Kambadur. 2000. Myostatin, a negative regulator of muscle growth, functions by inhibiting myoblast proliferation. *J. Biol. Chem.*, 275: 40235-40243.
54. Thomason, D. B., R. B. Biggs and F. W. Booth. 1989. Protein metabolism and beta-myosin heavy-chain mRNA in unweighted soleus muscle. *Am. J. Physiol*, 257: R300-R305.
55. Tidball, J. G. and M. J. Spencer. 2002. Expression of a calpastatin transgene slows muscle wasting and obviates changes in myosin isoform expression during murine muscle disuse. *J. Physiol*, 545: 819-828.
56. Tischler, M. E., E. J. Henriksen, K. A. Munoz, C. S. Stump, C. R. Woodman and C. R. Kirby. 1993. Spaceflight on STS-48 and earth-based unweighting produce similar effects on skeletal muscle of young rats. *J. Appl. Physiol*, 74: 2161-2165.
57. Tischler, M. E., S. Rosenberg, S. Satarug, E. J. Henriksen, C. R. Kirby, M. Tome and P. Chase. 1990. Different mechanisms of increased proteolysis in atrophy induced by denervation or unweighting of rat soleus muscle. *Metabolism*, 39: 756-763.
58. Tischler, M. E. and M. Slentz. 1995. Impact of weightlessness on muscle function. *ASGSB. Bull.*, 8: 73-81.
59. Toursel, T., L. Stevens, H. Granzier and Y. Mounier. 2002. Passive tension of rat skeletal soleus muscle fibers: effects of unloading conditions. *J. Appl. Physiol*, 92: 1465-1472.

60. Udaka, J., S. Ohmori, T. Terui, I. Ohtsuki, S. Ishiwata, S. Kurihara and N. Fukuda. 2008. Disease-induced preferential loss of the giant protein titin depresses muscle performance via abnormal sarcomeric organization. *J. Gen. Physiol*, 131: 33-41.
61. Widrick, J. J., S. T. Knuth, K. M. Norenberg, J. G. Romatowski, J. L. Bain, D. A. Riley, M. Karhanek, S. W. Trappe, T. A. Trappe, D. L. Costill and R. H. Fitts. 1999. Effect of a 17 day spaceflight on contractile properties of human soleus muscle fibres. *J. Physiol*, 516 (Pt 3): 915-930.
62. Widrick, J. J., J. G. Romatowski, J. L. Bain, S. W. Trappe, T. A. Trappe, J. L. Thompson, D. L. Costill, D. A. Riley and R. H. Fitts. 1997. Effect of 17 days of bed rest on peak isometric force and unloaded shortening velocity of human soleus fibers. *Am. J. Physiol*, 273: C1690-C1699.
63. Williams, A. B., G. M. Courten-Myers, J. E. Fischer, G. Luo, X. Sun and P. O. Hasselgren. 1999. Sepsis stimulates release of myofilaments in skeletal muscle by a calcium-dependent mechanism. *FASEB J.*, 13: 1435-1443.
64. Zimmerman, U. J., L. Boring, J. H. Pak, N. Mukerjee and K. K. Wang. 2000. The calpain small subunit gene is essential: its inactivation results in embryonic lethality. *IUBMB. Life*, 50: 63-68.

CHAPTER 2

INHIBITION OF CALPAIN PREVENTS MUSCLE WEAKNESS AND DISRUPTION OF SARCOMERE STRUCTURE DURING HINDLIMB SUSPENSION

Summary

Unloading skeletal muscle results in atrophy and a decreased ability of the remaining muscle to generate force. Reduced atrophy has been reported when calpain activity is inhibited during unloading, but the impact on force generating capability has not been established. Our hypothesis is that endogenous inhibition of the calpain system, through muscle specific over-expression of calpastatin, prevents the disruption of sarcomere structure and the decreased specific force (kN/m^2) observed with unloading. Wild type (*wt*) and calpastatin over-expressing transgenic (*cp*) mice were subjected to hindlimb suspension (HS). Following 3, 9, or 14 days of HS, soleus and extensor digitorum longus (EDL) muscles were removed from anesthetized mice and contractile properties were measured *in vitro*. EDL muscles were not affected by HS in *wt* or *cp* mice. Compared with soleus muscles of non-suspended control mice, soleus muscles of *wt* mice showed a 25% decline in mass after 14 days of HS while maximum isometric force (P_o) decreased by 40%, resulting in a specific P_o that was 35% lower than control values. Over the same time period, muscles of *cp* mice demonstrated 25% declines in both mass and P_o but no change in specific P_o . Consistent with the preservation of isometric force generating capability, soleus muscles of *cp* mice

maintained a high degree of order in sarcomere structure, in contrast to muscles of *wt* mice that demonstrated misalignment of z-lines and decreased uniformity of thick filament lengths following HS. Maximally activated muscles were also exposed to two stretches of 30% strain relative to fiber length. The magnitude of the deficit in force induced by the stretches increased with the duration of HS, but was not different for muscles of *cp* and *wt* mice. Thus, while isometric force generating capability and sarcomere structure were preserved during HS by calpain inhibition, the susceptibility to injury induced by lengthening contractions was not reduced. We conclude that inhibition of calpain activity during unloading preserves sarcomere structure such that the isometric force generating capability is not diminished, while the effects of unloading on lengthening contraction-induced injury likely occurs through calpain-independent mechanisms.

Introduction

Skeletal muscle atrophy and weakness are prominent features of diseases including cancer (Russell *et al.* 2009), sepsis (Williams *et al.* 1999), and diabetes (Price & Mitch 1998), as well as during bed rest (Widrick *et al.* 1997) and during the muscle unloading associated with travel to space (Gardetto *et al.* 1989; Widrick *et al.* 1999). The atrophy has been attributed to an imbalance created by factors that control protein synthesis and those that control protein degradation (Thomason *et al.* 1989). Several proteolytic systems contribute to the turnover of muscle proteins, including the lysosomal system, the caspase system, the ubiquitin-proteasome system, and the calpain system (Goll *et al.* 2008). An important role for the calpain system in skeletal muscle atrophy has been implicated by several investigators (Taillandier *et al.* 1996; Spencer *et al.*

1997; Enns & Belcastro 2006), but clear conclusions have not emerged. While some reports indicated increases in calpain mRNA in skeletal muscle during unloading by hindlimb suspension (HS) (Taillandier *et al.* 1996) or spinal cord transaction (Haddad *et al.* 2003), others showed no change in calpain mRNA with unloading by HS (Stevenson *et al.* 2003) or spaceflight (Ikemoto *et al.* 2001). Regardless, mRNA levels are not indicative of protein concentrations or activity (Croall & DeMartino 1991). Changes in calpain activity have been explored by isolating calpain from muscles following exercise or injury and incubating the protein with known substrates (Arthur *et al.* 1999; Reid & Belcastro 2000), but this approach ignores both endogenous calpain inhibitors present in the muscle *in vivo* and the intracellular calcium concentrations critical for calpain activation. Some of the aforementioned pitfalls were circumvented in studies using transgenic mice that over-expressed calpastatin, an endogenous inhibitor of calpain (Tidball & Spencer 2002). After 10 days of HS, the calpastatin over-expressing mice showed reduced muscle fiber atrophy and prevented the shift to faster myosin heavy chain isoforms typical of inactivity (Tidball & Spencer 2002).

In addition to inducing muscle atrophy, unloading also disrupts force generating capability, which decreases muscle performance and increases susceptibility to contraction-induced injury (Gardetto *et al.* 1989; Widrick *et al.* 1999; Trappe *et al.* 2009). Decreased muscle force generating capacity may provide an explanation for the lack of success of exercise countermeasures during muscle unloading in rats and humans (Haddad *et al.* 2006; Trappe *et al.* 2009). Our preliminary studies showed weakness of muscles following a period of HS (data not shown), defined as a decrease in maximum isometric force in excess of what can be explained by atrophy, i.e. a decreased specific force (kN/m²). To elucidate the contribution of the calpain system to the development of

both atrophy and weakness during unloading induced by HS, we analyzed the time course of the effects of *in vivo* inhibition of calpain by utilizing a line of transgenic mice with muscle-specific over-expression of calpastatin (Otani *et al.* 2004). Our working hypothesis is that the decreased specific force observed following the removal of weight bearing is due to the disruption of the underlying sarcomere structure by the calcium-dependent calpain system. Specifically, we hypothesized that following various periods of HS, atrophy, weakness, and susceptibility to lengthening contraction-induced injury would be less severe for muscles of transgenic calpastatin over-expressing (*cp*) mice than for muscles of wild type (*wt*) littermates. We further hypothesized that underlying sarcomere structure would be maintained during HS in *cp* but not *wt* mice.

Methods

All experiments were performed on 4- to 5-month old specific pathogen free (SPF) male C57BL/6 mice from a colony of transgenic calpastatin over-expressing (*cp*) mice and wild type (*wt*) littermates bred in house in the University of Michigan Unit for Laboratory Animal Medicine. All procedures were approved by the University of Michigan Committee for the Use and Care of Animals. A total of 26 *cp* and 29 *wt* mice were randomly assigned to one of four groups: experimental mice exposed to hind limb suspension (HS) for periods of 3, 9, or 14 days and non-suspended (control) mice that maintained normal levels of activity. During all operative procedures, mice were anesthetized with intraperitoneal injections of Avertin™ at a dose of 400 mg/kg tribromoethanol, with supplemental doses provided to maintain an adequate level of anesthesia to prevent response to tactile stimuli.

CP Mice

Breeding pairs of *cp* mice were obtained as a kind gift from Dr. Kenneth Polonsky at Washington University School of Medicine, St. Louis, MO. From these founder mice, we established an internal colony for this study. The transgene DNA was targeted to skeletal muscle using the murine muscle-specific creatine kinase promoter followed by a bovine growth hormone polyadenylation signal sequence (Otani *et al.* 2004).

Hindlimb Suspension

HS is a widely used method for unloading rodent hind limbs. Our method of HS was modified from that originally described by Morey (Morey 1979). Briefly, surgical tape (3M, Two Harbors, MN) was used to wrap the tail of each animal against a rigid metal wire piece with a manually bent upper hook connected to a rotating pulley. The tape was lightly soaked with liquid suture VetBond (3M, Two Harbor, MN) to create an instant cast. Care was taken to prevent any VetBond from dripping onto the animal's tail. During the casting process, mice were briefly restrained in a small terrycloth wrap with the tail exposed. Since the entire process of preparing the tail was completed within two minutes, no anesthetic was required during the procedure. After the tape and metal piece were attached, mice were released into a cage until the glue was dry. Once the tape hardened, the hind legs of the mice were lifted slightly off the floor of the cage by connecting the pulley to a metal rod inside the suspension cage. The rotating pulley system enabled mice to move from one end of the cage to the other with a full 360° range of motion and obtain food and water freely. Mice were observed daily for changes in appearance and activity.

In Vitro Muscle Contractile Properties

Under deep anesthesia, soleus and extensor digitorum longus (EDL) muscles of one limb were isolated from control mice, and from mice exposed to 3, 9, or 14 days of HS. 5-0 silk suture ties were secured around the distal and proximal tendons, and the muscles were carefully removed and placed in a horizontal bath containing buffered mammalian Ringer solution (composition in mM: 137 NaCl, 24 NaHCO₃, 11 glucose, 5 KCl, 2 CaCl₂, 1 MgSO₄, 1 NaH₂PO₄, and 0.025 tubocurarine chloride) maintained at 25 °C and bubbled with 95% O₂ / 5% CO₂ to stabilize pH at 7.4. One tendon of the muscle was tied securely to a force transducer (model BG-50, Kulite Semiconductor Products, Leonia, NJ) and the other tendon to the lever arm of a servomotor (model 305B, Aurora Scientific, Richmond Hill, ON, Canada). The contralateral soleus and EDL muscles were removed and prepared for future analyses of protein levels and activities or sarcomere structure. After removal of the muscles, mice were euthanized with an overdose of anesthetic and administration of a bilateral pneumothorax.

For measurement of isometric contractile properties, muscles were stimulated between two stainless steel plate electrodes. The voltage of single 0.2-ms square stimulation pulses and, subsequently, muscle length (L_o) were adjusted to obtain maximal twitch force. Muscle length was measured with calipers. With the muscle held at L_o , the force developed during trains of stimulation pulses was recorded, and stimulation frequency was increased until the maximum isometric tetanic force (P_o) was achieved. For EDL muscles, 300-ms trains of pulses were used, and 900-ms trains were used for soleus muscles. A stimulus frequency of 140 Hz was typically needed to achieve P_o for both EDL and soleus muscles of *cp* mice, whereas frequencies of 120 and 130 Hz elicited P_o for EDL and soleus muscles, respectively, of *wt* animals. For each

muscle, optimum fiber length (L_f) was calculated by multiplying L_o by previously determined L_f/L_o ratios for EDL and soleus muscles of 0.45 and 0.71, respectively (Brooks & Faulkner 1988).

Following assessment of the maximum isometric tetanic forces, EDL and soleus muscles were exposed to a single constant velocity stretch without activation (passive stretch) of 30% strain relative to L_f to obtain a measurement of the passive extension properties of the muscles. The velocity of the stretch was 2 L_f/s . The peak force achieved during the stretch was recorded. Each passive stretch was followed by a single maximum isometric contraction to verify that the stretch did not induce any injury. Following the passive stretch, each muscle was exposed to two additional 30% stretches also at 2 L_f/s initiated from the plateau of an isometric contraction at the stimulation frequency that elicited P_o . Prior to the stretch, EDL and soleus muscles were held isometric for the first 100 or 300 ms, respectively, of each contraction to allow near maximal activation, and stimulation was terminated at the end of the lengthening ramp. One minute of rest was allowed before the second lengthening contraction was initiated and P_o was measured once again 1 minute after the second lengthening contraction. The force deficit induced by the two lengthening contractions was calculated as the difference between the isometric forces measured before and after the stretches, expressed as a percentage of the force before the stretch.

After the force measurements, muscles were removed from the bath, the tendons were trimmed, and the muscle was blotted and weighed. Muscles were quick frozen in isopentane cooled with liquid nitrogen and stored at $-80\text{ }^{\circ}\text{C}$ for subsequent histological analyses. Total muscle fiber cross-sectional area (CSA) was calculated by dividing the muscle mass by the product of L_f and the density of mammalian skeletal muscle, 1.06

g/cm^3 . Specific P_o (kN/m^2) was calculated by dividing P_o by total fiber CSA for each muscle.

Myosin ATPase Activity

Frozen cross sections of 10 μm thickness were cut from the widest portion of the belly of each muscle. Cryosections were placed on microscope slides and incubated at various pH conditions to allow identification of Type 1 and Type 2 on the basis of myofibrillar ATPase activity, as previously described (Brooke & Kaiser 1970). Stained sections were visualized on a microscope (Leitz Laborlux, Leica; Wetzlar, Germany) and captured with a video camera (Diagnostic Instruments; Sterling Heights, MI), and the image analyzing software ImageJ was used to calculate individual fiber CSAs. For each muscle, individual fiber CSAs were evaluated from two to three fields at 20x magnification, with each field containing ~50 fibers. Fields were chosen randomly from the central portion of the muscle avoiding fields that reached the edge of the section. Images from sections of soleus muscles from $n = 4-6$ were analyzed for suspended and control *wt* and *cp* mice. Consequently, single fiber areas were measured for 400-600 fibers for each experimental group.

Calpastatin Western Blot

Total protein extracts from soleus muscles were prepared by homogenizing muscles in CytoBuster Protein Extraction System and protease blocking cocktails III and VIII from Calbiochem. Protein was resolved by SDS-PAGE and transferred to nitrocellulose membranes (Calbiochem). The membranes were blocked overnight at 4°C with 5% nonfat milk in phosphate-buffered saline containing 0.1% Tween 20. The

membranes were probed with polyclonal anti-CAST (Calbiochem, La Jolla, CA). Horseradish peroxidase-conjugated secondary antibodies were obtained from Santa Cruz BioTechnology Inc. (Santa Cruz, CA) and reagents for enhanced chemiluminescence purchased from Thermo Scientific (Rockford, IL).

Calpastatin Inhibitory Activity Analysis

Total protein extracts from soleus muscles were prepared by homogenizing muscle in CytoBuster Protein Extraction System. To verify the inhibitory capacity of the increased calpastatin protein levels, muscle homogenates from *cp* and *wt* mice soleus muscles were analyzed with the InnoZyme Calpain 1 and 2 Activity Kit from Calbiochem (La Jolla, CA). This assay detects calpain activity by measuring the fluorescence produced upon cleavage of a calpain specific site on a fluorescent dye, (DABCYL)-TPLK|SPPPSR-(EDANS). Fluorescence was visualized using the FlexStation3 plate reader at the Center for Chemical Genomics in the Life Sciences Institute at University of Michigan.

Electron Microscopy

Soleus muscles from control mice and mice that were exposed to 14 days of HS were removed, pinned at a fixed taut length, and immediately placed in 0.1 M cacodylate-buffered Karnovsky's fixative solution (3% glutaraldehyde and 3% formaldehyde). After the tissues were fixed, each muscle was divided into three parts to allow both cross and longitudinal sections and fixed for 4 hours at 40 °C, pH 7.4. The muscles were then washed overnight in rinsing cacodylate buffer, post-fixed in a buffered solution of 1% osmium tetroxide, and dehydrated through a graded ethanol

series. Each section was propylene oxide embedded in epoxy resin and polymerized for 3 days at 450 °C and 1 day at 600 °C. Sections were cut on a Sorvall MT5000 ultramicrotome (DuPont, Newton, CT, USA) and stained with 1% Toluidine Blue for light microscopic evaluation, and ultra-thin sections were obtained by cutting the specimens with a diamond knife on the same ultramicrotome and post-staining in 1% uranyl acetate and lead citrate. These sections were examined with a Philips CM-10 transmission electron microscope (Philips Electronic Instruments Co., Mahwah, NJ, USA) operating at 60 kV. Micrographs were analyzed using ImageJ to quantify the width of the A-bands through measurements of the lengths of individual thick filaments. For control mice, twenty filaments were measured from two regions of muscles from two different animals, and for mice exposed to 14 days of HS, three regions of muscles from four different mice were analyzed for a total of 640 thick filaments measured.

Statistics

All data are presented as means \pm 1 S.E.M. unless indicated otherwise. The effects of genotype (*wt*, *cp*) and duration of unloading (none, 3, 9, 14 days) on muscle mass, P_o , specific P_o , peak force during passive stretches, force deficits following lengthening contractions, single fiber CSAs, and thick filament lengths were determined by two factor analysis of variance (ANOVA) with a level of significance at $P < 0.05$. Individual differences were determined by Bonferroni post hoc analyses.

Results

Phenotype of Calpastatin Over-Expressing Mice

Similar to the levels of calpastatin over-expression previously reported in pooled hind limb muscle by Polonsky's group (Otani *et al.* 2004) calpastatin levels were increased ~20 fold in soleus muscles of *cp* compared with *wt* mice (Fig. 2.1A). The ability of this level of calpastatin over-expression in the soleus muscles to inhibit calpain activity was demonstrated using the fluorometric calpain activity assay. The sensitivity of this assay was not sufficient to detect the endogenous calpain activities in the extremely small volume of homogenates obtained from individual soleus muscles. Thus, our approach was to assess the ability of endogenous calpastatin activity in the muscle homogenates to inhibit known concentrations of exogenous calpain (5 µg/ml). When exogenous calpain was added to *wt* muscle homogenates, cleavage of the fluorescent protein increased substantially (Fig 2.1B). In contrast, the *cp* muscle homogenates demonstrated no calpain activity above baseline even when 5 µg/ml exogenous calpain was added to the *cp* muscle homogenates (Fig 2.1B), indicating that the muscles of *cp* mice possessed substantial capacity for inhibiting calpain activity.

Despite the high levels of calpastatin in the muscles of *cp* mice, the body masses of the *cp* mice, 28.3 ± 0.6 grams, and *wt* littermates, 28.5 ± 0.4 grams, were not different, nor were the muscle masses for soleus or EDL muscles from control *cp* and *wt* mice (Fig. 2.1C). Consistent with the similarity of muscle masses between *cp* and *wt* mice, P_0 was not different for either soleus or EDL muscles of control *cp* and *wt* mice (data not shown). When normalized by total muscle fiber CSA, specific P_0 values for EDL muscles of *cp* and *wt* mice were also not different, but soleus muscles of *cp* mice

showed a small amount of weakness as reflected in a specific P_o that was just over 10% lower for muscles of *cp* compared with *wt* mice (Fig. 2.1D). Finally, with respect to the susceptibility to lengthening contraction-induced injury, maximally activated soleus and EDL muscles of both *cp* and *wt* mice suffered a deficit in isometric force of ~8% following two lengthening contractions of 30% strain, with no differences between muscles or groups of mice (Fig. 2.1E).

Response to Hind Limb Suspension.

Body Mass. All mice used in this study were weighed prior to HS and at the point when they were sacrificed. Although most mice lost a small amount of mass during the period of HS, some mice actually showed slight gains, with no difference between the *cp* and *wt* mice. Moreover, the loss in body mass was not progressive, that is, mice suspended for 14 days did not show a greater loss of mass than those suspended for 3 or 9 days. Overall, for the 40 mice that experienced any period of HS, the average change in weight was a loss of $4.2\% \pm 0.8\%$.

Soleus Muscle Atrophy. Compared with control muscles, 14 days of HS induced a decline in soleus muscle wet mass of 25% that was not different for *cp* and *wt* mice, although the decrease became statistically significant after only 3 days for muscles of *wt* mice, compared with 14 days for *cp* mice (Fig. 2.2). Similarly, analysis of the individual single fiber CSAs showed no overall effect of genotype on the CSA of either type 1 ($P = 0.65$) or type 2 ($P = 0.12$) fibers, either in control mice or following HS (Fig 2.3). Analysis of the effect of HS on CSA of type 1 fibers showed a trend ($P = 0.08$) for a decline by Day 9 and a significant decline ($P = 0.02$) of 30% by Day 14. In contrast, while the CSAs of type 2 fibers were trending downward for soleus muscles of both *cp* and *wt* mice, the

decrease in CSA compared with control muscles of ~12% after 14 days did not reach statistical significance ($P = 0.18$).

Soleus Muscle Isometric Contractile Properties. With the loss of soleus muscle mass and fiber CSA, a coincident loss in force was observed (Fig. 2.4). Whereas muscle mass showed only a trend for a further decrease beyond 3 days of HS for *wt* mice, the decrease in P_o for *wt* mice continued to progress out to Day 14, at which point P_o was 40% lower than the value for soleus muscles of control *wt* mice. Consistent with the progressive loss of force with HS by soleus muscles of *wt* mice, along with no further decrease in mass after Day 3, specific P_o declined throughout the entire duration of HS. Although the 6.5% decrease in specific P_o after 3 days of HS was not statistically significant, by 9 days, specific P_o was 28% lower than the value for muscles of control *wt* mice (Fig. 2.5). Specific P_o continued to decline such that, after 14 days of HS, the value was decreased by 35% compared with the control value. In contrast to the profound weakness induced by HS in soleus muscles of *wt* mice, the specific P_o for soleus muscles of *cp* mice exposed to HS showed no decrease compared with the value for soleus muscles of control *cp* mice even after 14 days of HS (Fig. 2.5).

Sarcomere Structure. The maintenance of isometric force generating capacity in the muscles of *cp* mice suggested there was preservation of the underlying myofibrillar structure in the *cp* mice. Therefore, sarcomere ultrastructure in muscles of *cp* and *wt* mice was examined by electron microscopy (Fig. 2.6). Control muscles from both *wt* and *cp* mice demonstrated a highly ordered array of well-aligned sarcomeres with great consistency of A-band widths (Figs. 2.6A, 2.6C). Following 14 days of HS, a clear loss of the sarcomeric organization within muscles of *wt* mice was observed (Fig. 2.6B). Also clear visually was an increased variability in the width of the A-bands. In contrast, in

muscles of *cp* mice exposed to 14 days of HS, the alignment of sarcomeres and the uniformity of the A-band widths were maintained to a much larger degree than in *wt* mice (Fig 2.6D). These observations were supported by quantitative analysis of individual thick filament lengths (Fig. 2.7). In control muscles, thick filament lengths were highly uniform and were not different for soleus muscles of *wt* and *cp* mice. Compared with the uniformity in the lengths of the thick filaments in sarcomeres of control muscles, HS resulted in a substantial increase in muscles of *wt* mice in the variability of the thick filament lengths (Fig. 2.7). Although neither the mean nor median thick filament lengths changed for muscles of *wt* mice following 14 days of HS, sarcomeres contained coexisting combinations of short and long thick filaments, resulting in a doubling of the standard deviation. In contrast, soleus muscles from the *cp* mice maintained roughly the same uniformity in thick filament lengths even after 14 days of HS (Fig. 2.7).

Passive Resistance to Stretch. The decreased uniformity of thick filament lengths following HS for *wt* mice was accompanied by a substantial decrease in the resistance to passive stretch, as reflected in the lower peak force during the stretch (Fig. 2.8). Moreover, in *cp* mice, peak passive force was unaffected by HS consistent with the maintenance in these muscles of a uniformity of thick filament lengths.

Susceptibility to Contraction Induced Injury. Two 30% lengthening contractions of maximally activated soleus muscles caused significant deficits in isometric force that worsened progressively after periods of HS. For *wt* mice, the amount of injury, as measured by the force deficit one minute after the second lengthening contraction, increased steadily to reach a level nearly 4-fold greater than that of control muscles by Day 14 (Fig. 2.9). Soleus muscles of *cp* mice also demonstrated a marked increase in susceptibility to injury after HS such that after 14 days the force deficit induced by

lengthening contractions for muscles of *cp* mice was not different from that induced in *wt* mice (Fig. 2.9).

EDL Muscle Mass and Contractile Properties. The effects of HS on EDL muscles were minimal. In *wt* mice, EDL muscle mass showed a transient decrease of 20% in *wt* mice at Day 3, but mass recovered by Day 9 and remained unchanged during the remainder of the period of HS (Fig 2.10). The small decrease in mass was not accompanied by a decrease in force generation, as neither P_o nor specific P_o was affected by HS. For EDL muscles of *cp* mice, both the mass and the contractile properties remained unchanged throughout the 14 days of HS (Fig 2.10).

Discussion

Progressive skeletal muscle atrophy and weakness are among the primary effects of skeletal muscle unloading, immobilization, and spaceflight (Gardetto *et al.* 1989; Tischler *et al.* 1993; Riley *et al.* 1995; Widrick *et al.* 1999). Previous work showed that inhibition of the protease calpain, through over-expression of calpastatin in a transgenic mouse model, reduced the amount of muscle fiber atrophy in response to 10 days of HS (Tidball & Spencer 2002), but the impact of calpain inhibition on skeletal muscle function has not previously been addressed. The major finding of the present study was that in contrast to the progressive decrease with HS in maximum isometric specific force exhibited by soleus muscles of *wt* mice, the development of muscle weakness was completely prevented during 14 days of HS when calpain was inhibited by increased *in vivo* expression of calpastatin. The protection of the muscles of *cp* mice from developing weakness with unloading is consistent with our hypothesis that the decreased specific force observed following the removal of weight bearing is due to the

disruption by the calpain system of the underlying sarcomere structure. Further support for this hypothesis was provided by a second key finding in the present study that the maintenance of specific P_o in *cp* mice during HS was accompanied by a striking preservation of sarcomere ultrastructure compared with the disorganization in sarcomere structure observed after 14 days of HS in *wt* mice. Our observation that calpain inhibition in our transgenic model did not prevent atrophy after 14 days of unloading likely reflects the longer time period of unloading in our study compared to the study of Tidball and Spencer (Tidball & Spencer 2002) who studied mice exposed to 10 days of HS. We similarly showed no significant loss of soleus muscle mass at 9 days in *cp* mice as well as a 13% further loss of mass between 9 and 14 days.

Mice deficient in either of two muscle-specific ubiquitin ligases, Muscle RING Finger 1 (MuRF1) or Muscle Atrophy F-box (MAFbx, also known as atrogin-1), have also displayed an attenuation of muscle atrophy leading to the conclusion that the ubiquitin-proteasome system is required for muscle atrophy in response to disuse (Bodine *et al.* 2001a), although those experiments employed denervation rather than HS to trigger atrophy in the muscles. The proteasome has been shown to degrade purified actin and myosin, but specific interactions between myofibrillar proteins appear to protect intact myofibrils from ubiquitin-dependent degradation, with the rate-limiting step in the degradation of myofibrillar proteins proposed to be their dissociation from the myofibril (Solomon & Goldberg 1996). One hypothesis is that cleavage of sarcomeric proteins by calpain may be necessary to provide substrate for the ubiquitin-proteasome system (Kandarian & Stevenson 2002). An important role of calpain in cytoskeletal remodeling during the early phase of the muscle response to alterations in loading is supported by several investigations (Enns & Belcastro 2006; Vermaelen *et al.* 2007), and the

preservation in the present study of sarcomere structure and specific P_o under circumstances when calpain was inhibited during unloading provides strong support for the conclusion that calpain targets the force generating infrastructure during disuse. Despite substantial support for the coordinated action of calpain and the ubiquitin-proteasome system to mediate muscle atrophy in response to unloading, the present finding that inhibition of calpain during 14 days of HS did not prevent atrophy coupled with the findings that following 14 days of denervation, muscle mass decreased 30% and 20% in mice deficient in MuRF1 or MAFbx, respectively (Bodine *et al.* 2001b), suggests that the inhibition or even prevention of protein degradation may be insufficient to protect muscle completely from a loss in mass during unloading. Alternate or additional approaches targeting the enhancement of protein synthesis and muscle growth (Bodine *et al.* 2001c) rather than the inhibition of protein degradation may be necessary to fully counteract the atrophy associated with disuse.

One known calpain substrate and hypothesized *in vivo* target of calpain is the giant sarcomeric protein titin (Goto *et al.* 2003; Lim *et al.* 2004; Raynaud *et al.* 2005; Udaka *et al.* 2008; Goll *et al.* 2008). Titin contains high-affinity calpain binding sites where the protein is cleaved (Raynaud *et al.* 2005). Titin is well recognized as the main determinant within muscle fibers of passive tension (Horowitz *et al.* 1986; Funatsu *et al.* 1990) and may serve as a regulator of thick filament length during sarcomere assembly (Whiting *et al.* 1989; Trinick 1994). Recently, Udaka and colleagues (Udaka *et al.* 2008) reported that muscle disuse, achieved through immobilization of a limb by casting, induced changes within sarcomeres that were correlated with the proteolytic cleavage of titin. Among the responses to immobilization that were associated with a preferential loss of titin were decreased mean thick filament length, decreased uniformity of thick

filament length, decreased maximum isometric specific force, and decreased passive force (Udaka *et al.* 2008). We show here strong evidence that the changes in passive force and increased variability of thick filament length can be prevented in muscles where calpain activity is inhibited providing *in vivo* evidence for the role of calpain mediated protein cleavage in these functional changes that occur during HS. Furthermore, the maintenance of passive tension and the preservation of the uniformity in thick filaments lengths for muscles of *cp* mice, in combination with the results by Udaka and colleagues, are consistent with the hypothesis that calpain targets titin and the inhibition of calpain may protect against loss in titin function, at least to some extent. An additional calpain substrate that may be targeted during HS is the intermediate filament protein desmin (Enns *et al.* 2007). Desmin functions to maintain sarcomeres within adjacent myofibrils in register, and deficiency of desmin results in muscle weakness (Sam *et al.* 2000). Our electron micrographs showed a loss following HS of the alignment of sarcomeres in the muscles of *wt* mice along with the substantial reduction in specific P_o . The observation that, in *cp* mice, specific P_o was unaffected by HS and sarcomere alignment was maintained is consistent with the hypothesis that additional proteins responsibility for sarcomere integrity, such as desmin, may also be spared by the inhibition of calpain. Collectively, these findings provide evidence for a model in which muscle unloading increases *in vivo* calpain mediated cleavage sarcomere proteins, possibly titin and desmin, leading to alterations within the sarcomere that decrease force generating capacity.

A surprising observation in the present study was that, although muscles of *cp* mice maintained specific force during HS, the muscles of *cp* mice were not protected to any great extent from the increased susceptibility to lengthening contraction-induced

injury observed during HS. In many disease states such as muscular dystrophy and aging, the increased susceptibility to contraction induced injury is tightly associated with muscle weakness (Brooks & Faulkner 1996; Consolino & Brooks 2004). Our results showed that the preservation of sarcomeric structure and force production afforded by the inhibition of calpain was not accompanied by maintenance of the ability to withstand the additional stress associated with lengthening contractions. These data support the conclusion that the increased susceptibility to contraction-induced injury and muscle weakness induced by HS are likely occurring through distinct cellular mechanisms and the effect of HS to increase contraction-induced injury is not mediated by calpain-dependent proteolytic activity.

Our data substantiate the common finding that the EDL muscle, which is comprised primarily of type 2 fibers, is minimally affected by unloading (Darr & Schultz 1989; Thompson & Shoeman 1998; Fitts *et al.* 2001). Although it is generally accepted that fast muscles are less sensitive to disuse-induced atrophy than slow muscles (Baldwin & Haddad 2002), the mechanisms underlying these differences between fast and slow muscles remain an area of active investigation. Fast muscles may be less susceptible than slow muscles to HS due to differential activation of downstream cellular responses to HS in type 1 and type 2 fibers. Previous work demonstrated that slow soleus muscles exhibited increased calpain activation during atrophy within 12 hours of HS, whereas a significant increase in calpain activity was not observed in fast gastrocnemius muscles until the muscles had been unloaded for more than 3 days (Enns & Belcastro 2006). Moreover, 5 days of hindlimb immobilization resulted in increased levels of both autolyzed calpain 1 and autolyzed calpain 2 in soleus muscles but no change in either calpain 1 or 2 in fast plantaris muscles (Vermaelen *et al.* 2007).

Thus, the sensitivity of type 1 fibers to disuse atrophy may be related to fiber-type specificity of the activation pattern of calpain following HS. Finally, the lack of atrophy of EDL muscles during HS may be a consequence of the small amount of loading of the muscles provided by flexing the ankle and lifting the hind paws against gravity, rather than a complete insensitivity of type 2 fibers to disuse atrophy. Regardless of the precise mechanisms for the different response of slow and fast muscles, our studies demonstrate that if activation of calpain is inhibited in slow muscle, many of the effects of HS on muscle contractile function and sarcomeric structure can be prevented.

In summary, this study provides clear evidence that inhibition of the calpain system during HS preserves sarcomere structure and prevents the development of muscle weakness in soleus muscles. These findings support our working hypothesis that the decreased specific force observed following the removal of weight bearing is due to the disruption of the underlying sarcomere structure by calpains. Protection from sarcomeric disruption by the inhibition of calpain, perhaps through the inhibition of cleavage of sarcomeric proteins such as titin, is also supported by our observation of the maintenance of passive tension and uniformity of thick filament lengths in soleus muscles of *cp* mice exposed to 14 days of HS. Finally, our findings that the loss of soleus muscle mass associated with unloading was not prevented in the *cp* mice and that the risk for disruption of the myofibrillar structure when challenged with lengthening contractions was substantially elevated by unloading in *cp* mice suggest that inhibition of the calpain system is not sufficient to completely protect muscles from the structural and functional deficits associated with disuse. Thus, calpain inhibition may be an important and effective target for preventing muscle weakness during disuse, by minimizing proteolytic damage to the force generating apparatus, especially in combination with

additional pharmacological or physical therapies aimed at preventing muscle atrophy and injury.

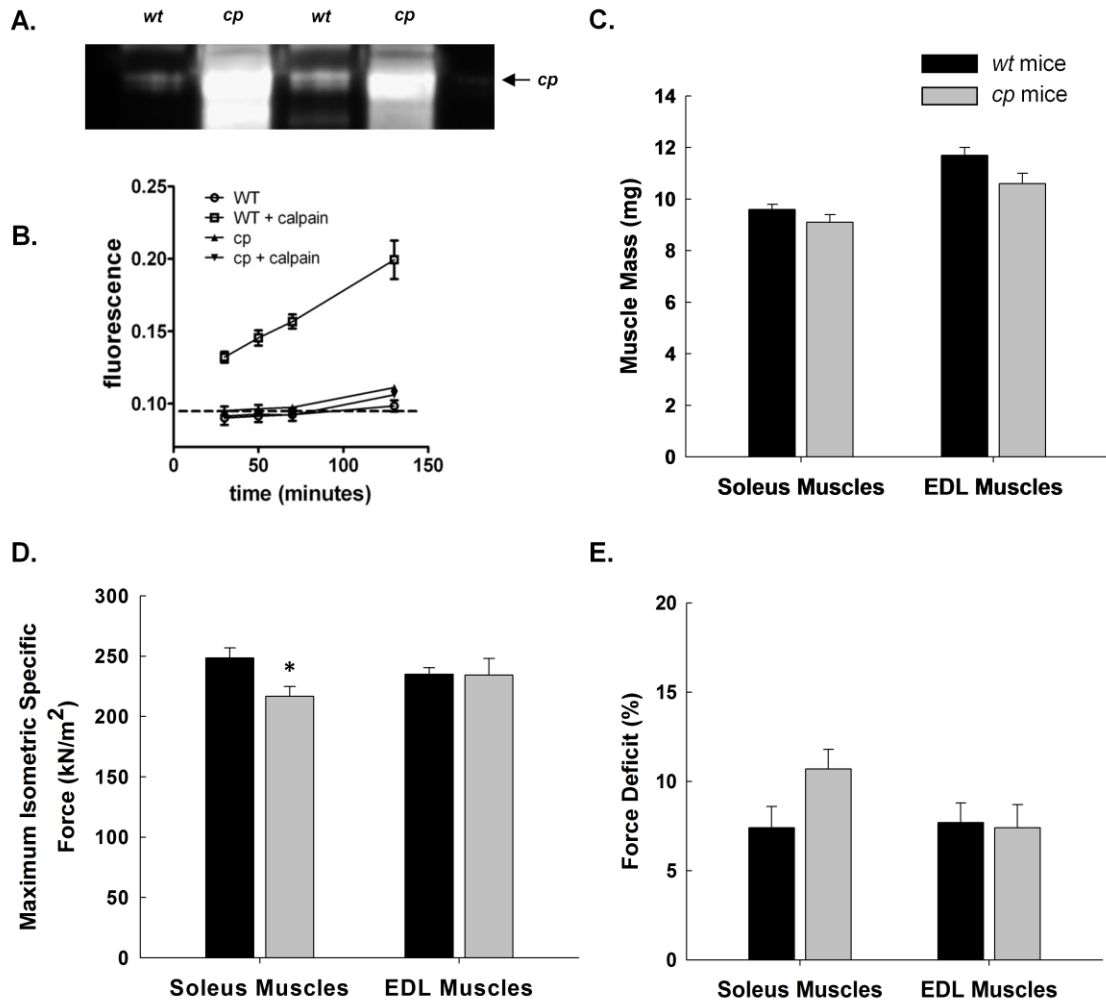


Figure 2.1. Characterization of *cp* mice. Data are shown for **A.** confirmation by Western blot of over-expression of human calpastatin in soleus muscles of *cp* but not *wt* mice, **B.** Calpain activity measurements in muscle lysates from *wt* (open symbols) and *cp* (filled symbols) mice, **C.** muscle mass expressed in milligrams, **D.** maximum isometric specific force expressed in kilonewtons per square meter, and **E.** the deficit in isometric force measured one minute following two lengthening contractions expressed as the percent decline relative to the initial force. In panel B, the dashed line represents the background level of fluorescence. Marked activity was detected only in *wt* lysates (squares) in the presence of exogenously added calpain (5 μ g/mL), and this calpain activity was completely inhibited in lysates from *cp* mice (inverted triangles). Data are means \pm SEM, $n=3$. All values for *wt* lysates with exogenous calpain were significantly ($p<0.05$) above baseline as well as above the values for all other groups. Values for *cp* lysates were not different from baseline at any point. In panels C-E, bars represent means \pm 1 S.E.M. for soleus and extensor digitorum longus (EDL) muscles of *wt* (black bars) and *cp* (gray bars) mice and the asterisk (*) indicates significant ($p<0.05$) difference between the value of *cp* and *wt* mice.

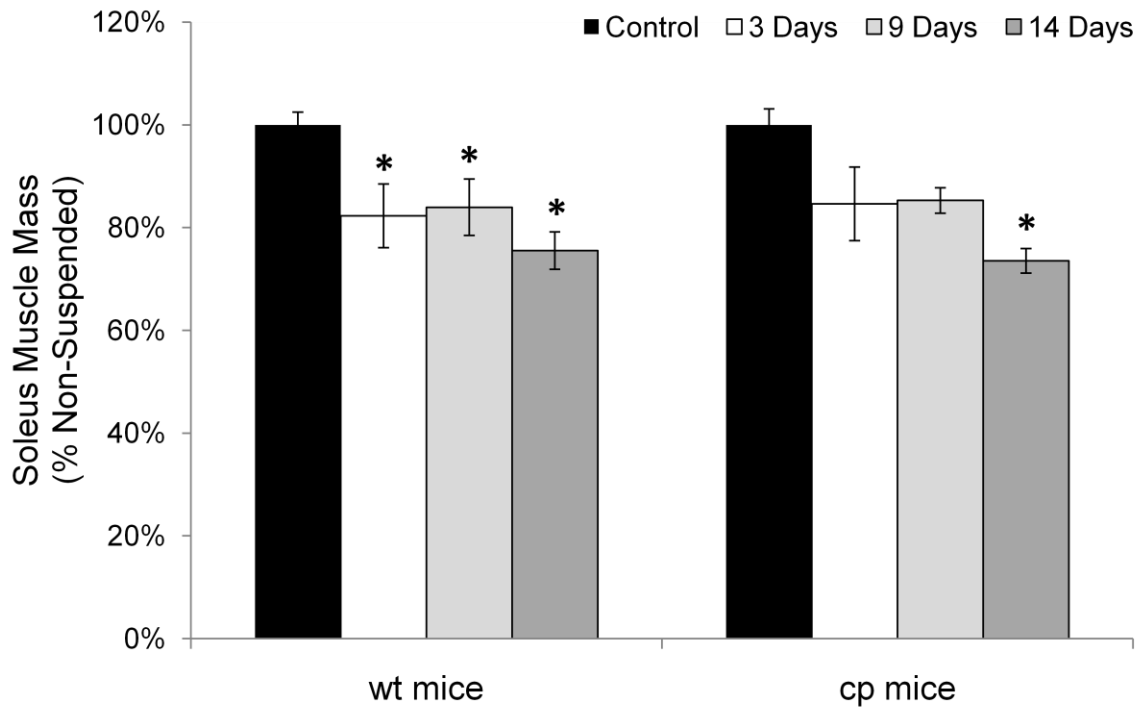
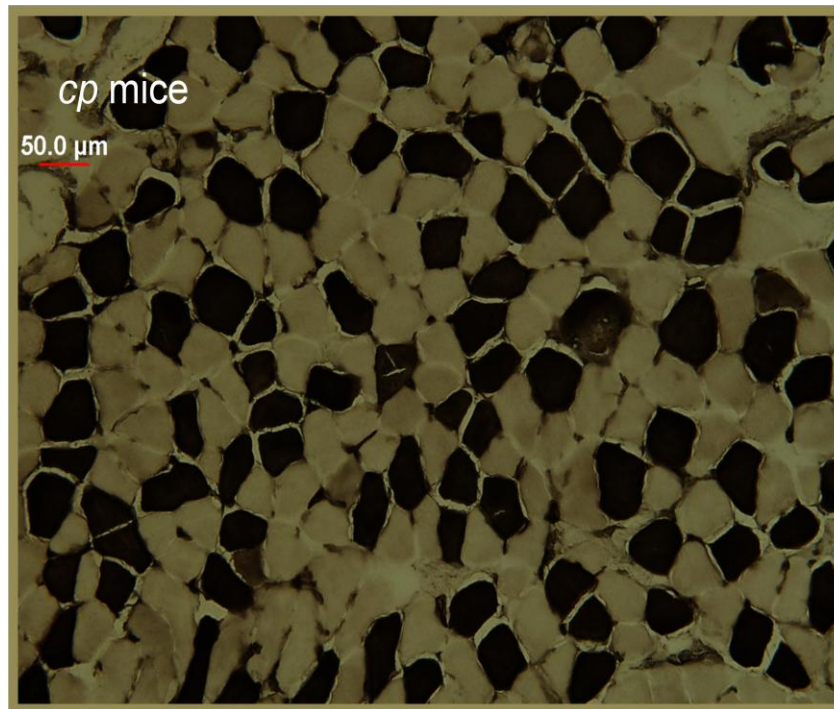
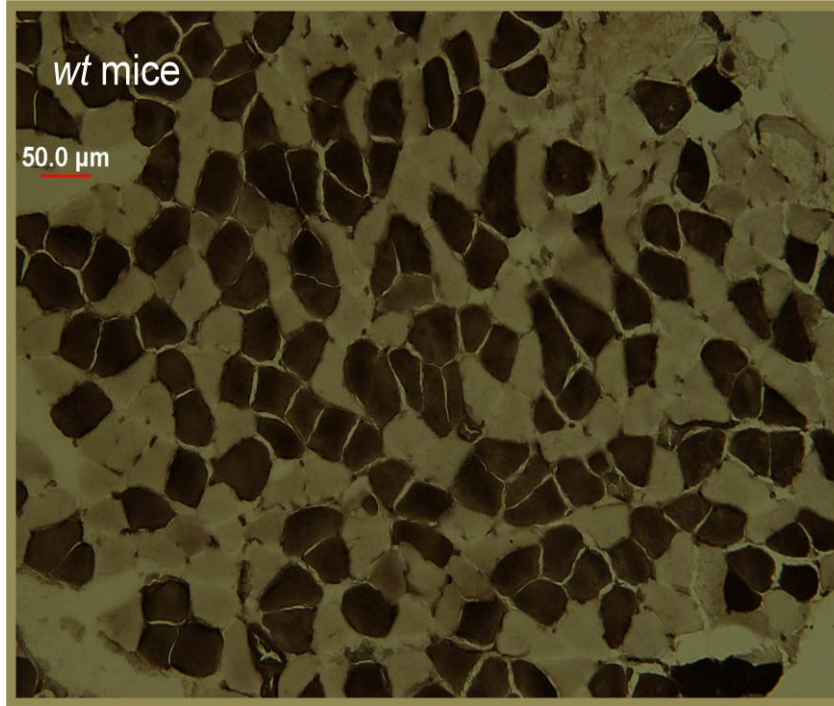


Figure 2.2. Soleus muscle mass for wt and cp mice following hindlimb suspension. Data are shown for masses of soleus muscles of transgenic calpastatin over-expressing mice (cp mice) on the right and wild type littermates (wt mice) on the left that were either non-suspended (Control, black bars) or exposed to 3 (white bars), 9 (light gray bars), or 14 (dark gray bars) days of hindlimb suspension. Data are expressed as a percentage of the value for muscles of the controls. Bars represent means \pm 1 s.e.m. The asterisks (*) indicate significant ($p < 0.05$) differences from the respective values for control mice.



A.

Figure 2.3 A. Representative cross sections for soleus muscles of control non-suspended wt and cp mice. Sections were assayed for myosin ATPase activity such that the type 1 fibers stain dark and the type 2 fibers stain light.

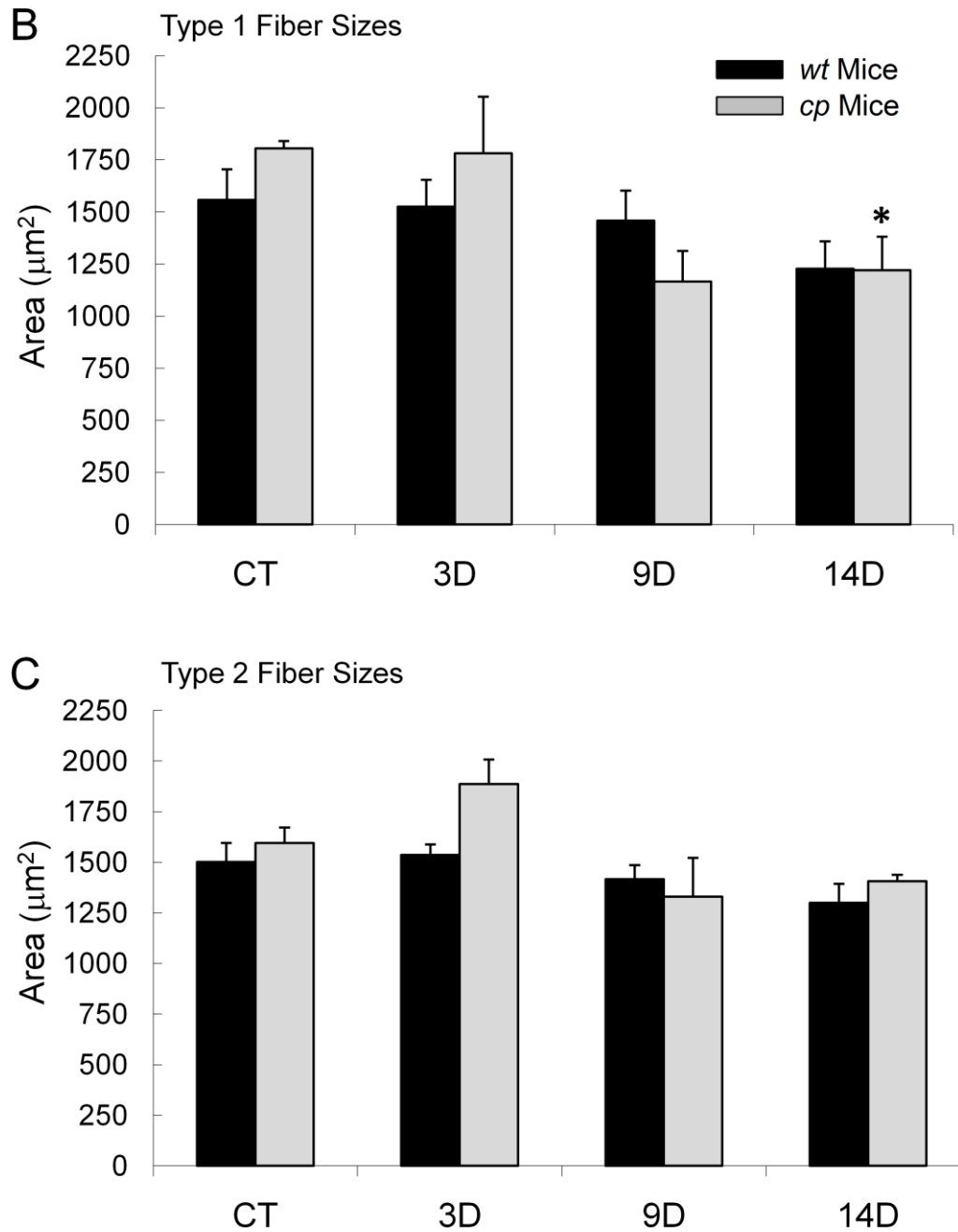


Figure 2.3 B and C. Individual fiber cross-sectional areas (CSAs) for soleus muscles following hindlimb suspension. Data are shown for the average fibers CSAs expressed in μm^2 for **B.** type 1 fibers and **C.** type 2 fibers in soleus muscles of wild type (*wt* Mice, black bars) and calpastatin over-expressing mice (*cp* Mice, gray bars) that were either non-suspended (CT) or were exposed to 3 (3D), 9 (9D), or 14 (14D) days of hindlimb suspension. Bars represent means \pm 1 s.e.m. The asterisk (*) indicate significant ($p < 0.05$) differences from the respective values for non-suspended control mice.

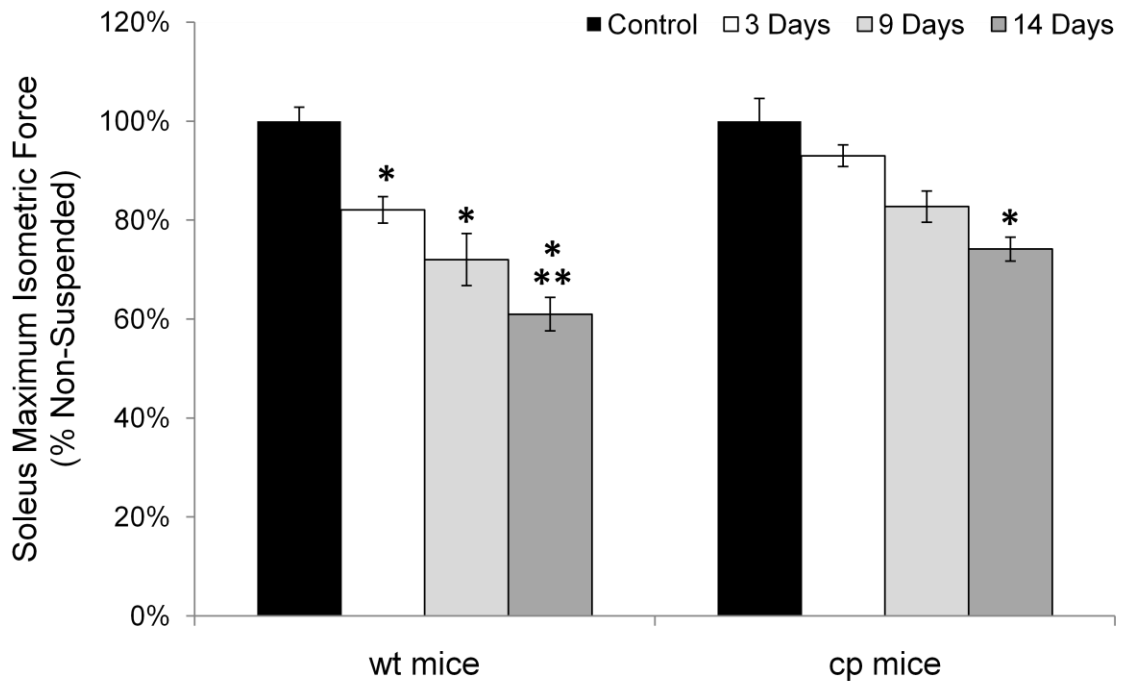


Figure 2.4. Soleus muscle maximum isometric forces for wt and cp mice following hindlimb suspension. Data are shown for maximum isometric tetanic forces (P_0) of soleus muscles of transgenic calpastatin over-expressing mice (cp mice) on the right and wild type littermates (wt mice) on the left that were either non-suspended (Control, black bars) or exposed to 3 (white bars), 9 (light gray bars), or 14 (dark gray bars) days of hindlimb suspension. Data are expressed as a percentage of the value for muscles of the controls. Bars represent means \pm 1 s.e.m. The asterisks (*) indicate significant ($p < 0.05$) differences from the respective values for control mice. Double asterisks (**) indicate significant ($p < 0.05$) differences from the 3 Day value for mice of the same genotype.

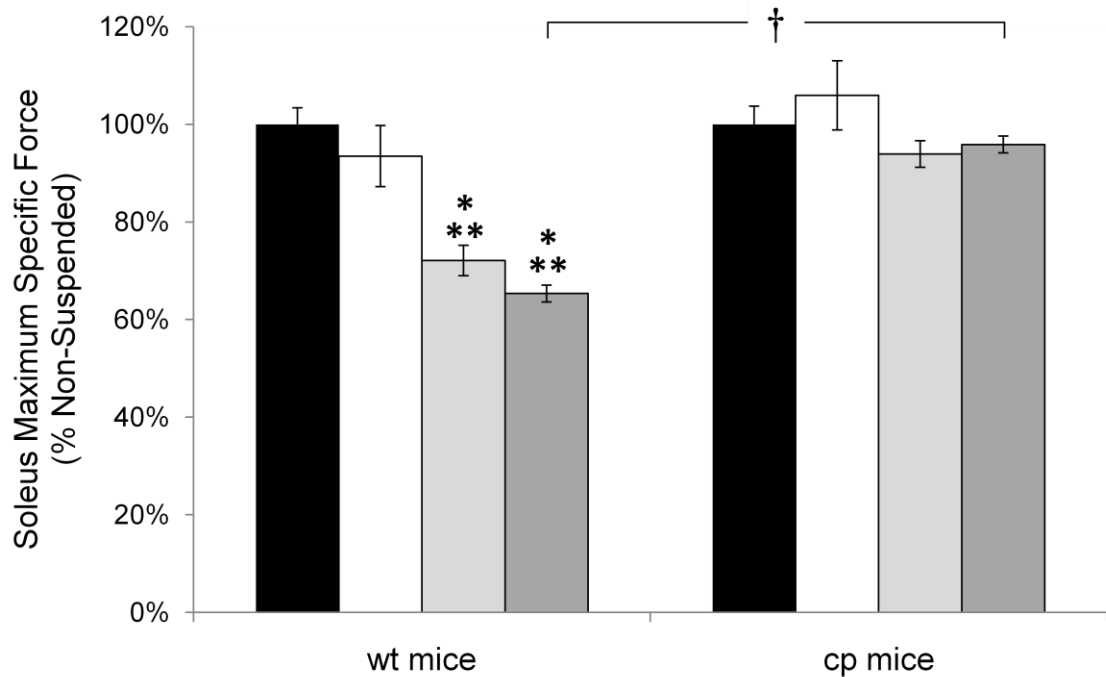


Figure 2.5. Soleus muscle maximum isometric specific forces for wt and cp mice following hind limb suspension. Data are shown for maximum isometric specific force (specific P_0) of soleus muscles of transgenic calpastatin over-expressing mice (cp mice) on the right and wild type littermates (wt mice) on the left that were either non-suspended (Control, black bars) or exposed to 3 (white bars), 9 (light gray bars), or 14 (dark gray bars) days of hindlimb suspension. Data are expressed as a percentage of the value for muscles of the controls. Bars represent means \pm 1 s.e.m. The asterisks (*) indicate significant ($p < 0.05$) differences from the respective values for control mice. Double asterisks (**) indicate significant ($p < 0.05$) differences from the 3 Day value for mice of the same genotype and the dagger (†) indicates a significant ($p < 0.05$) difference between cp and wt mice for the same period of hindlimb suspension.

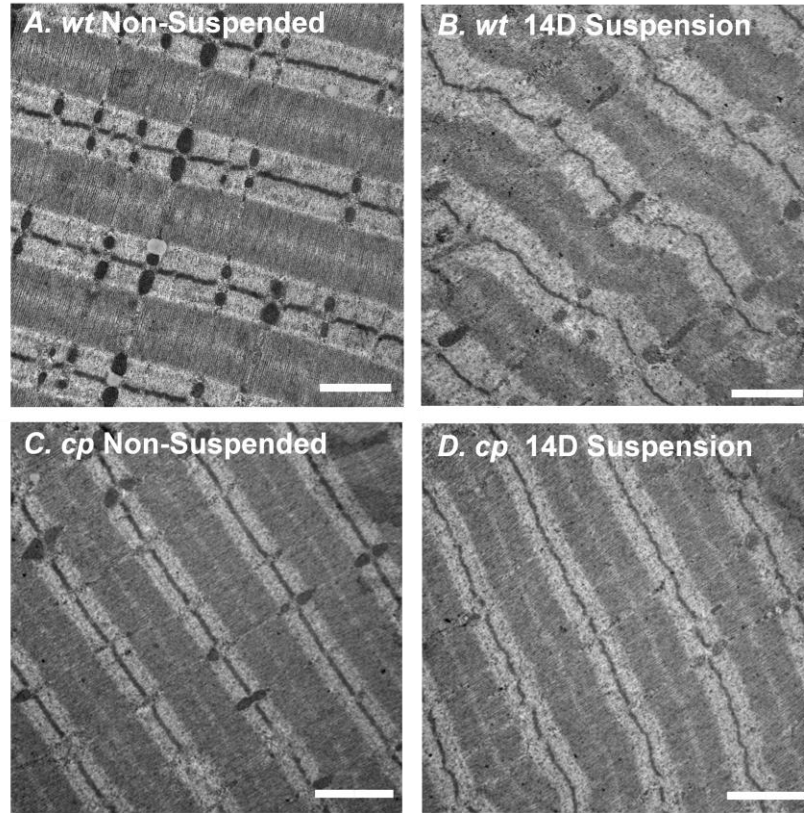


Figure 2.6. Sarcomere structure for soleus muscles of non-suspended *wt* and *cp* mice and mice exposed to 14 days of hindlimb suspension. Representative electron micrographs (EM) from soleus muscles of *wt* (A., B.) and *cp* (C., D.) mice that were either not suspended (A., C.) or exposed to 14 days of hindlimb suspension (B., D.). Scale bars = 1 μ m.

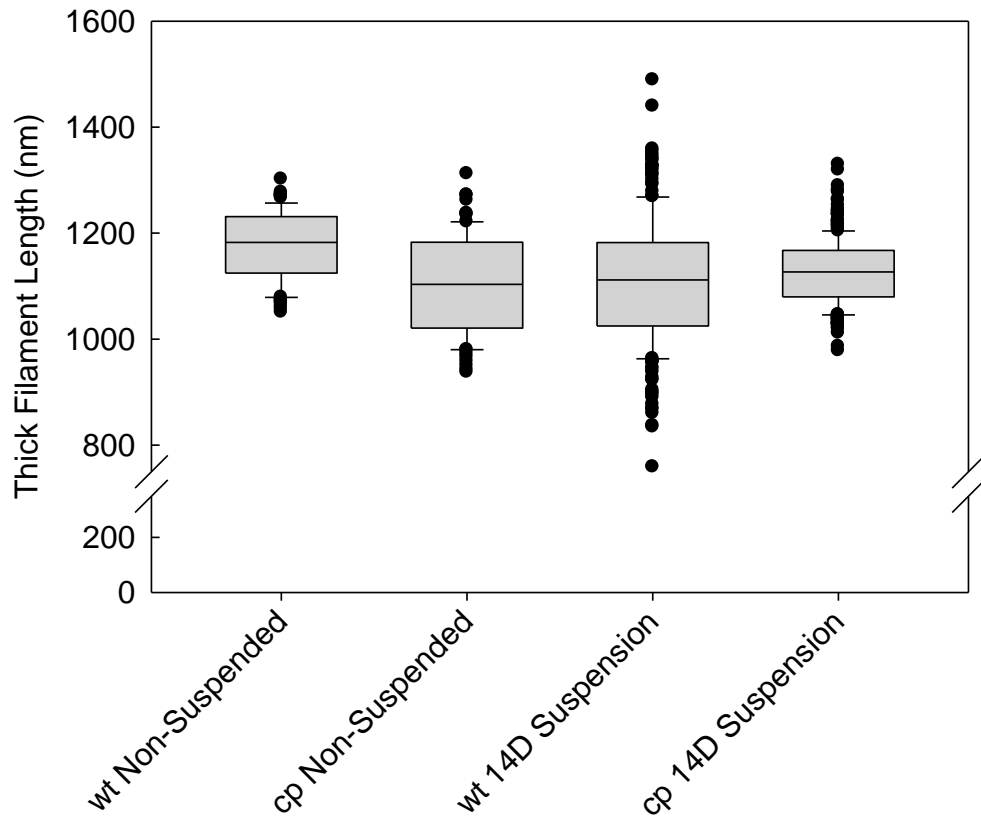


Figure 2.7. Thick filament lengths for soleus muscles of non-suspended wt and cp mice and mice exposed to 14 days of hindlimb suspension. Thick filament lengths measured from muscle EMs are shown in a box plot representation. The line within the boxes indicates the median, while the top and bottom edges of the box indicate 75th and 25th percentiles, respectively. The brackets above and below the boxes indicate 90th and 10th percentiles, respectively and the additional symbols are values that fall outside the 10th to 90th %ile range. Neither means nor medians were different among the groups, but note increased variability in thick filament lengths for muscle sof wt mice after hindlimb suspension.

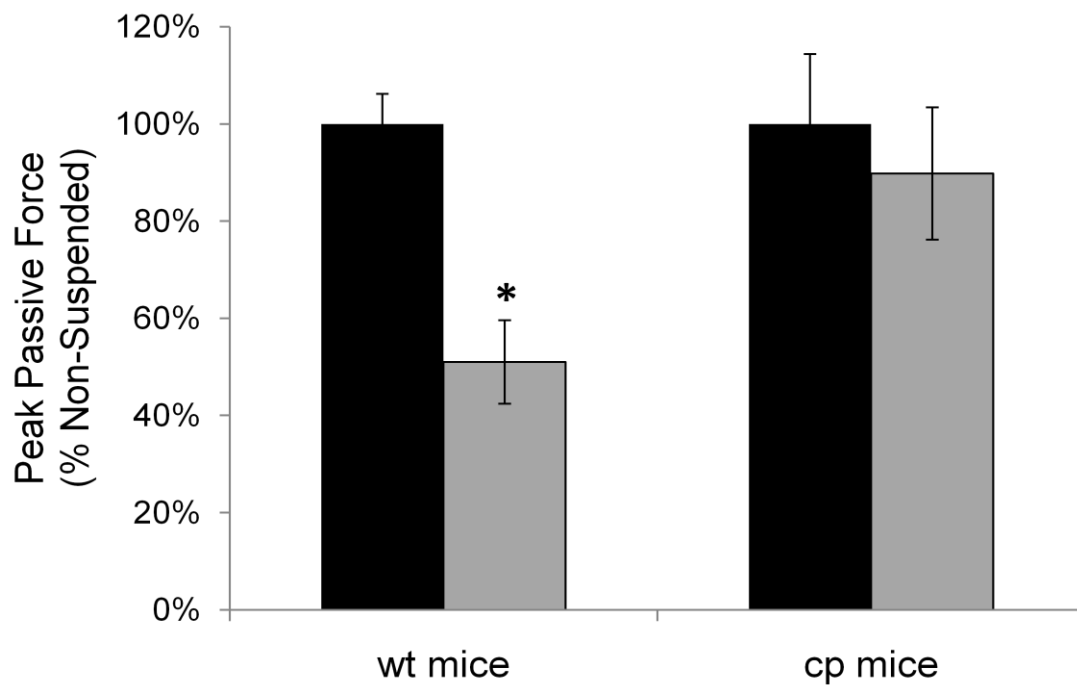


Figure 2.8. Changes in passive resistance to stretch for soleus muscles of wt and cp mice following hindlimb suspension. Data are shown for the peak force during a passive stretch for soleus muscles of transgenic calpastatin over-expressing mice (cp mice) on the right and wild type littermates (wt mice) on the left that were either non-suspended (Control, black bars) or exposed to 14 days of HS (gray bars). Data are expressed as a percentage of the value for muscles of the control mice. Bars represent means \pm 1 s.e.m. The asterisk (*) indicates significant ($p < 0.05$) difference from the control value.

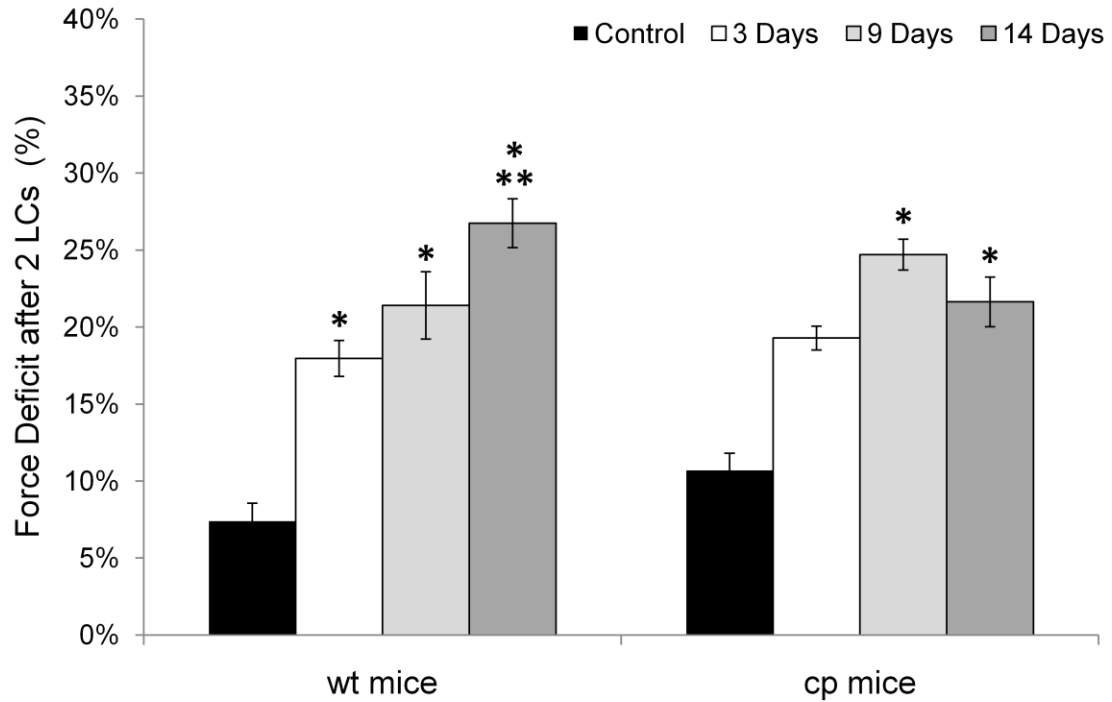


Figure 2.9. Force deficits following lengthening contractions of soleus muscles of wt and cp mice following hindlimb suspension. Data are shown for the deficit in isometric force induced following two lengthening contractions of maximally activated soleus muscles of transgenic calpastatin over-expressing mice (cp mice) on the right and wild type littermates (wt mice) on the left that were either non-suspended (Control, black bars) or exposed to 3 (white bars), 9 (light gray bars), or 14 (dark gray bars) days of hindlimb suspension. Data are expressed as the difference between the initial isometric force and the force immediately following the stretches expressed as a percentage of the initial force for each group. Bars represent means \pm 1 s.e.m. The asterisk (*) indicates a significant ($p < 0.05$) differences from the value for control mice and double asterisks (**) indicate a significant ($p < 0.05$) difference from the 3 Day value for mice of the same genotype.

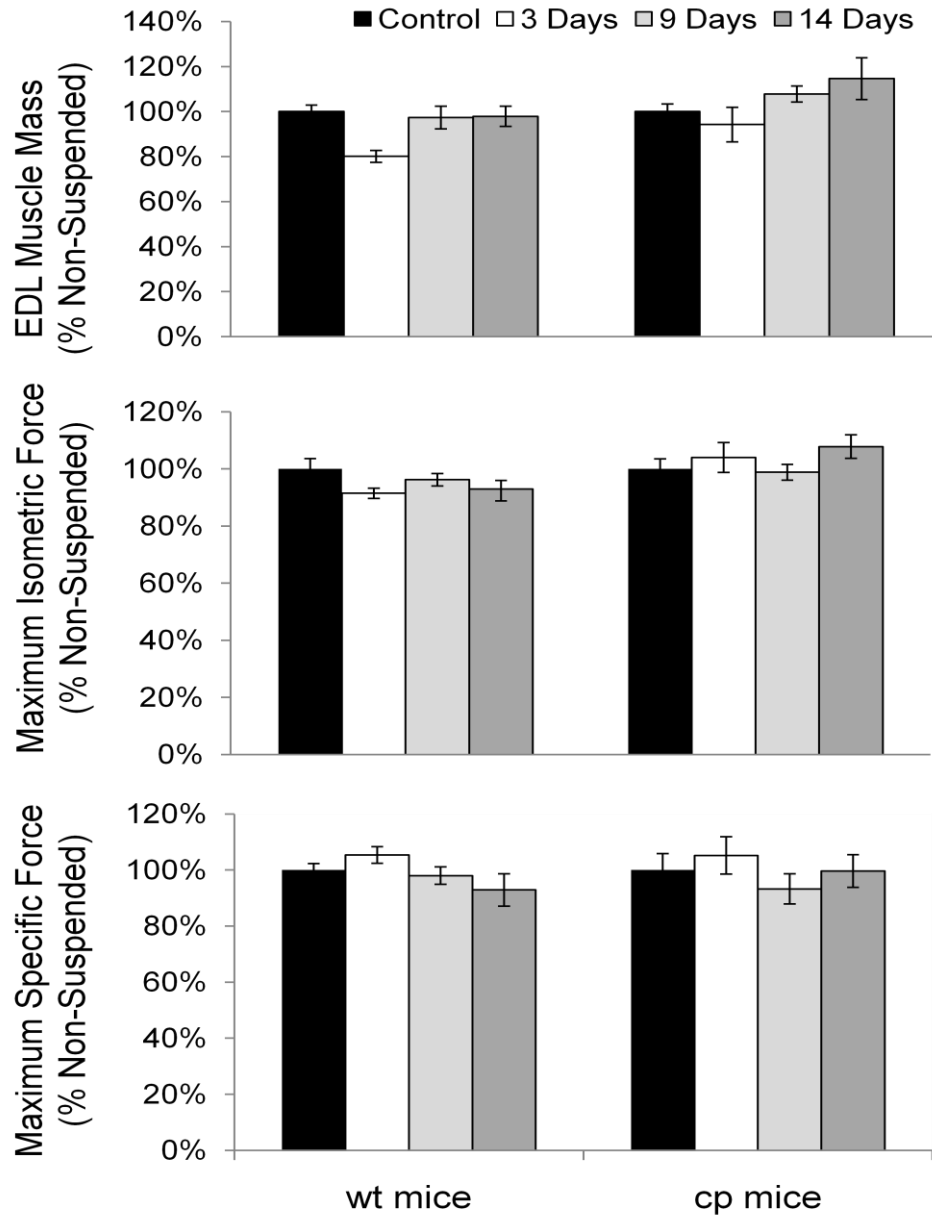


Figure 2.10. Masses, maximum isometric forces, and maximum specific forces for EDL muscle of wt and cp mice following HS. Data are shown for **A.** muscle mass, **B.** maximum isometric tetanic force (P_o), and **C.** specific P_o for EDL muscles of transgenic calpastatin over-expressing mice (cp mice) on the right and wild type littermates (wt mice) on the left that were either not exposed to hindlimb suspension (control, black bars) or were exposed to 3 (white bars), 9 (light gray bars), or 14 (dark gray bars) days of hindlimb suspension. Data are expressed as a percentage of the value for muscles of the non-suspended controls. Bars represent means \pm 1 s.e.m. The asterisks (*) indicate significant ($p < 0.05$) differences from the respective values for non-suspended mice.

References

1. Arthur, G. D., T. S. Booker and A. N. Belcastro. 1999. Exercise promotes a subcellular redistribution of calcium-stimulated protease activity in striated muscle. *Can. J. Physiol. Pharmacol.*, 77: 42-47.
2. Baldwin, K. M. and F. Haddad. 2002. Skeletal muscle plasticity: cellular and molecular responses to altered physical activity paradigms. *Am. J. Phys. Med. Rehabil.*, 81: S40-S51.
3. Bodine, S. C., E. Latres, S. Baumhueter, V. K. Lai, L. Nunez, B. A. Clarke, W. T. Poueymirou, F. J. Panaro, E. Na, K. Dharmarajan, Z. Q. Pan, D. M. Valenzuela, T. M. DeChiara, T. N. Stitt, G. D. Yancopoulos and D. J. Glass. 2001b. Identification of ubiquitin ligases required for skeletal muscle atrophy. *Science*, 294: 1704-1708.
4. Bodine, S. C., E. Latres, S. Baumhueter, V. K. Lai, L. Nunez, B. A. Clarke, W. T. Poueymirou, F. J. Panaro, E. Na, K. Dharmarajan, Z. Q. Pan, D. M. Valenzuela, T. M. DeChiara, T. N. Stitt, G. D. Yancopoulos and D. J. Glass. 2001a. Identification of ubiquitin ligases required for skeletal muscle atrophy. *Science*, 294: 1704-1708.
5. Bodine, S. C., T. N. Stitt, M. Gonzalez, W. O. Kline, G. L. Stover, R. Bauerlein, E. Zlotchenko, A. Scrimgeour, J. C. Lawrence, D. J. Glass and G. D. Yancopoulos. 2001c. Akt/mTOR pathway is a crucial regulator of skeletal muscle hypertrophy and can prevent muscle atrophy in vivo. *Nat. Cell Biol.*, 3: 1014-1019.
6. Brooke, M. H. and K. K. Kaiser. 1970. Muscle fiber types: how many and what kind? *Arch. Neur.*, 23: 369-379.

7. Brooks, S. V. and J. A. Faulkner. 1988. Contractile properties of skeletal muscles from young, adult and aged mice. *J. Physiol.*, 404: 71-82.
8. Brooks, S. V. and J. A. Faulkner. 1996. The magnitude of the initial injury induced by stretches of maximally activated muscle fibres of mice and rats increases in old age. *J. Physiol.*, 497: 573-580.
9. Consolino, C. M. and S. V. Brooks. 2004. Susceptibility to sarcomere injury induced by single stretches of maximally activated muscles of mdx mice. *J. Appl. Physiol.*, 96: 633-638.
10. Croall, D. E. and G. N. DeMartino. 1991. Calcium-activated neutral protease (calpain) system: structure, function, and regulation. *Physiol. Rev.*, 71: 813-847.
11. Darr, K. C. and E. Schultz. 1989. Hindlimb suspension suppresses muscle growth and satellite cell proliferation. *J. Appl. Physiol.*, 67: 1827-1834.
12. Enns, D. L. and A. N. Belcastro. 2006. Early activation and redistribution of calpain activity in skeletal muscle during hindlimb unweighting and reweighting. *Can. J. Physiol. Pharmacol.*, 84: 601-609.
13. Enns, D. L., T. Raastad, I. Ugelstad and A. N. Belcastro. 2007. Calpain/calpastatin activities and substrate depletion patterns during hindlimb unweighting and reweighting in skeletal muscle. *Eur. J. Appl. Physiol.*, 100: 445-455.
14. Fitts, R. H., D. R. Riley and J. J. Widrick. 2001. Functional and structural adaptations of skeletal muscle to microgravity. *J. Exp. Biol.*, 204: 3201-3208.
15. Funatsu, T., H. Higuchi and S. Ishiwata. 1990. Elastic filaments in skeletal muscle revealed by selective removal of thin filaments with plasma gelsolin. *J. Cell Biol.*, 110: 53-62.

16. Gardetto, P. R., J. M. Schluter and R. H. Fitts. 1989. Contractile function of single muscle fibers after hindlimb suspension. *J. Appl. Physiol.*, 66: 2739-2749.
17. Goll, D. E., G. Neti, S. W. Mares and V. F. Thompson. 2008. Myofibrillar protein turnover: the proteasome and the calpains. *J. Anim. Sci.*, 86: E19-E35.
18. Goto, K., R. Okuyama, M. Honda, H. Uchida, T. Akema, Y. Ohira and T. Yoshioka. 2003. Profiles of connectin (titin) in atrophied soleus muscle induced by unloading of rats. *J. Appl. Physiol.*, 94: 897-902.
19. Haddad, F., G. R. Adams, P. W. Bodell and K. M. Baldwin. 2006. Isometric resistance exercise fails to counteract skeletal muscle atrophy processes during the initial stages of unloading. *J. Appl. Physiol.*, 100: 433-441.
20. Haddad, F., R. R. Roy, H. Zhong, V. R. Edgerton and K. M. Baldwin. 2003. Atrophy responses to muscle inactivity. II. Molecular markers of protein deficits. *J. Appl. Physiol.*, 95: 791-802.
21. Horowitz, R., E. S. Kempner, M. E. Bisher and R. J. Podolsky. 1986. A physiological role for titin and nebulin in skeletal muscle. *Nature*, 323: 160-164.
22. Ikemoto, M., T. Nikawa, S. Takeda, C. Watanabe, T. Kitano, K. M. Baldwin, R. Izumi, I. Nonaka, T. Towatari, S. Teshima, K. Rokutan and K. Kishi. 2001. Space shuttle flight (STS-90) enhances degradation of rat myosin heavy chain in association with activation of ubiquitin-proteasome pathway. *FASEB J.*, 15: 1279-1281.
23. Kandarian, S. C. and E. J. Stevenson. 2002. Molecular events in skeletal muscle during disuse atrophy. *Exerc. Sport Sci. Rev.*, 30: 111-116.

24. Lim, C. C., C. Zuppinger, X. Guo, G. M. Kuster, M. Helmes, H. M. Eppenberger, T. M. Suter, R. Liao and D. B. Sawyer. 2004. Anthracyclines induce calpain-dependent titin proteolysis and necrosis in cardiomyocytes. *J. Biol. Chem.*, 279: 8290-8299.
25. Morey, E. R. 1979. Spaceflight and bone turnover: correlation with a new rat model of weightlessness. *BioScience*, 29: 168-172.
26. Otani, K., D. H. Han, E. L. Ford, P. M. Garcia-Roves, H. Ye, Y. Horikawa, G. I. Bell, J. O. Holloszy and K. S. Polonsky. 2004. Calpain system regulates muscle mass and glucose transporter GLUT4 turnover. *J. Biol. Chem.*, 279: 20915-20920.
27. Price, S. R. and W. E. Mitch. 1998. Mechanisms stimulating protein degradation to cause muscle atrophy. *Curr. Opin. Clin. Nutr. Metab. Care*, 1: 79-83.
28. Raynaud, F., E. Fernandez, G. Coulis, L. Aubry, X. Vignon, N. Bleimling, M. Gautel, Y. Benyamin and A. Ouali. 2005. Calpain 1-titin interactions concentrate calpain 1 in the Z-band edges and in the N2-line region within the skeletal myofibril. *FEBS J.*, 272: 2578-2590.
29. Reid, W. D. and A. N. Belcastro. 2000. Time course of diaphragm injury and calpain activity during resistive loading. *Am. J. Respir. Crit. Care Med.*, 162: 1801-1806.
30. Riley, D. A., J. L. Thompson, B. B. Krippendorf and G. R. Slocum. 1995. Review of spaceflight and hindlimb suspension unloading induced sarcomere damage and repair. *Basic Appl. Myol.*, 5: 139-145.

31. Russell, S. T., P. M. Siren, M. J. Siren and M. J. Tisdale. 2009. Attenuation of skeletal muscle atrophy in cancer cachexia by D-myo-inositol 1,2,6-triphosphate. *Cancer Chemother. Pharmacol.*, 64: 517-527.
32. Sam, M., S. Shah, J. Friden, D. J. Milner, Y. Capetanaki and R. L. Lieber. 2000. Desmin knockout muscles generate lower stress and are less vulnerable to injury compared with wild-type muscles. *Am. J. Physiol. (Cell)*, 279: C1116-C1122.
33. Solomon, V. and A. L. Goldberg. 1996. Importance of the ATP-ubiquitin-proteasome pathway in the degradation of soluble and myofibrillar proteins in rabbit muscle extracts. *J. Biol. Chem.*, 271: 26690-26697.
34. Spencer, M. J., B. Lu and J. G. Tidball. 1997. Calpain II expression is increased by changes in mechanical loading of muscle in vivo. *J. Cell Biochem.*, 64: 55-66.
35. Stevenson, E. J., P. G. Giresi, A. Koncarevic and S. C. Kandarian. 2003. Global analysis of gene expression patterns during disuse atrophy in rat skeletal muscle. *J. Physiol.*, 551: 33-48.
36. Taillandier, D., E. Aurousseau, D. Meynial-Denis, D. Bechet, M. Ferrara, P. Cottin, A. Ducastaing, X. Bigard, C. Y. Guezennec, H. P. Schmid and . 1996. Coordinate activation of lysosomal, Ca²⁺-activated and ATP-ubiquitin-dependent proteinases in the unweighted rat soleus muscle. *Biochem. J.*, 316: 65-72.
37. Thomason, D. B., R. B. Biggs and F. W. Booth. 1989. Protein metabolism and beta-myosin heavy-chain mRNA in unweighted soleus muscle. *Am. J. Physiol.*, 257: R300-R305.
38. Thompson, L. V. and J. A. Shoeman. 1998. Contractile function of single muscle fibers after hindlimb unweighting in aged rats. *J. Appl. Physiol.*, 84: 229-235.

39. Tidball, J. G. and M. J. Spencer. 2002. Expression of a calpastatin transgene slows muscle wasting and obviates changes in myosin isoform expression during murine muscle disuse. *J. Physiol.*, 545: 819-828.
40. Tischler, M. E., E. J. Henriksen, K. A. Munoz, C. S. Stump, C. R. Woodman and C. R. Kirby. 1993. Spaceflight on STS-48 and earth-based unweighting produce similar effects on skeletal muscle of young rats. *J. Appl. Physiol.*, 74: 2161-2165.
41. Trappe, S., D. Costill, P. Gallagher, A. Creer, J. R. Peters, H. Evans, D. A. Riley and R. H. Fitts. 2009. Exercise in space: human skeletal muscle after 6 months aboard the International Space Station. *J. Appl. Physiol.*, 106: 1159-1168.
42. Trinick, J. 1994. Titin and nebulin: protein rulers in muscle? *Trends Biochem. Sci.*, 19: 405-409.
43. Udaka, J., S. Ohmori, T. Terui, I. Ohtsuki, S. Ishiwata, S. Kurihara and N. Fukuda. 2008. Disuse-induced preferential loss of the giant protein titin depresses muscle performance via abnormal sarcomeric organization. *J. Gen. Physiol.*, 131: 33-41.
44. Vermaelen, M., P. Sirvent, F. Raynaud, C. Astier, J. Mercier, A. Lacampagne and O. Cazorla. 2007. Differential localization of autolyzed calpains 1 and 2 in slow and fast skeletal muscles in the early phase of atrophy. *Am. J. Physiol. Cell Physiol.*, 292: C1723-C1731.
45. Whiting, A., J. Wardale and J. Trinick. 1989. Does titin regulate the length of muscle thick filaments? *J. Mol. Biol.*, 205: 263-268.

46. Widrick, J. J., S. T. Knuth, K. M. Norenberg, J. G. Romatowski, J. L. Bain, D. A. Riley, M. Karhanek, S. W. Trappe, T. A. Trappe, D. L. Costill and R. H. Fitts. 1999. Effect of a 17 day spaceflight on contractile properties of human soleus muscle fibres. *J. Physiol.*, 516: 915-930.
47. Widrick, J. J., J. G. Romatowski, J. L. Bain, S. W. Trappe, T. A. Trappe, J. L. Thompson, D. L. Costill, D. A. Riley and R. H. Fitts. 1997. Effect of 17 days of bed rest on peak isometric force and unloaded shortening velocity of human soleus fibers. *Am. J. Physiol.*, 273: C1690-C1699.
48. Williams, A. B., G. M. courten-Myers, J. E. Fischer, G. Luo, X. Sun and P. O. Hasselgren. 1999. Sepsis stimulates release of myofilaments in skeletal muscle by a calcium-dependent mechanism. *FASEB J.*, 13: 1435-1443.

CHAPTER 3

TREATMENT WITH DEACETYLASE INHIBITORS DURING HINDLIMB SUSPENSION DOES NOT PREVENT MUSCLE WEAKNESS BUT RESULTS IN LARGER INDIVIDUAL FIBERS

Summary

Deacetylase inhibitors have been reported to increase myotube size in culture and to induce muscle fiber hypertrophy and improvements in force generation in dystrophin-deficient mice. Our objective was to investigate whether treatment with the deacetylase inhibitor trichostatin A (TSA) provides protection from the loss of muscle mass and function in healthy wild type mice subjected to hindlimb suspension (HS). Mice were exposed to 14 or 21 days of HS with daily administration of either TSA or a saline vehicle to test the hypothesis that, compared with the unloaded muscles in vehicle treated mice, muscles in the mice treated with TSA would show greater muscle masses, higher maximum isometric forces, higher specific forces normalized for cross-sectional area (CSA), larger individual fiber CSAs, and lower susceptibility to contraction-induced injury. Following 14 or 21 days of HS, soleus muscles lost slightly less mass in TSA (30%) compared with vehicle (40%) treated mice, but the loss of force generating capacity induced by HS was not similarly prevented by TSA treatment. In fact, specific force (kN/m^2) showed a tendency for a continued downward trend throughout the period of HS for muscles of TSA treated mice. Susceptibility to injury, as assessed by the

deficit in isometric force production following two lengthening contractions, was not different between muscles of TSA and vehicle treated mice for either non-suspended controls or following 14 or 21 days of HS. Despite similar masses of soleus muscles from TSA and vehicle treated mice exposed to 21 days of HS, individual fiber CSAs were 30-40% larger and the number of fibers appearing in muscle cross sections was ~30% smaller in the TSA treated mice. These findings suggest an as yet unappreciated impact of TSA treatment on muscle architecture, which warrants future investigation. Based on only slight amelioration of the loss of muscle mass induced by HS provided by treatment with TSA that was more than compensated for by negative effects on force generating capacity, we conclude that the pharmacological use of deacetylase inhibitors to prevent muscle atrophy and maintain muscle function under circumstances of muscle disuse is not supported.

Introduction

Muscle atrophy and weakness are prominent features of diseases including cancer (Russell *et al.* 2009), muscular dystrophy (Spencer & Mellgren 2002), sepsis (Williams *et al.* 1999), and diabetes (Price & Mitch 1998), as well as during bed rest (Widrick *et al.* 1997) and the muscle unloading during space exploration (Gardetto *et al.* 1989; Widrick *et al.* 1999). Multiple studies utilizing drugs, genetic modifications, and exercise as therapeutic interventions have been undertaken to counteract the atrophy and weakness that unloading induces in skeletal muscle (Criswell *et al.* 1998; McMahon *et al.* 2003; Haddad *et al.* 2006; Arbogast *et al.* 2007; Trappe *et al.* 2009). While most investigations have targeted systems that mediate protein degradation within skeletal muscles during disuse, a few studies have provided insight into attenuation of skeletal

muscle atrophy by modulation of positive or negative regulators of muscle growth.

One positive regulator of muscle growth, IGF-I, has been shown to act at least in part through the inhibition of protein degradation by suppressing the expression of muscle specific ubiquitin ligases (Sacheck *et al.* 2004), but over-expression of IGF-I in a transgenic mouse model did not prevent muscle atrophy induced by HS (Criswell *et al.* 1998). Other investigators have examined the effectiveness of the inhibition of myostatin to ameliorate disuse atrophy of skeletal muscle. Myostatin (GDF-8) is a member of the transforming growth factor-beta (TGF- β) family of cytokines and functions as a negative regulator of skeletal muscle mass (McPherron *et al.* 1997). Inactivation of the myostatin gene as well as postnatal inhibition of myostatin both result in significant increases in skeletal muscle mass (Zhu *et al.* 2000; Grobet *et al.* 2003; Whittemore *et al.* 2003). Moreover, myostatin-deficient mice demonstrated resistance to muscle atrophy induced by glucocorticoid treatment (Gilson *et al.* 2007), and finally, myostatin expression has been reported to increase following HS (Carlson *et al.* 1999; Lalani *et al.* 2000). Thus, while the potential of the inhibition of myostatin as a countermeasure for disuse atrophy appears a promising hypothesis, myostatin-deficient mice actually lost more muscle mass than wild type controls following HS (McMahon *et al.* 2003).

Recently, treatment with deacetylase inhibitors has been explored as an approach to ameliorating muscle atrophy. Protein acetylation positively influences cell proliferation and differentiation, and studies of C2C12 skeletal muscle cell lines and primary human myoblast cultures showed that treatment with deacetylase inhibitors, including trichostatin A (TSA), valproic acid, and phenylbutyrate, resulted in the formation of larger myotubes compared with myotubes formed in cultures in the absence of the drugs (Iezzi *et al.* 2002; Iezzi *et al.* 2004). The effect of deacetylase inhibitors on

muscle cell size *in vitro* prompted an investigation of the efficacy of this pharmacological intervention to improve muscle fiber size and skeletal muscle function in dystrophic muscles (Minetti *et al.* 2006). Treatment of *mdx* mice, a model of Duchenne muscular dystrophy, with TSA improved exercise performance, increased muscle force generation, and decreased susceptibility to contraction-induced injury to levels comparable to those of wild type mice. An astonishing increase in individual muscle fiber cross-sectional areas (CSA) in *mdx* mice in response to TSA treatment of nearly two-fold relative to those in either untreated *mdx* mice or in wild type control mice was also reported in the Minetti *et al.* study, as were beneficial effects in mice deficient in alpha-sarcoglycan, a model of limb girdle muscular dystrophy type 2D (Minetti *et al.* 2006).

Although deacetylase inhibitors have been shown to induce increases in muscle cell size *in vitro* and in dystrophic mice, the ability of promoting protein acetylation as a means to alleviate disuse muscle atrophy in healthy mice has not been explored. Inasmuch as muscle regeneration has been reported to be impaired during HS (Darr & Schultz 1989; Mozdziak *et al.* 1998; Mitchell & Pavlath 2004; Fujino *et al.* 2005), the possibility that treatment with deacetylase inhibitors may counteract atrophy through the promotion of regenerative processes does not seem an unreasonable hypothesis. Thus, the objective of the present study was to investigate the effects on wild type mice of treatment with the deacetylase inhibitor TSA during HS on the severity of skeletal muscle atrophy and loss of force generating capacity. Mice were exposed to 14 or 21 days of HS with daily administration of either TSA or saline vehicle to test the hypothesis that, compared with the unloaded muscles in vehicle treated mice, muscles in the mice treated with TSA would show greater muscle masses, higher maximum isometric forces,

larger individual fiber cross-sectional areas, and lower susceptibility to contraction-induced injury.

Methods

All experiments were performed on 4-month-old specific pathogen free (SPF) male C57BL/6 mice purchased from the Jackson Laboratories (Bar Harbor, ME). All procedures were approved by the University of Michigan Committee for the Use and Care of Animals. A total of 36 mice were randomly assigned to one of six groups. The first two groups of mice were treated with TSA and exposed to HS for either 14 (TSA-14D) or 21 (TSA-21D) days. Another two groups of mice were injected with vehicle and exposed to HS for either 14 (CON-14D) or 21 (CON-21D) days. A fifth group of mice was treated with TSA for 21 days but not exposed to HS (TSA-NS). Finally, the last group of mice served as undisturbed controls and were not treated with TSA or exposed to HS (CON-NS). During all post-HS experimental procedures, the mice were anesthetized with intraperitoneal injections of 2% Avertin™ at a dose of 400 mg/kg tribromoethanol, with supplemental doses provided to maintain an adequate level of anesthesia to prevent response to tactile stimuli.

Injections of TSA

For all treated mice, TSA was administered daily by intraperitoneal injection. The dose of TSA used was 0.6 mg per kg diluted in saline consistent with the dose used previously in mice (Minetti et al., 2006). Untreated mice also received daily injections of the same volume of the saline vehicle, but without drug.

Hindlimb Suspension

HS is a widely used method for unloading rodent hind limbs. Our method of HS was modified from that originally described by Morey (Morey 1979). Briefly, surgical tape (3M, Two Harbors, MN) was used to wrap the tail of each animal against a rigid metal wire piece with a manually bent upper hook connected to a rotating pulley. The tape was lightly soaked with liquid suture VetBond (3M, Two Harbor, MN) to create an instant cast. Care was taken to prevent any VetBond from dripping onto the animal's tail. During the casting process, mice were briefly restrained in a small terrycloth wrap with the tail exposed. Since the entire process of preparing the tail was completed within two minutes, no anesthetic was required during the procedure. After the tape and metal piece were attached, mice were released into a cage until the glue was dry. Once the tape hardened, the hind legs of the mice were lifted slightly off the floor of the cage by connecting the pulley to a metal rod inside the suspension cage. The rotating pulley system enabled mice to move from one end of the cage to the other with a full 360° range of motion and obtain food and water freely. Mice were observed daily for changes in appearance and activity.

In Vitro Muscle Contractile Properties

Based on widespread reports that the soleus muscles are among the most sensitive to the atrophy associated with HS, and supported by our own observations in our previous study (Chapter 2) that showed no atrophy of mouse EDL muscles after 14 days of HS, we chose to focus our analyses in this study on soleus muscles. At the end of all treatment periods, soleus muscles in one limb were isolated under deep anesthesia. 5-0 silk suture ties were secured around the distal and proximal tendons,

and the muscles were carefully removed and placed in a horizontal bath containing buffered mammalian Ringer solution (composition in mM: 137 NaCl, 24 NaHCO₃, 11 glucose, 5 KCl, 2 CaCl₂, 1 MgSO₄, 1 NaH₂PO₄, and 0.025 tubocurarine chloride) maintained at 25 °C and bubbled with 95% O₂ / 5% CO₂ to stabilize pH at 7.4. One tendon of the muscle was tied securely to a force transducer (model BG-50, Kulite Semiconductor Products, Leonia, NJ) and the other tendon to the lever arm of a servomotor (model 305B, Aurora Scientific, Richmond Hill, ON, Canada). The contralateral muscle was removed and prepared for future analyses. After removal of the muscles, animals were euthanized with an overdose of anesthetic and administration of a bilateral pneumothorax.

For measurement of isometric contractile properties, muscles were stimulated between two stainless steel plate electrodes. The voltage of single 0.2-ms square stimulation pulses and, subsequently, muscle length (L_o) were adjusted to obtain maximal twitch force. Muscle length was measured with calipers. With the muscle held at L_o , the force developed during 900-ms trains of stimulation pulses was recorded, and stimulation frequency was increased until the maximum isometric tetanic force (P_o) was achieved. A stimulus frequency of 120 Hz typically elicited P_o for all muscles. For each muscle, optimum fiber length (L_f) was calculated by multiplying L_o by previously determined L_f/L_o ratio for soleus muscles of 0.71 (Brooks & Faulkner 1988).

Following assessment of isometric contractile properties, maximally activated muscles were exposed to two stretches of 30% strain relative to L_f at a velocity of 2 L_f/s initiated from the plateau of an isometric contraction. The stimulation frequency that elicited P_o was used during the lengthening contractions. Muscles were held isometric for 300 ms to allow near maximal activation, and stimulation was terminated at the end of

the lengthening ramp. One minute of rest was allowed before the second lengthening contraction was initiated. P_o was measured once again 1 minute after the two lengthening contractions. The force deficit induced by the lengthening contractions was calculated as the difference between the isometric forces measured before and after the stretches, expressed as a percentage of the force before the stretch.

After the force measurements, muscles were removed from the bath, the tendons were trimmed, and the muscle was blotted and weighed. Muscles were quick frozen in isopentane cooled with liquid nitrogen and stored at $-80\text{ }^{\circ}\text{C}$ for subsequent histological analyses. Total muscle fiber cross-sectional area (CSA) was calculated by dividing the muscle mass by the product of L_f and the density of mammalian skeletal muscle, 1.06 g/cm^3 . Specific P_o (in kN/m^2) was calculated by dividing P_o by total fiber CSA for each muscle.

Myosin ATPase Activity

Frozen cross sections of $10\text{ }\mu\text{m}$ thickness were cut from the widest portion of the belly of each muscle. Cryosections were placed on microscope slides and incubated at varying pH conditions to measure myofibrillar ATPase activity, as previously described (Brooke 1970). Muscle fibers were classified as type 1 or type 2 on the basis of myofibrillar ATPase activity. Stained sections were visualized on a microscope (Leitz Laborlux, Leica; Wetzlar, Germany) and captured with a video camera (Diagnostic Instruments; Sterling Heights, MI) and the image analyzing software ImageJ was used to calculate individual fiber areas. For each muscle, individual fiber CSAs were evaluated from two entire cross sections and separated by fiber type. Total counts of type 1 and

type 2 fibers in each whole cross section were also performed using the ImageJ image-analysis system.

Statistics

All data are presented as means \pm 1 S.E.M. unless indicated otherwise. The effects of treatment (CON, TSA) and duration of HS (NS, 14D, or 21D) on muscle mass, P_o , specific P_o , force deficits following lengthening contractions, single fiber CSAs, and fiber counts were determined by two factor analysis of variance (ANOVA) with a level of significance set a priori at $P < 0.05$. Individual differences were determined by Bonferroni post hoc analyses.

Results

Effect of TSA on wild-type mice

Body masses were not different between CON-NS and TSA-NS mice, but there was a small 14% decrease in soleus muscle mass following 21 days of TSA injections (Fig.3.1A). Despite the slightly smaller mass of the muscles of TSA-NS compared with CON-NS mice, the values of P_o for TSA-NS and CON-NS were not significantly different (Fig. 3.1B). Furthermore, when P_o was normalized by total muscle fiber CSA, specific P_o values were also not different between the two groups of mice (Fig. 3.1C). Finally, similar deficits in isometric force were observed for muscles of TSA-NS and CON-NS mice following the two lengthening contractions (Fig. 3.1D). Collectively, these findings suggest that TSA treatment alone had minimal effects on the structure and function of soleus muscles in healthy control mice. Based on these findings that 21 days of TSA

treatment had only a small impact on the muscles in non-suspended animals, we reasoned that the additional animal use required to include a control group of mice treated with TSA for 14 days but not exposed to HS was not justified.

Response to Hindlimb Suspension

Body Mass. All mice used in this study were weighed prior to HS and at the point when they were sacrificed. Most mice lost a small amount of weight during the period of HS, with no differences between TSA treated and vehicle treated mice. Moreover, the weight loss was not progressive, that is, mice suspended for 21 days did not show greater weight loss than those suspended for 14 days. Overall, for the 24 mice that experienced any period of HS, the average change in weight was a loss of $8\% \pm 1\%$.

Soleus Muscle Mass. Compared with soleus muscles of CON-NS mice, muscles of CON-14D mice showed a loss of mass of ~40% with no further decrease observed for muscles of CON-21D mice (Fig. 3.2). Similarly, compared with soleus muscles of TSA-NS, muscles of TSA-14D and TSA-21D also showed substantial loss of mass, with no difference between the 14 day and 21 day time points (Fig. 3.2). Despite the significant decrease in mass following HS observed for soleus muscles of TSA treated mice, the decrease for the TSA treated mice was only 30% compared with the 40% decrease observed for vehicle treated mice, such that the relative masses of muscles of TSA treated mice were significantly greater than those of muscles of vehicle treated mice after both 14 and 21 days of HS (Fig. 3.2).

Contractile Properties. Coincident with the losses of mass were decreasing values of P_o . Compared with the P_o for CON-NS mice, P_o was 47% lower for muscles of CON-14D mice and 53% lower for muscles of CON-21D mice (Fig. 3.3). This greater

loss of force than mass during HS for the vehicle treated mice resulted in 21% and 30% lower values of specific P_o for muscles of CON-14D and CON-21D, respectively, compared with the muscles of CON-NS mice (Fig. 3.4). Despite the moderate attenuation of the loss of muscle mass observed for TSA treated mice, force values were not similarly spared. P_o for muscles of TSA-21D mice was 50% lower than the value for TSA-NS mice (Fig. 3.3), a decrease of similar magnitude for that observed in vehicle treated mice. Again, a greater loss of force than mass during HS of TSA treated mice indicates that muscles in the treated mice were weaker than those in non-suspended mice. Significantly lower values for specific P_o were observed for muscles of both TSA-14D (24%) and TSA-21D (40%) mice compared with the values for TSA-NS mice (Fig. 3.4). Furthermore, the specific P_o of muscles of TSA treated mice decreased from 185 ± 8 kN/m² for the TSA-14D group to 146 ± 9 kN/m² for the TSA-21D group, although the decrease did not reach statistical significance ($p = 0.1$).

Susceptibility to Contraction Induced Injury. The two 30% lengthening contractions of maximally activated soleus muscles caused significant deficits in the isometric force of soleus muscles of TSA treated and vehicle treated mice that were not different between the groups at any time point studied (Fig. 3.5). Despite the lack of difference between muscles of TSA and CON mice at any time point, force deficit was 70% greater for muscles of CON-14D compared with CON-NS mice, whereas force deficit did not increase with HS for muscles of TSA treated mice.

Muscle Fiber Sizes. Comparisons of the single fiber CSAs in soleus muscles exposed to 21 days of HS showed substantially larger fibers in TSA treated compared with vehicle treated mice. Type 1 fibers in muscles of TSA-21D mice were 43% larger than the type 1 fibers in the muscles of CON-21D mice (Fig. 3.6A). Similarly, type 2

fibers were larger for muscles of TSA-21D compared with CON-21D mice, although the magnitude of the difference, 32%, was slightly less than was seen for type 1 fibers. The 30% to 40% larger fibers in the TSA-21D muscles compared with the CON-21D muscles far exceeded the ~10% attenuation in the loss of muscle mass observed during HS with TSA treatment (Fig. 3.2). Moreover, the absolute masses of the soleus muscles of TSA-21D (6.5 ± 0.2 mg) and CON-21D (6.4 ± 0.2 mg) mice were not different. In an attempt to reconcile the increase in average single fiber CSAs with no difference in muscle mass, we generated frequency histograms from the fiber CSA data (Fig. 3.6B). Consistent with larger mean fibers CSAs for both type 1 and type 2 fibers of the TSA treated mice, the frequency histograms showed clear shifts to the right for both fiber types, with considerable numbers of very large fibers present in the muscles of the TSA treated mice. For muscles of CON-21D mice, fewer than 10% of the fibers had CSAs of $2500 \mu\text{m}^2$ or greater, whereas nearly 40% of the fibers in the muscles of the TSA-21D mice exceeded $2500 \mu\text{m}^2$. Furthermore, in muscles of TSA-21D mice, fewer than 20% of the fibers were smaller than $1000 \mu\text{m}^2$ compared with twice as many fibers in that size range in the muscles of the CON-21D mice (Fig. 3.6B).

Muscle Fiber Numbers. The similarity in muscle masses for TSA-21D and CON-21D mice, coupled with the substantially larger individual fiber CSAs in the muscles of TSA-21D indicates that those muscles may have fewer fibers. Total fiber counts from muscle cross sections showed ~30% fewer fibers in the muscles of TSA-21D compared with CON-21D mice (Fig. 3.7).

Discussion

Deacetylase inhibitors have been reported to increase myotube size in culture

(Iezzi *et al.* 2004) and to induce muscle fiber hypertrophy and improvements in force generation in dystrophin-deficient mice (Minetti *et al.* 2006). Our objective was to investigate whether treatment with the deacetylase inhibitor trichostatin A (TSA) provided protection from the loss of muscle mass and function in healthy wild type mice subjected to HS. Consistent with our hypothesis, muscles in mice treated with TSA lost slightly less mass than those of vehicle treated mice over the course of 21 days of HS, however, contrary to our hypothesis, the loss of force as well as specific force was not different for TSA and vehicle treated mice. In fact, there was a trend for greater loss of specific force for the TSA treated mice. Thus, any beneficial effect provided by TSA treatment to maintain muscle mass was overcome by the weakness of the remaining muscle. These findings are contrary to reports that 12 weeks of TSA treatment restored specific force values for muscles of *mdx* mice to wild type values (Minetti *et al.* 2006). Whether the relatively short duration of treatment incorporated in the present study explains our contrary findings is unknown, but the continued downward trend in specific force during HS for the muscles of our TSA treated mice argues against that possibility.

The larger CSAs of fibers in the TSA-21D compared with CON-21D groups are consistent with increased fiber sizes for muscles of *mdx* mice, in which after 45 days of TSA treatment the average single fiber CSA was 2X greater than the CSAs of either untreated *mdx* mice or wild type control mice (Minetti *et al.* 2006). The increase in fiber sizes induced by TSA treatment in *mdx* mice was accompanied by increased expression of the TGF- β family member follistatin (Minetti *et al.* 2006). Increased follistatin levels have also been reported in muscles of TSA treated wild type mice in which muscle fiber degeneration and regeneration was induced by cardiotoxin injection (Iezzi *et al.* 2004). In addition, muscle fibers harvested from TSA-treated *mdx* mice gave rise to satellite cells

that showed increased follistatin expression and formed myotubes of larger diameter than those formed from cells harvested from tissues of untreated mice (Minetti *et al.* 2006), and the up-regulation of follistatin *in vivo* observed following treatment with TSA correlated with increased expression of markers of satellite cell activation and improved regeneration of injured muscles in wild type mice (Iezzi *et al.* 2004). The *in vivo* findings are consistent with previous work showing that TSA treatment of C2C12 myoblasts increased follistatin expression and preventing follistatin transcription rendered myoblasts insensitive to TSA. Furthermore, treatment of C2C12 cells with follistatin inhibitors greatly reduced TSA-mediated myoblast fusion (Iezzi *et al.* 2004). Based on the combination of the *in vitro* and *in vivo* experiments described above, a reasonable hypothesis for the mechanism underlying the action of TSA appears to be that deacetylase inhibitors activate follistatin expression in injured muscles promoting enhanced activation, proliferation and fusion of satellite cells into hypernucleated myotubes and subsequent fusion of the newly formed myotubes with mature myofibers. To propose such a mechanism in our unloaded muscles requires one to accept that muscle fibers can simultaneously atrophy and “hypertrophy,” i.e. newly formed myotubes are capable of fusing with atrophying fibers in unloaded muscles.

If individual fibers in our TSA treated animals were undergoing “hypertrophy,” additional changes in the architecture of the muscle must be proposed to account for the aggregate of our morphological data, showing that following HS there were (1) no differences in muscle mass or length between TSA treated and vehicle treated mice, (2) significantly greater individual fiber CSAs in TSA treated mice, and (3) significantly fewer fibers appearing in muscle cross sections of TSA treated mice. The similar muscle masses for TSA and vehicle treated mice coupled with the 30-40% larger fiber CSAs in

the muscles of the TSA treated compared with vehicle treated mice suggests that the muscles in the TSA treated mice may have been losing muscle fibers during the 21 days of HS. Our expectation is that fiber loss would occur as severely atrophic fibers ultimately disappear, yet our fiber size data shows no indication of the presence of severely atrophic fibers in the muscles of the TSA treated mice, although such a population of fibers may be observed at earlier time points. An alternate explanation is that the substantially larger fibers in the muscles of the TSA treated mice caused an increased angle of pennation in the muscle resulting in a decreased number of fibers in a cross section (Maxwell *et al.* 1974). Our findings are consistent with this scenario in principle, but the dramatic increase in pennation angle required to account for the 30% fewer fibers per cross-section for muscles of TSA-21D compared with CON-21D mice is unlikely. Such a change in architecture also necessitates that the muscles of the TSA-21D mice have shorter muscle fibers than muscles of CON-21D mice. The muscles of both TSA treated and vehicle treated mice showed decreases in muscle length with HS (data not shown), but the muscle lengths were not different between the TSA and vehicle treated groups after either 14 or 21 days of HS. More detailed analyses of the changes in muscle architecture during HS with TSA treatment is required to determine whether the muscles of TSA treated mice atrophy through fiber loss or decreases in fiber length. The possibility that individual fibers simultaneously hypertrophy through deacetylase inhibitor mediated activation of satellite cells is an intriguing and potentially highly significant finding and warrants future investigation.

To assess any effects of treatment with deacetylase inhibitors on susceptibility to contraction-induced injury, we subjected all muscles to an injurious protocol of lengthening contractions. Whereas 14 days of HS increased susceptibility to injury of

muscles in vehicle treated mice with no further increase observed following 21 days, muscles in TSA treated mice showed no increase in injury susceptibility during HS. The nearly two-fold increase in force deficit following lengthening contractions observed for muscles of CON-14D compared with CON-NS mice is consistent with the findings of our previous study (Chapter 2). The observation that neither 14 nor 21 days of HS increased susceptibility to contraction-induced injury in TSA treated mice could be explained by the presence in the TSA treated mice of newly regenerated muscle fibers as newly regenerated fibers have been reported to be more resistant to contraction-induced injury (Devor & Faulkner 1999). The presence of newly regenerated fibers in muscles of TSA-14D or TSA-21D mice may be consistent with the hypothesis outlined above for the actions of TSA treatment to stimulate the activation of satellite cells enhancing regeneration, although any effect on susceptibility to contraction-induced injury as a result of the TSA treatment was not sufficient to reduce the magnitude of the force deficit compared with the values recorded for muscles of vehicle treated mice.

In summary, the findings of the present study show that treatment with the deacetylase inhibitor TSA resulted in a slight amelioration of the loss of muscle mass induced by unloading skeletal muscle during HS. Any effect of the deacetylase inhibitor to preserve muscle mass, however, was more than compensated for by negative effects on force generating capacity such that, following HS, muscles of TSA and vehicle treated mice were not different with respect to isometric force production. Despite the lack of beneficial effects of TSA treatment on mass or force, single fiber CSAs were 30-40% larger in TSA treated compared with vehicle treated mice following 21 days of HS. These findings suggest that TSA treatment during HS may induce the fusion of newly formed hypernucleated myotubes with atrophying muscle, but definitive studies are

required to directly test this hypothesis. Thus, although treatment with deacetylase inhibitors is not effective for protecting muscles from the losses of mass and force generating capacity associated with disuse, TSA treatment appears to be an extremely powerful inducer of fiber growth.

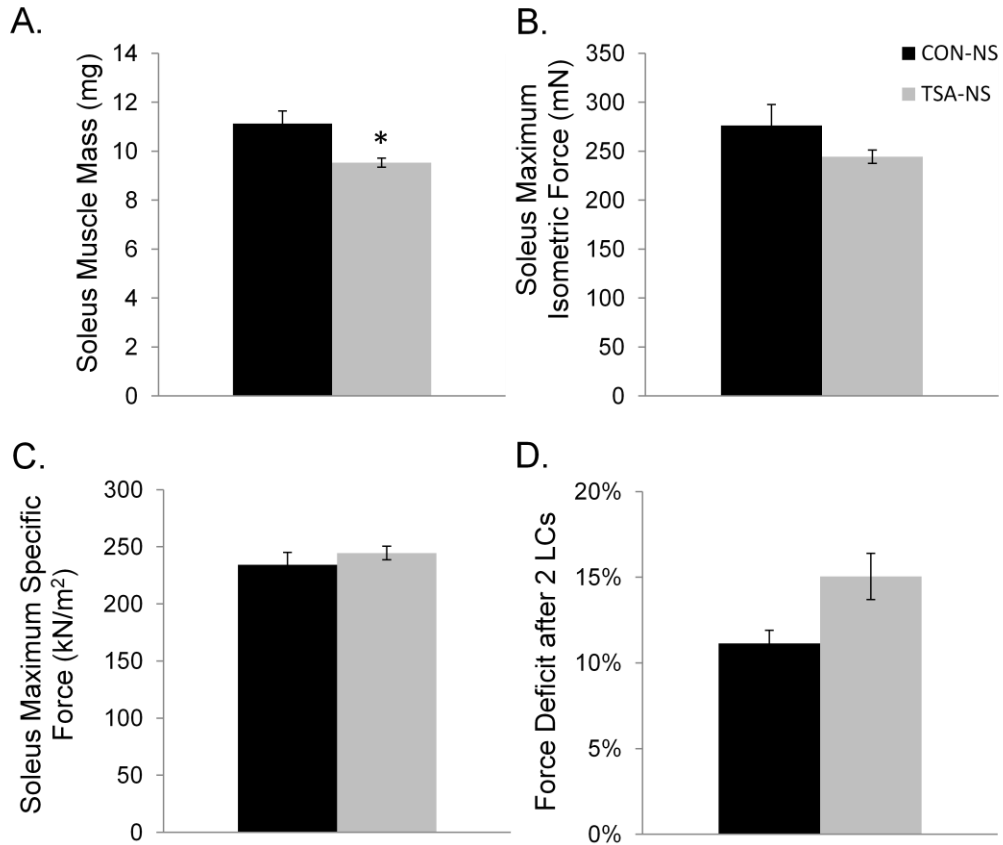


Figure 3.1. Effects of 21 days of TSA treatment on soleus muscles of non-suspended mice. Data are shown for **A.** muscle mass expressed in milligrams, **B.** maximum isometric tetanic force (P_o) expressed in millinewtons, **C.** specific P_o expressed in kilonewtons per square meter, and **D.** the deficit in isometric force measured one minute following two lengthening contractions expressed as the percent decline relative to the initial force for soleus of muscles of untreated (CON, black bars) and TSA treated (TSA, gray bars) mice. Bars represent means \pm 1 s.e.m. and the asterisk (*) indicates a significant ($p < 0.05$) difference between the TSA-NS and CON-NS values.

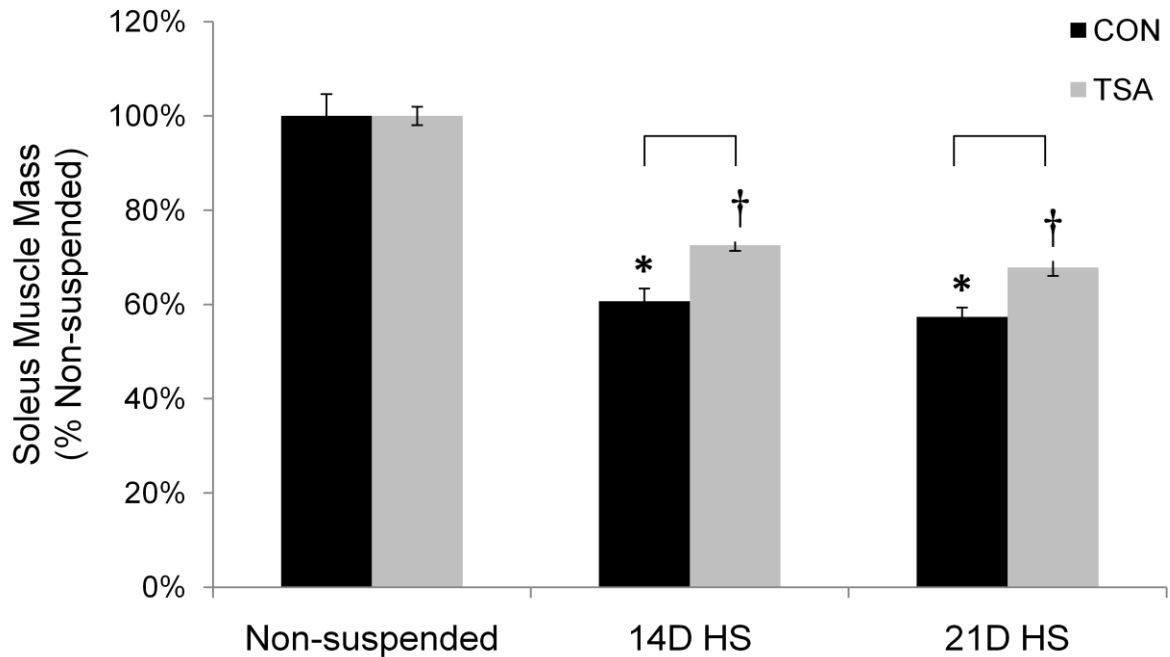


Figure 3.2. Soleus muscle mass following 14 and 21 days of hindlimb suspension for TSA and vehicle treated mice. Data are shown for mass for soleus muscles of vehicle treated (CON, black bars) and TSA treated (TSA, gray bars) mice that were either not exposed to hindlimb suspension (Non-suspended) or were exposed to either 14 (14D HS) or 21 (21D HS) days of hindlimb suspension. Data are expressed as a percentage of the value for muscles of the non-suspended controls. Bars represent means \pm 1 s.e.m. The asterisks (*) and daggers (†) indicate significant ($p < 0.05$) differences from the respective values for non-suspended mice and the brackets indicate differences between the TSA and CON values.

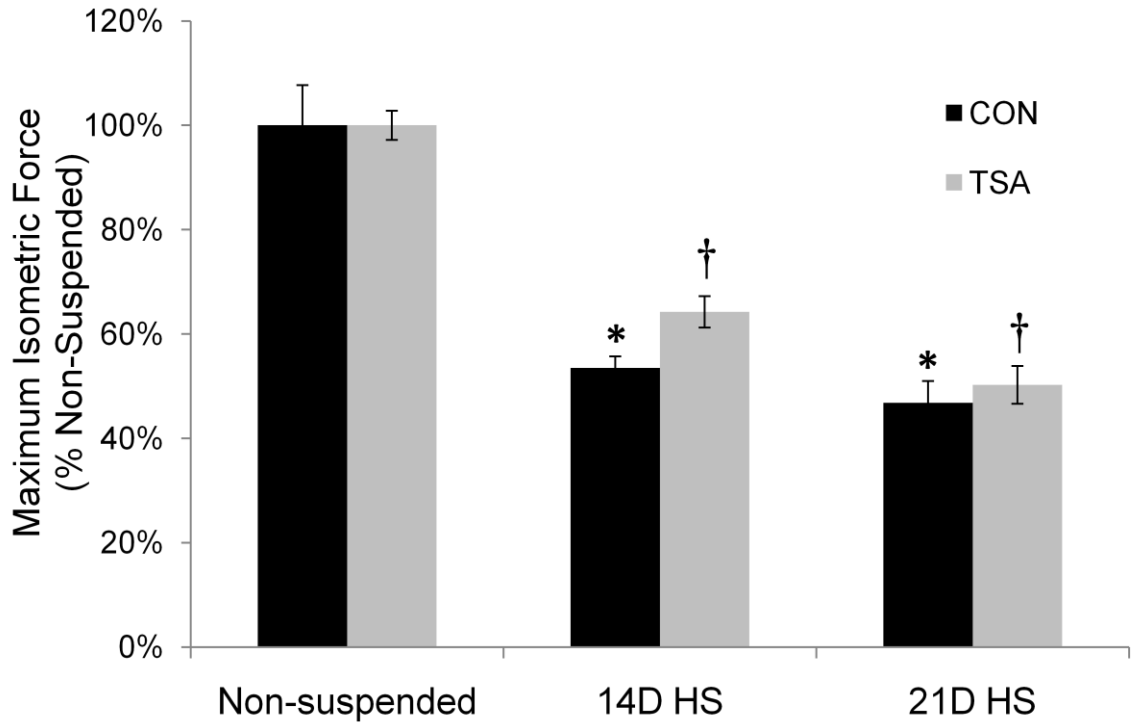


Figure 3.3. Soleus muscle maximum isometric force following 14 and 21 days of hindlimb suspension for TSA and vehicle treated mice. Data are shown for maximum isometric tetanic force (P_0) for soleus muscles of vehicle treated (CON, black bars) and TSA treated (TSA, gray bars) mice that were either not exposed to hindlimb suspension (Non-suspended) or were exposed to either 14 (14D HS) or 21 (21D HS) days of hindlimb suspension. Data are expressed as a percentage of the value for muscles of the non-suspended controls. Bars represent means \pm 1 s.e.m. The asterisks (*) and daggers (†) indicate significant ($p < 0.05$) differences from the respective values for non-suspended mice.

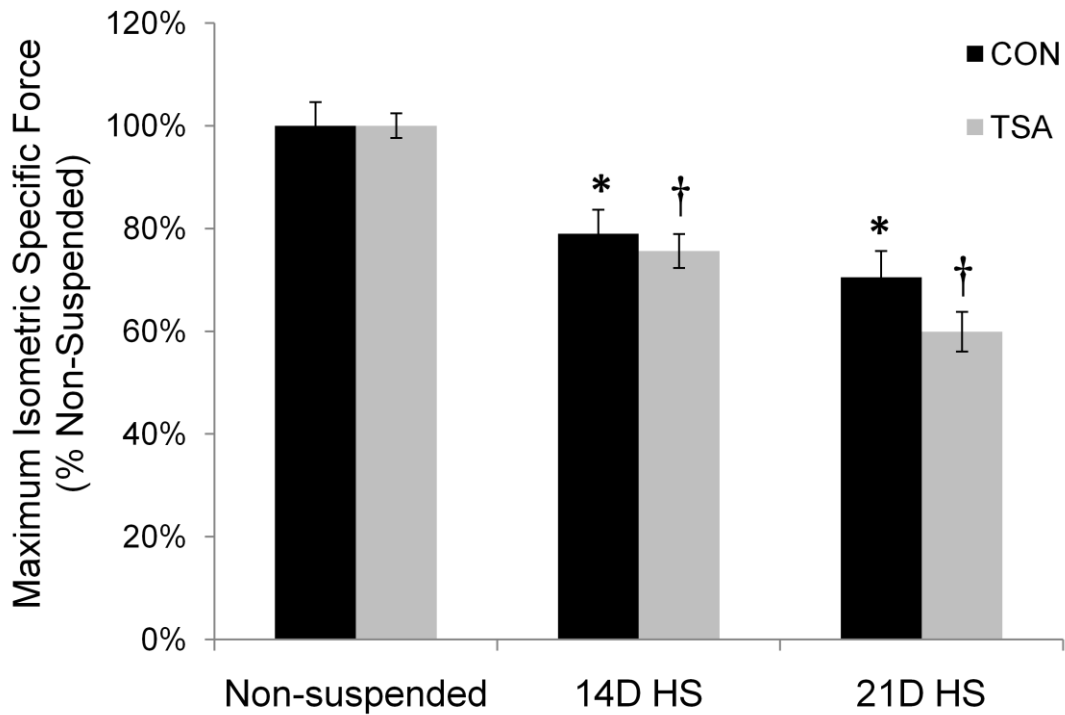


Figure 3.4. Soleus muscle maximum isometric specific force following 14 and 21 days of hindlimb suspension for TSA and vehicle treated mice. Data are shown for maximum isometric tetanic force (specific P_0) for soleus muscles of vehicle treated (CON, black bars) and TSA treated (TSA, gray bars) mice that were either not exposed to hindlimb suspension (Non-suspended) or were exposed to either 14 (14D HS) or 21 (21D HS) days of hindlimb suspension. Data are expressed as a percentage of the value for muscles of the non-suspended controls. Bars represent means \pm 1 s.e.m. The asterisks (*) and daggers (†) indicate significant ($p < 0.05$) differences from the respective values for non-suspended mice.

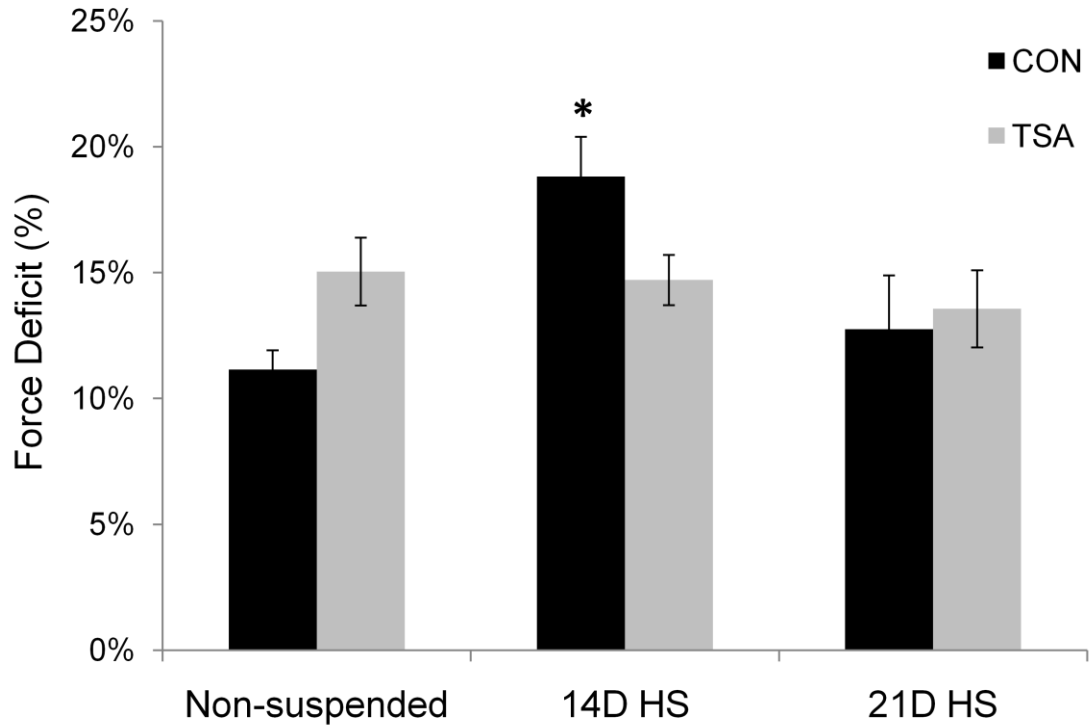


Figure 3.5. Force deficits following lengthening contractions of soleus muscles following 14 and 21 days of hindlimb suspension for TSA and vehicle treated mice. Data are shown for the deficit in isometric force induced following two lengthening contractions of maximally activated soleus muscles of vehicle treated (CON, black bars) and TSA treated (TSA, gray bars) mice that were either not exposed to hindlimb suspension (Non-suspended) or were exposed to either 14 (14D HS) or 21 (21D HS) days of hindlimb suspension. Data are expressed as the difference between the initial isometric force and the force immediately following the stretches expressed as a percentage of the initial force for each group. Bars represent means \pm 1 s.e.m. The asterisk (*) indicates a significant ($p < 0.05$) differences from the value for non-suspended mice.

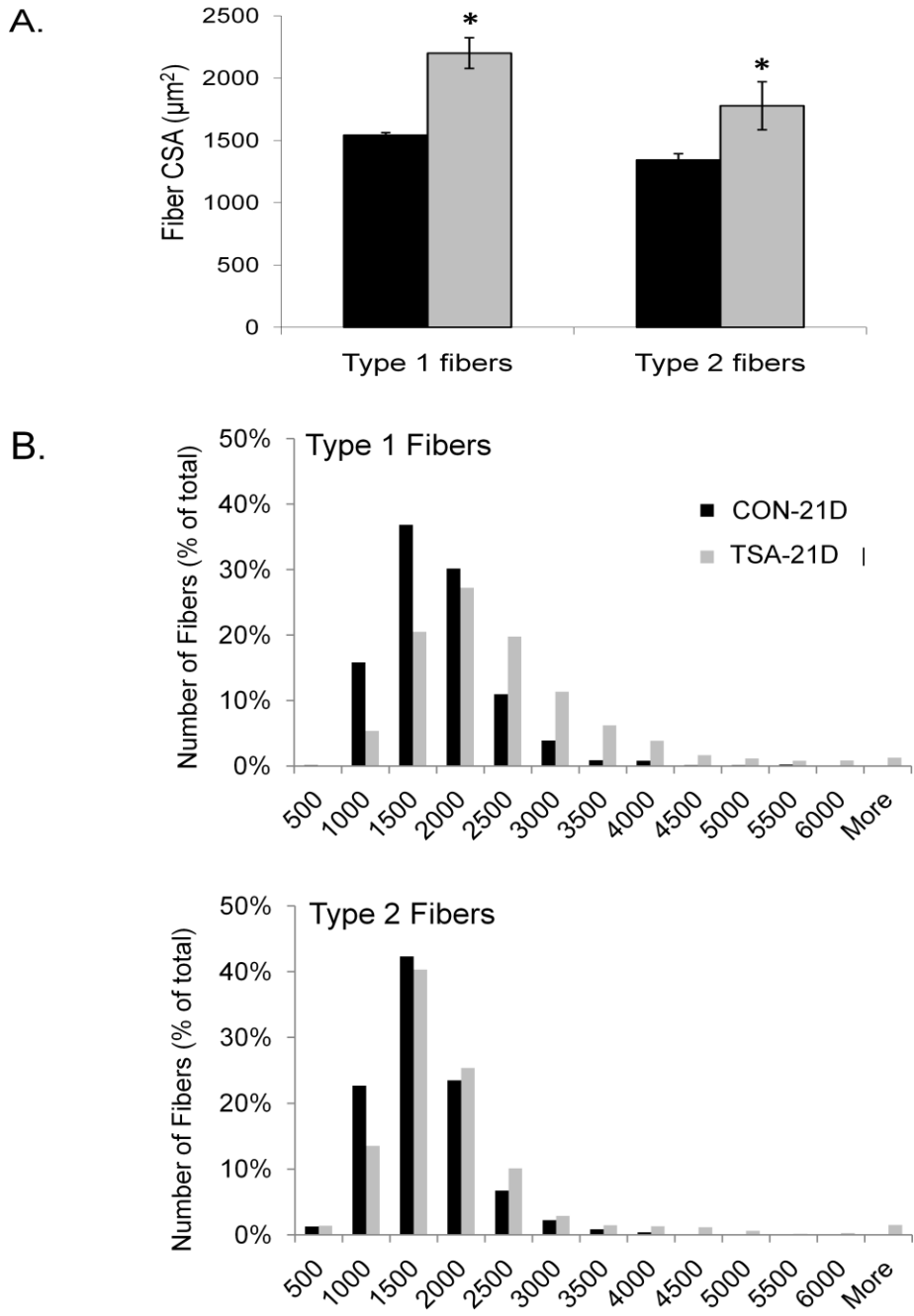


Figure 3.6. Individual fiber cross-sectional areas (CSAs) for soleus muscles following 21 days of hindlimb suspension for TSA and vehicle treated mice. Data are shown for **A.** the average fibers CSAs expressed in μm^2 and **B.** frequency distribution of fiber CSAs in soleus muscles of vehicle treated (CON-21D, black bars) and TSA treated (TSA-21D, gray bars) mice that were exposed to 21 days of hindlimb suspension. In panel A. Bars represent means \pm 1 s.e.m. The asterisks (*) indicate a significant ($p < 0.05$) differences between the TSA-21D and CON-21D values.

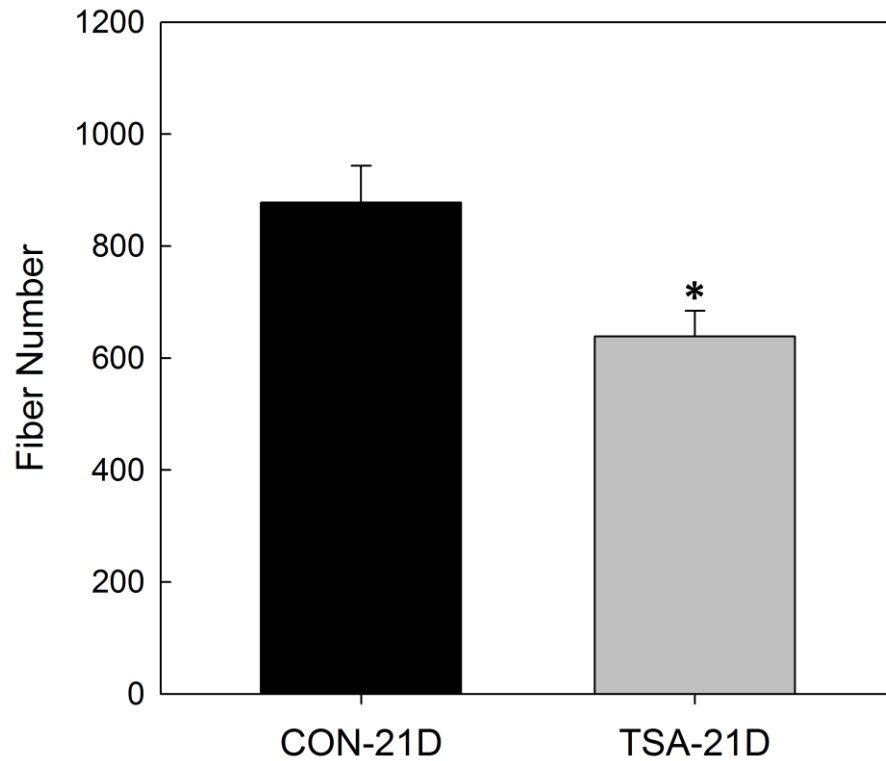


Figure 3.7. Total number of fibers that appear in a muscle cross section for soleus muscles following 21 days of hindlimb suspension for TSA and vehicle treated mice. Data are shown for the average number of fibers appearing in muscle cross sections for soleus muscles of vehicle treated (CON-21D, black bars) and TSA treated (TSA-21D, gray bars) mice that were exposed to 21 days of hindlimb suspension. Bars represent means \pm 1 s.e.m. The asterisk (*) indicates a significant ($p < 0.05$) differences between the TSA-21D and CON-21D values.

References

1. Arbogast, S., J. Smith, Y. Matuszczak, B. J. Hardin, J. S. Moylan, J. D. Smith, J. Ware, A. R. Kennedy and M. B. Reid. 2007. Bowman-Birk inhibitor concentrate prevents atrophy, weakness, and oxidative stress in soleus muscle of hindlimb-unloaded mice. *J. Appl. Physiol.*, 102: 956-964.
2. Brooke, M. H. a. K. K. K. 1970. Muscle fiber types: how many and what kind?. *Arch. Neurol.*, 23: 369-379.
3. Brooks, S. V. and J. A. Faulkner. 1988. Contractile properties of skeletal muscles from young, adult and aged mice. *J. Physiol.*, 404: 71-82.
4. Carlson, C. J., F. W. Booth and S. E. Gordon. 1999. Skeletal muscle myostatin mRNA expression is fiber-type specific and increases during hindlimb unloading. *Am. J. Physiol.*, 277: R601-R606.
5. Criswell, D. S., F. W. Booth, F. DeMayo, R. J. Schwartz, S. E. Gordon and M. L. Fiorotto. 1998. Overexpression of IGF-I in skeletal muscle of transgenic mice does not prevent unloading-induced atrophy. *Am. J. Physiol.*, 275: E373-E379.
6. Darr, K. C. and E. Schultz. 1989. Hindlimb suspension suppresses muscle growth and satellite cell proliferation. *J. Appl. Physiol.*, 67: 1827-1834.
7. Devor, S. T. and J. A. Faulkner. 1999. Regeneration of new fibers in muscles of old rats reduces contraction-induced injury. *J. Appl. Physiol.*, 87: 750-756.
8. Fujino, H., H. Kohzuki, I. Takeda, T. Kiyooka, T. Miyasaka, S. Mohri, J. Shimizu and F. Kajiya. 2005. Regression of capillary network in atrophied soleus muscle induced by hindlimb unweighting. *J. Appl. Physiol.*, 98: 1407-1413.
9. Gardetto, P. R., J. M. Schluter and R. H. Fitts. 1989. Contractile function of single muscle fibers after hindlimb suspension. *J. Appl. Physiol.*, 66: 2739-2749.

10. Gilson, H., O. Schakman, L. Combaret, P. Lause, L. Grobet, D. Attaix, J. M. Ketelslegers and J. P. Thissen. 2007. Myostatin gene deletion prevents glucocorticoid-induced muscle atrophy. *Endocrinology*, 148: 452-460.
11. Grobet, L., D. Pirottin, F. Farnir, D. Poncelet, L. J. Royo, B. Brouwers, E. Christians, D. Desmecht, F. Coignoul, R. Kahn and M. Georges. 2003. Modulating skeletal muscle mass by postnatal, muscle-specific inactivation of the myostatin gene. *Genesis*, 35: 227-238.
12. Haddad, F., G. R. Adams, P. W. Bodell and K. M. Baldwin. 2006. Isometric resistance exercise fails to counteract skeletal muscle atrophy processes during the initial stages of unloading. *J. Appl. Physiol.*, 100: 433-441.
13. Iezzi, S., G. Cossu, C. Nervi, V. Sartorelli and P. L. Puri. 2002. Stage-specific modulation of skeletal myogenesis by inhibitors of nuclear deacetylases. *Proc. Natl. Acad. Sci. U. S. A.*, 99: 7757-7762.
14. Iezzi, S., P. M. Di, C. Serra, G. Caretti, C. Simone, E. Maklan, G. Minetti, P. Zhao, E. P. Hoffman, P. L. Puri and V. Sartorelli. 2004. Deacetylase inhibitors increase muscle cell size by promoting myoblast recruitment and fusion through induction of follistatin. *Dev. Cell*, 6: 673-684.
15. Lalani, R., S. Bhasin, F. Byhower, R. Tarnuzzer, M. Grant, R. Shen, S. Asa, S. Ezzat and N. F. Gonzalez-Cadavid. 2000. Myostatin and insulin-like growth factor-I and -II expression in the muscle of rats exposed to the microgravity environment of the NeuroLab space shuttle flight. *J. Endocrinol.*, 167: 417-428.
16. Maxwell, L. C., J. A. Faulkner and G. J. Hyatt. 1974. Estimation of number of fibers in guinea pig skeletal muscles. *J. Appl. Physiol.*, 37: 259-264.

17. McMahon, C. D., L. Popovic, J. M. Oldham, F. Jeanplong, H. K. Smith, R. Kambadur, M. Sharma, L. Maxwell and J. J. Bass. 2003. Myostatin-deficient mice lose more skeletal muscle mass than wild-type controls during hindlimb suspension. *Am. J. Physiol. Endocrinol. Metab.*, 285: E82-E87.
18. McPherron, A. C., A. M. Lawler and S. J. Lee. 1997. Regulation of skeletal muscle mass in mice by a new TGF-beta superfamily member. *Nature*, 387: 83-90.
19. Minetti, G. C., C. Colussi, R. Adami, C. Serra, C. Mozzetta, V. Parente, S. Fortuni, S. Straino, M. Sampaolesi, P. M. Di, B. Illi, P. Gallinari, C. Steinkuhler, M. C. Capogrossi, V. Sartorelli, R. Bottinelli, C. Gaetano and P. L. Puri. 2006. Functional and morphological recovery of dystrophic muscles in mice treated with deacetylase inhibitors. *Nat. Med.*, 12: 1147-1150.
20. Mitchell, P. O. and G. K. Pavlath. 2004. Skeletal muscle atrophy leads to loss and dysfunction of muscle precursor cells. *Am. J. Physiol. Cell Physiol.*, 287: C1753-C1762.
21. Morey, E. R. 1979. Spaceflight and bone turnover: correlation with a new rat model of weightlessness. *BioScience*, 29: 168-172.
22. Mozdziak, P. E., Q. Truong, A. Macius and E. Schultz. 1998. Hindlimb suspension reduces muscle regeneration. *Eur. J. Appl. Physiol. Occup. Physiol.*, 78: 136-140.
23. Price, S. R. and W. E. Mitch. 1998. Mechanisms stimulating protein degradation to cause muscle atrophy. *Curr. Opin. Clin. Nutr. Metab. Care*, 1: 79-83.

24. Russell, S. T., P. M. Siren, M. J. Siren and M. J. Tisdale. 2009. Attenuation of skeletal muscle atrophy in cancer cachexia by D-myo-inositol 1,2,6-triphosphate. *Cancer Chemother. Pharmacol.*, 64: 517-527.
25. Satchek, J. M., A. Ohtsuka, S. C. McLary and A. L. Goldberg. 2004. IGF-I stimulates muscle growth by suppressing protein breakdown and expression of atrophy-related ubiquitin ligases, atrogin-1 and MuRF1. *Am. J. Physiol. Endocrinol. Metab.*, 287: E591-E601.
26. Spencer, M. J. and R. L. Mellgren. 2002. Overexpression of a calpastatin transgene in mdx muscle reduces dystrophic pathology. *Hum. Mol. Genet.*, 11: 2645-2655.
27. Trappe, S., D. Costill, P. Gallagher, A. Creer, J. R. Peters, H. Evans, D. A. Riley and R. H. Fitts. 2009. Exercise in space: human skeletal muscle after 6 months aboard the International Space Station. *J. Appl. Physiol.*, 106: 1159-1168.
28. Whittemore, L. A., K. Song, X. Li, J. Aghajanian, M. Davies, S. Girgenrath, J. J. Hill, M. Jalenak, P. Kelley, A. Knight, R. Maylor, D. O'Hara, A. Pearson, A. Quazi, S. Ryerson, X. Y. Tan, K. N. Tomkinson, G. M. Veldman, A. Widom, J. F. Wright, S. Wudyka, L. Zhao and N. M. Wolfman. 2003. Inhibition of myostatin in adult mice increases skeletal muscle mass and strength. *Biochem. Biophys. Res. Commun.*, 300: 965-971.
29. Widrick, J. J., S. T. Knuth, K. M. Norenberg, J. G. Romatowski, J. L. Bain, D. A. Riley, M. Karhanek, S. W. Trappe, T. A. Trappe, D. L. Costill and R. H. Fitts. 1999. Effect of a 17 day spaceflight on contractile properties of human soleus muscle fibres. *J. Physiol.*, 516 (Pt 3): 915-930.

30. Widrick, J. J., J. G. Romatowski, J. L. Bain, S. W. Trappe, T. A. Trappe, J. L. Thompson, D. L. Costill, D. A. Riley and R. H. Fitts. 1997. Effect of 17 days of bed rest on peak isometric force and unloaded shortening velocity of human soleus fibers. *Am. J. Physiol.*, 273: C1690-C1699.
31. Williams, A. B., G. M. Courten-Myers, J. E. Fischer, G. Luo, X. Sun and P. O. Hasselgren. 1999. Sepsis stimulates release of myofilaments in skeletal muscle by a calcium-dependent mechanism. *FASEB J.*, 13: 1435-1443.
32. Zhu, X., M. Hadhazy, M. Wehling, J. G. Tidball and E. M. McNally. 2000. Dominant negative myostatin produces hypertrophy without hyperplasia in muscle. *FEBS Lett.*, 474: 71-75.

CHAPTER 4

SUMMARY AND CONCLUSIONS

Summary and Significance of Major Findings

For decades, the adaptive changes in fiber size, muscle mass, and contractility of skeletal muscle resulting from unloading in both humans and animals have been well documented. Yet due to the complexities and unknowns of the mechanisms by which unloading induces changes in skeletal muscle structure and function, no effective remedies have been identified. The purpose of this thesis was to investigate the impact of manipulating pathways that modulate either muscle protein degradation or muscle growth pathways on the decrease in skeletal muscle mass and force generating capacity that occurs in response to disuse. Using hindlimb suspension (HS) to unload soleus muscles of mice the overall hypothesis was tested that inhibition of either calpain activity or protein deacetylase activity would ameliorate the development of muscle atrophy and weakness.

Chapter 2 Summary. Previous work supporting important roles for both the calpain and ubiquitin-proteasome systems to mediate the muscle atrophy induced by unloading suggests that important functional connections exist between these two protein degradation pathways. The working hypothesis tested in Chapter 2 was that increased calpain activity in response to unloading targets specific myofibrillar proteins

leading to the disruption of the underlying sarcomere structure and providing substrate for ubiquitination. Thus, the specific hypothesis was that following various periods of HS, atrophy, weakness, susceptibility to contraction-induced injury, and sarcomere disruption would be less severe for muscles in which calpain activity was inhibited. Calpain activity was inhibited through transgenic muscle-specific over-expression of calpastatin.

The most significant finding of the study was that the development of muscle weakness was completely prevented during HS in the calpastatin over-expressing mice. Consistent with the maintenance of specific force during the period of unloading, electron microscopy demonstrated that calpain inhibition also preserved sarcomere structure. The preservation of sarcomere structure in the calpastatin over-expressing mice during HS was in contrast to substantial disruption of sarcomeres observed in muscles of wild type mice exposed to HS. We also demonstrated that calpain inhibition prevented the decrease in passive tension observed in wild type mice during HS. This finding in addition to reports that immobilization induced changes within sarcomeres that were correlated with the cleavage of titin (Udaka *et al.* 2008) and studies indicating that titin has specific binding sites for calpain cleavage (Raynaud *et al.* 2005) are consistent with the hypothesis that calpain targets titin and the inhibition of calpain may protect titin.

The beneficial effects of calpain inhibition during unloading, to maintain sarcomere structure and to prevent any decrease in maximum isometric specific force, did not extend to a prevention of the increase in susceptibility to lengthening contraction-induced injury induced by HS. These data suggest that the muscle weakness and the increased susceptibility to contraction-induced injury induced by HS are occurring through distinct cellular mechanisms and the effect of HS to increase contraction-

induced injury is not mediated by calpain-dependent proteolytic activity. Finally, calpain inhibition in our transgenic model did not prevent muscle atrophy after 14 days of HS. This result, coupled with the findings that mice deficient in either of two muscle-specific ubiquitin ligases, MuRF1 or MAFbx (atrogen-1), showed decreases in muscle mass of 30% and 20%, respectively, following 14 days of denervation (Bodine *et al.* 2001a), suggests that the inhibition or even prevention of protein degradation may be insufficient to protect muscle completely from a loss in mass during unloading.

Chapter 2 Significance to the Field. As stated above, the most significant finding of the study was the prevention of the development of muscle weakness during HS under circumstances when calpain proteolytic activity was inhibited. This finding is consistent with our hypothesis that the decreased specific force observed following unloading is due to the disruption of the underlying sarcomere structure by the calpain system. Our results provide evidence that unloading leads to sustained increases in calcium concentration by an unknown mechanism, which leads to activation of the calpains that mediate the cleavage of contractile proteins within the sarcomeres resulting in skeletal muscle disruption and weakness. Previous work demonstrated that mice deficient in muscle-specific ubiquitin ligases displayed an attenuation of disuse muscle atrophy (Bodine *et al.* 2001b), even though ubiquitination does not appear to target proteins within intact sarcomeres (Solomon & Goldberg 1996; Cohen *et al.* 2009). Thus, others have hypothesized that additional degradation pathways are necessary for the initial cleavage of sarcomeric proteins to provide substrates for the ubiquitin-proteasome system (Koochmaraie 1992; Tidball & Spencer 2002; Goll *et al.* 2003; Fareed *et al.* 2006). The present findings provide strong support for a critical role of the calpain system in

targeting the force generating infrastructure of sarcomeres during disuse. Overall, our results provide evidence for a model in which muscle unloading increases *in vivo* calpain mediated cleavage sarcomere proteins, possibly titin and desmin, leading to alterations within the sarcomere that decrease force generating capacity.

Chapter 3 Summary. Recent investigations have used pharmacological interventions or genetic modifications that induce skeletal muscle growth as means of ameliorating muscle atrophy induced by unloading. Most of these studies have revealed that while such interventions were effective in inducing hypertrophy in muscles of normally ambulating mice, muscle atrophy induced by unloading was not prevented (Criswell *et al.* 1998; McMahon *et al.* 2003). However, one class of drugs, the deacetylase inhibitors, has been shown to increase myotube size *in vitro* (Iezzi *et al.* 2004), improve regeneration of injured muscles in wild type mice *in vivo* (Iezzi *et al.* 2004), and induce muscle fiber hypertrophy and improvements in muscle contractility in dystrophic mice (Minetti *et al.* 2006). The deacetylase inhibitors appear to act on muscle through the induction of the TGF- β family member follistatin (Iezzi *et al.* 2004), which serves as an endogenous inhibitor of myostatin, that promotes activation and proliferation of satellite cells and enhances the fusion of satellite cells into hypernucleated myotubes and perhaps into mature myofibers (Iezzi *et al.* 2004; Minetti *et al.* 2006; Gilson *et al.* 2009). Neither the effects nor effectiveness of these drugs on skeletal muscles of healthy mice during unloading had been explored. Inasmuch as muscle regeneration has been reported to be impaired during HS (Darr & Schultz 1989; Mozdziak *et al.* 1998; Mitchell & Pavlath 2004; Fujino *et al.* 2005), the possibility that treatment with a deacetylase inhibitor may counteract atrophy through the promotion of

regenerative processes does not seem an unreasonable hypothesis. Thus, the work described in Chapter 3 tested the specific hypothesis that inhibition of deacetylases by treating muscles with trichostatin A (TSA) would provide protection from the loss of muscle mass and weakness in healthy wild type mice subjected to HS.

We observed only a slight amelioration of the loss of muscle mass in the mice treated with TSA compared with vehicle treated mice during 21 days of HS, and the loss of force as well as specific force generating capability was not different for TSA and vehicle treated mice. Despite the lack of protective effects of TSA treatment on muscle mass or force during 21 days of HS, histological analyses showed the presence of substantially larger fibers in the muscles of TSA compared with vehicle treated mice. The larger fibers in muscles of TSA treated animals were observed with no difference between the groups for absolute muscle mass or length suggesting a loss of fibers from the muscles of the TSA treated mice, but more definitive morphological and architecture studies are required to test that hypothesis definitively. In summary, the findings of this study provide little support for the use of deacetylase inhibitors to alleviate the structural and functional deficits associated with unloading. Moreover, until the totality of the effects of the TSA treatment is better understood, the use of the drug under any circumstances should be pursued cautiously.

Chapter 3 Significance to the Field. The findings of this study have both basic science significance as well as applied or clinical significance. First, with respect to the application of treatment with deacetylase inhibitors to lessen the negative effects of muscle disuse, such as during bed rest, immobilization of a limb by casting, or during space flight, our findings indicate that any small benefit provided to maintain muscle

mass was overcome by the weakness of the remaining muscle. Thus, the beneficial effects of treatment with deacetylase inhibitors reported for muscles of dystrophic mice do not appear to extend to the setting of protecting control muscles during disuse. Although treatment with TSA was ineffective for protecting muscles from weakness, after 21 days of HS, individual fiber CSAs were 30-40% larger in muscles of TSA treated mice compared with those in muscles of vehicle treated mice. These findings indicate that inhibition of deacetylase activity is capable of inducing fiber growth, even in atrophying muscle.

Our results are also of significance for the understanding of potential biological effects of deacetylase inhibitors in skeletal muscle. Our observation that muscles in TSA and vehicle treated mice were of similar mass following 21 days of HS but were composed of fibers with greatly differing CSAs indicates that the TSA treatment must be inducing some rather dramatic architectural changes in the muscles. One possibility is that the muscles of the TSA treated mice lost fibers during the period of unloading, an hypothesis that is supported by the fewer fibers present in the cross sections of muscles of TSA compared with vehicle treated mice. An alternative explanation for the observation of fewer fibers appearing in the cross sections of the TSA treated group is that the presence of larger fibers in these muscles resulted in an increased angle of pennation causing fewer fibers to span any given cross section (Maxwell *et al.* 1974). Although an increased pennation angle in the muscles of TSA treated animals represents a reasonable hypothesis, in principle, to account for the similarity in overall mass with the vehicle treated muscles, a scenario of more pennate fibers also necessitates shorter fibers in the muscles of the TSA treated mice. We cannot currently definitively explain these findings, but neither outright fiber loss nor “atrophy” of fibers

through reductions in fiber length accompanied by the simultaneous “hypertrophy” of fiber CSA are typical responses to either muscle unloading or regeneration, and these phenomena warrant future investigation.

Future Directions

Consistent with our findings in Chapter 3, the presence of extremely large fibers in muscles of mice treated with TSA was reported by Minetti et al. for *mdx* mice. Fiber CSAs were a full 2x larger in muscles of *mdx* mice treated with TSA compared with either untreated *mdx* or wild type mice (Minetti *et al.* 2006). Neither muscle masses nor fiber numbers were reported by Minetti and colleagues, but the fiber size data indicates that either muscle masses were two-fold larger or additional undetermined changes were being induced in those muscles as appears to be the case in our TSA treated mice exposed to HS. An additional possibility to explain the entirety of the morphological data from our TSA treated animals is the hypothesis that, while muscle fibers were undergoing atrophy associated with unloading, some of the fibers were fusing together. Although the possibility of fusion of mature myofibers represents the most reasonable interpretation of the aggregate of our morphological data, there is no precedent for such a phenomenon. The fusion of mature myofibers seems highly unlikely as it would require substantial tissue remodeling, but as such the changes should be readily apparent if one were to examine the development of the muscle atrophy and the fiber “hypertrophy” over the course of the period of HS in conjunction with TSA treatment.

The studies described in Chapter 2 provide support for the hypothesis that in the early days and perhaps weeks following the unloading of muscle, disruption of sarcomere structure is mediated by increased calpain activity. The hypothesis that one

of the early and functionally important molecular targets of the calpain system is the cleavage of titin is supported by our observation of the maintenance of passive tension and uniformity of thick filament lengths in soleus muscles of calpastatin over-expressing mice exposed to 14 days of HS. Future studies should pursue this hypothesis directly through analyses of changes in titin levels during HS under circumstances of calpain inhibition. In addition, analysis of permeabilized single fibers from soleus muscles of unloaded wild type and calpastatin over-expressing mice can provide a more specific assessment of the contributions of calpain targeting of titin protein and the subsequent effects on passive tension. Moreover, the ability of the inhibition of calpain proteolytic activity during HS suspension to prevent a decrease in specific force generation during isometric contractions without providing protection from an increased susceptibility to contraction-induced injury as well raises important questions regarding the mechanisms underlying the initiation of contraction-induced injury. Clearly, the threshold in terms of the level of sarcomere disruption that impairs isometric force generation is greater than that for tolerating lengthening contractions without damage.

While inhibition of the calpain system was able to ameliorate the muscle weakness that normally develops during disuse, muscle atrophy was not prevented. The persistence of muscle atrophy in response to disuse in muscles in which calpain activity was substantially inhibited fits with the views of investigators who have suggested that multiple molecular systems may be mediating the increased protein degradation during atrophy (Jackman & Kandarian 2004; Kandarian & Jackman 2006). Although this multifactorial effect might be at play, a few of these protein degradation pathways may be able to prevent the bulk of the atrophy and weakness. Taking into account the prevention of muscle weakness mediated by inhibition of the calpain system

in this thesis and the previous finding that knocking out the skeletal muscle specific ubiquitin ligases reduced muscle atrophy (Bodine *et al.* 2001b), future studies could study the effects of disuse on MuRF1(-/-) or MAFbx(-/-) mice that over-express calpastatin as a means of also inhibiting the proteolytic activity of the calpains. A synergistic inhibition of these two major degradative pathways during disuse could be sufficient to prevent muscle weakness and atrophy. However, given the working model that the ubiquitin-proteasome system operates “downstream” of the calpains, inhibition of both systems may not provide any additive effect. Inhibition or even outright prevention of protein degradation may be insufficient to protect muscle completely from a loss in mass during unloading. Alternatively, the effects of inhibition of the ubiquitin proteasome system may not be the result of directly inhibiting degradation of the myofilaments, but instead regulation of levels of other key signaling proteins important for maintaining muscle protein synthesis or muscle mass. This possibility suggests that approaches targeting the enhancement of protein synthesis and muscle growth (Bodine *et al.* 2001c), rather than the inhibition of protein degradation, may be necessary to fully counteract the atrophy associated with disuse.

One target with potential for enhancing muscle growth, supported by previous work studying deacetylase inhibitors (Iezzi *et al.* 2004; Minetti *et al.* 2006) is follistatin. Gilson and her colleagues (Gilson *et al.* 2009) recently showed that over-expression of follistatin increased skeletal muscle satellite cell proliferation and muscle hypertrophy through a mechanism that was independent of the myostatin inhibitory function of follistatin. Future studies could assess the effects of follistatin over-expression during disuse as a way to induce hypertrophy through increased satellite cell proliferation. While an increase in muscle growth may be insufficient on its own to overcome the

strong stimulatory effects of unloading on protein degradation pathways, follistatin over-expression could be incorporated in conjunction with other therapies that inhibit sarcomere disruption, such as calpastatin over-expression.

In addition, the IGF-1/PI3K/Akt pathway stimulates muscle hypertrophy through both its effects to induce protein synthesis and to inhibit the FOXO family of transcription factors that induce the upregulation of the skeletal muscle specific ubiquitin ligases MuRF1 and MAFbx (reviewed in Glass, 2005). Yet, upregulation of IGF-1 was not sufficient to block atrophy during unloading by HS (Criswell *et al.* 1998). However, a more recent study showed that over-expression of IGF-1 by means of electroporation induced a small but significant amelioration of the loss of muscle mass and density in soleus muscles (Alzghoul *et al.* 2004). Despite these potentially promising findings (Alzghoul *et al.* 2004), the issue remains of developing an effective means of activating the Akt/PI3K pathway in an appropriate and muscle-specific manner. Thus, future studies should find ways to activate the pathway in suspended rodents in order to determine the specific contributions on skeletal muscle weakness and atrophy during disuse.

Another pathway that may be involved in disuse-mediated muscle atrophy is the Nuclear Factor (NF) κ B pathway. The NF κ B/Rel family consists of a number of distinct subunits, including p50/p105, p52/p100, p65 (RelA), RelB, and c-Rel, each expressed in skeletal muscle (Bar-Shai *et al.* 2005). NF κ B family members play critical roles in modulating the specificity of NF κ B function, via the formation of a range of homo and heterodimers (Hayden & Ghosh 2008). While key regulatory roles for NF κ B have been described in detail in immune cells, the function(s) of NF κ B in muscle is poorly understood. In skeletal muscle, NF κ B has been shown to modulate expression of a

number of genes associated with myogenesis (Bakkar *et al.* 2008; Dahlman *et al.* 2009), catabolism-related genes in muscles of adult mice (Bar-Shai *et al.* 2005; Peterson & Guttridge 2008; Van *et al.* 2009), and cyto-protective proteins during adaptation to contractile activity (Vasilaki *et al.* 2006). The specificity of the responses of skeletal muscle cells to NF κ B activation is also unclear, but it is likely to be largely due to subtle differences in NF κ B activation such as κ B binding sequences and NF κ B dimer formation that regulate expression of specific genes (Bakkar *et al.* 2008). For example, skeletal muscle atrophy due to unloading is associated with NF κ B activation, although no change in the nuclear content of the p65 subunit is observed indicating that disuse atrophy-induced NF κ B activation does not involve the canonical activation pathway (Hunter *et al.* 2002; Bar-Shai *et al.* 2005). Rather, the non-canonical NF κ B was implicated in studies of knock out mice for p50 or bcl-3 (an I κ B family member) in which muscles were protected from fiber atrophy following 10 days of HS (Hunter & Kandarian 2004), suggesting that NF κ B may play a causative role in the response to disuse rather than being activated as a consequence of atrophy. Although the conclusion of Hunter and Kandarian (2004) was that disuse atrophy requires the non-canonical NF κ B pathway, neither the upstream signals nor the downstream target genes are known. Future studies using microarray analysis of the genes that are altered during HS in p50 (-/-) or bcl-3 (-/-) mice would be useful to identify candidate triggers and downstream targets mediating the muscle atrophy.

Taking together the data from Chapters 2 and 3, we propose that the mechanisms underlying the muscle weakness and muscle atrophy involve distinct molecular pathways. These separate pathways can be observed under conditions where the inhibition of calpain activity in calpastatin over-expressing mice completely

blocked the effects of muscle disuse that cause muscle weakness but muscle atrophy was not prevented. Conversely, while the effects of TSA to ameliorate the loss of muscle mass during HS were not dramatic, TSA treatment did partially prevent the loss in muscle mass without improving muscle weakness and resulted in dramatic increases in fiber CSAs. This latter effect is consistent with results observed in myostatin deficient mice, which have marked muscular hypertrophy, but the muscles are actually weaker in terms of force production per cross sectional area and more susceptible to injury (Mendias *et al.* 2006). Therefore, since the muscles ability to produce force and its cross-sectional area are key determinants of the overall ability of muscle to produce specific force, our studies suggest that therapies for muscle dysfunction following disuse will likely need to target calpain mediated muscle fiber damage along with the future fully characterized pathways that may mediate the bulk of the muscle atrophy.

References

1. Alzghoul, M. B., D. Gerrard, B. A. Watkins and K. Hannon. 2004. Ectopic expression of IGF-I and Shh by skeletal muscle inhibits disuse-mediated skeletal muscle atrophy and bone osteopenia in vivo. *FASEB J.*, 18: 221-223.
2. Bakkar, N., J. Wang, K. J. Ladner, H. Wang, J. M. Dahlman, M. Carathers, S. Acharyya, M. A. Rudnicki, A. D. Hollenbach and D. C. Guttridge. 2008. IKK/NF-kappaB regulates skeletal myogenesis via a signaling switch to inhibit differentiation and promote mitochondrial biogenesis. *J. Cell Biol.*, 180: 787-802.
3. Bar-Shai, M., E. Carmeli and A. Z. Reznick. 2005. The role of NF-kappaB in protein breakdown in immobilization, aging, and exercise: from basic processes to promotion of health. *Ann. N. Y. Acad. Sci.*, 1057: 431-447.
4. Bodine, S. C., E. Latres, S. Baumhueter, V. K. Lai, L. Nunez, B. A. Clarke, W. T. Poueymirou, F. J. Panaro, E. Na, K. Dharmarajan, Z. Q. Pan, D. M. Valenzuela, T. M. DeChiara, T. N. Stitt, G. D. Yancopoulos and D. J. Glass. 2001a. Identification of ubiquitin ligases required for skeletal muscle atrophy. *Science*, 294: 1704-1708.
5. Bodine, S. C., E. Latres, S. Baumhueter, V. K. Lai, L. Nunez, B. A. Clarke, W. T. Poueymirou, F. J. Panaro, E. Na, K. Dharmarajan, Z. Q. Pan, D. M. Valenzuela, T. M. DeChiara, T. N. Stitt, G. D. Yancopoulos and D. J. Glass. 2001b. Identification of ubiquitin ligases required for skeletal muscle atrophy. *Science*, 294: 1704-1708.

6. Bodine, S. C., T. N. Stitt, M. Gonzalez, W. O. Kline, G. L. Stover, R. Bauerlein, E. Zlotchenko, A. Scrimgeour, J. C. Lawrence, D. J. Glass and G. D. Yancopoulos. 2001c. Akt/mTOR pathway is a crucial regulator of skeletal muscle hypertrophy and can prevent muscle atrophy in vivo. *Nat. Cell Biol.*, 3: 1014-1019.
7. Cohen, S., J. J. Brault, S. P. Gygi, D. J. Glass, D. M. Valenzuela, C. Gartner, E. Latres and A. L. Goldberg. 2009. During muscle atrophy, thick, but not thin, filament components are degraded by MuRF1-dependent ubiquitylation. *J. Cell Biol.*, 185: 1083-1095.
8. Criswell, D. S., F. W. Booth, F. DeMayo, R. J. Schwartz, S. E. Gordon and M. L. Fiorotto. 1998. Overexpression of IGF-I in skeletal muscle of transgenic mice does not prevent unloading-induced atrophy. *Am. J. Physiol.*, 275: E373-E379.
9. Dahlman, J. M., J. Wang, N. Bakkar and D. C. Guttridge. 2009. The RelA/p65 subunit of NF-kappaB specifically regulates cyclin D1 protein stability: implications for cell cycle withdrawal and skeletal myogenesis. *J. Cell Biochem.*, 106: 42-51.
10. Darr, K. C. and E. Schultz. 1989. Hindlimb suspension suppresses muscle growth and satellite cell proliferation. *J. Appl. Physiol.*, 67: 1827-1834.
11. Fareed, M. U., A. R. Evenson, W. Wei, M. Menconi, V. Poylin, V. Petkova, B. Pignol and P. O. Hasselgren. 2006. Treatment of rats with calpain inhibitors prevents sepsis-induced muscle proteolysis independent of atrogen-1/MAFbx and MuRF1 expression. *Am. J. Physiol. Regul. Integr. Comp. Physiol.*, 290: R1589-R1597.

12. Fujino, H., H. Kohzuki, I. Takeda, T. Kiyooka, T. Miyasaka, S. Mohri, J. Shimizu and F. Kajiya. 2005. Regression of capillary network in atrophied soleus muscle induced by hindlimb unweighting. *J. Appl. Physiol.*, 98: 1407-1413.
13. Gilson, H., O. Schakman, S. Kalista, P. Lause, K. Tsuchida and J. P. Thissen. 2009. Follistatin induces muscle hypertrophy through satellite cell proliferation and inhibition of both myostatin and activin. *Am. J. Physiol. Endocrinol. Metab.*, 297: E157-E164.
14. Goll, D. E., V. F. Thompson, H. Li, W. Wei and J. Cong. 2003. The calpain system. *Physiol. Rev.*, 83: 731-801.
15. Hayden, M. S. and S. Ghosh. 2008. Shared principles in NF-kappaB signaling. *Cell*, 132: 344-362.
16. Hunter, R. B. and S. C. Kandarian. 2004. Disruption of either the Nfkb1 or the Bcl3 gene inhibits skeletal muscle atrophy. *J. Clin. Invest.*, 114: 1504-1511.
17. Hunter, R. B., E. Stevenson, A. Koncarevic, H. Mitchell-Felton, D. A. Essig and S. C. Kandarian. 2002. Activation of an alternative NF-kappaB pathway in skeletal muscle during disuse atrophy. *FASEB J.*, 16: 529-538.
18. Iezzi, S., P. M. Di, C. Serra, G. Caretti, C. Simone, E. Maklan, G. Minetti, P. Zhao, E. P. Hoffman, P. L. Puri and V. Sartorelli. 2004. Deacetylase inhibitors increase muscle cell size by promoting myoblast recruitment and fusion through induction of follistatin. *Dev. Cell.*, 6: 673-684.
19. Jackman, R. W. and S. C. Kandarian. 2004. The molecular basis of skeletal muscle atrophy. *Am. J. Physiol. Cell Physiol.*, 287: C834-C843.
20. Kandarian, S. C. and R. W. Jackman. 2006. Intracellular signaling during skeletal muscle atrophy. *Muscle Nerve*, 33: 155-165.

21. Koohmaraie, M. 1992. Ovine skeletal muscle multicatalytic proteinase complex (proteasome): purification, characterization, and comparison of its effects on myofibrils with mu-calpains. *J. Anim. Sci.*, 70: 3697-3708.
22. Maxwell, L. C., J. A. Faulkner and G. J. Hyatt. 1974. Estimation of number of fibers in guinea pig skeletal muscles. *J. Appl. Physiol.*, 37: 259-264.
23. McMahon, C. D., L. Popovic, J. M. Oldham, F. Jeanplong, H. K. Smith, R. Kambadur, M. Sharma, L. Maxwell and J. J. Bass. 2003. Myostatin-deficient mice lose more skeletal muscle mass than wild-type controls during hindlimb suspension. *Am. J. Physiol. Endocrinol. Metab.*, 285: E82-E87.
24. Mendias, C. L., J. E. Marcin, D. R. Calderon and J. A. Faulkner. 2006. Contractile properties of EDL and soleus muscles of myostatin-deficient mice. *J. Appl. Physiol.*, 101: 898-905.
25. Minetti, G. C., C. Colussi, R. Adami, C. Serra, C. Mozzetta, V. Parente, S. Fortuni, S. Straino, M. Sampaolesi, P. M. Di, B. Illi, P. Gallinari, C. Steinkuhler, M. C. Capogrossi, V. Sartorelli, R. Bottinelli, C. Gaetano and P. L. Puri. 2006. Functional and morphological recovery of dystrophic muscles in mice treated with deacetylase inhibitors. *Nat. Med.*, 12: 1147-1150.
26. Mitchell, P. O. and G. K. Pavlath. 2004. Skeletal muscle atrophy leads to loss and dysfunction of muscle precursor cells. *Am. J. Physiol. Cell Physiol.*, 287: C1753-C1762.
27. Mozdziak, P. E., Q. Truong, A. Macius and E. Schultz. 1998. Hindlimb suspension reduces muscle regeneration. *Eur. J. Appl. Physiol. Occup. Physiol.*, 78: 136-140.

28. Peterson, J. M. and D. C. Guttridge. 2008. Skeletal muscle diseases, inflammation, and NF-kappaB signaling: insights and opportunities for therapeutic intervention. *Int. Rev. Immunol.*, 27: 375-387.
29. Raynaud, F., E. Fernandez, G. Coulis, L. Aubry, X. Vignon, N. Bleimling, M. Gautel, Y. Benyamin and A. Ouali. 2005. Calpain 1-titin interactions concentrate calpain 1 in the Z-band edges and in the N2-line region within the skeletal myofibril. *FEBS J.*, 272: 2578-2590.
30. Solomon, V. and A. L. Goldberg. 1996. Importance of the ATP-ubiquitin-proteasome pathway in the degradation of soluble and myofibrillar proteins in rabbit muscle extracts. *J. Biol. Chem.*, 271: 26690-26697.
31. Tidball, J. G. and M. J. Spencer. 2002. Expression of a calpastatin transgene slows muscle wasting and obviates changes in myosin isoform expression during murine muscle disuse. *J. Physiol.*, 545: 819-828.
32. Udaka, J., S. Ohmori, T. Terui, I. Ohtsuki, S. Ishiwata, S. Kurihara and N. Fukuda. 2008. Disuse-induced preferential loss of the giant protein titin depresses muscle performance via abnormal sarcomeric organization. *J. Gen. Physiol.*, 131: 33-41.
33. Van, G. D., J. S. Damrauer, R. W. Jackman and S. C. Kandarian. 2009. The IkappaB kinases IKKalpha and IKKbeta are necessary and sufficient for skeletal muscle atrophy. *FASEB J.*, 23: 362-370.
34. Vasilaki, A., F. McArdle, L. M. Iwanejko and A. McArdle. 2006. Adaptive responses of mouse skeletal muscle to contractile activity: The effect of age. *Mech. Ageing Dev.*, 127: 830-839.